José Víctor del Razo Sarmina

Coordinated Electric Vehicle Charging in Residential and Highway Environments

Technische
Universität
München

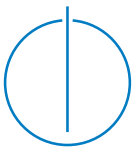

Technische Universität München

Fakultät für Informatik

Coordinated Electric Vehicle Charging in Residential and Highway Environments

José Víctor del Razo Sarmina

Vollständiger Abdruck der von der Fakultät für Informatik der Technischen Universität München zur Erlangung des akademischen Grades eines

Doktors der Naturwissenschaften (Dr. rer. nat.)

genehmigten Dissertation.

Vorsitzende(r): Univ.-Prof. Dr. Nils Thuerey

Prüfer der Dissertation:

1. Univ.-Prof. Dr. Hans-Arno Jacobsen
2. Prof. Dr. Anders Andersen,
   UiT The Arctic University of Norway

Die Dissertation wurde am 22.06.2016 bei der Technischen Universität München eingereicht und durch die Fakultät für Informatik am 21.09.2016 angenommen.

Abstract

Electric vehicles (EVs) could contribute towards the reduction of CO2 emissions and the integration of renewable energies. To do so, efficient and applicable control mechanisms need to be in place and a critical mass of EVs needs to be available. In this work, two greatly different methods towards achieving these objectives are presented.

We propose the Vehicle-Originating-Signals (VOS) approach for charging control of a fleet of electric vehicles (EV) in an electricity distribution network. The VOS approach enables EVs in a fleet to compute signals reflecting their need for charge and willingness to supply power. An aggregator collects these signals and implements the control with minor computational effort. The goal of the approach is to manage the EV load such that the total power consumption, including inflexible demand and solar generation, closely follows a given target profile. We evaluate the VOS approach on a scenario for Munich, Germany, based on a mobility survey and real electricity demand and solar generation data. We compare our approach against a centralized optimization and show that it achieves a competitive performance. Then, we present a statistical method to evaluate the performance and limitations of our approach. We also introduce two extensions to the approach: a method for further reducing the communication requirements and examples of alternative signals designs.

To reduce the effects of limited range and long charging times of EVs, and therefore increase adoption rates, we propose a smart scheduling approach for EVs to plan charging stops on a highway with limited charging infrastructure. This approach aims to minimize the total travel time for each EV based on the A* algorithm with constraint verification and a peer-to-peer scheduling system. By considering the estimated state of the charging stations, we achieve indirect coordination between EVs. We introduce a simulation framework with trips generated using a data-driven approach and support for time-varying highway parameters. Furthermore, we apply our approach to a use-case for the German highway A9 from Munich to Berlin. Results show that the smart scheduling approach significantly reduces the total travel times and adapts to changes on the highway, for example, slow traffic on a given segment. Our approach can be generalized beyond fast-charging to account for different technologies such as hydrogen or battery swapping stations.

Zusammenfassung

Elektrofahrzeuge können zur Reduzierung der CO2-Emission und zur Integration erneuerbarer Energien beitragen. Um dies zu ermöglichen, müssen sowohl effiziente und anwendbare Steuerungsmechanismen als auch eine bestimmte Mindestanzahl an Elektrofahrzeugen vorhanden sein. Inhalt der vorliegenden Arbeit ist die Ausarbeitung zwei sehr unterschiedlicher Methoden, die die oben genannten Zielsetzungen unterstützen.

Der erste Lösungsansatz, die Vehicle-Originating-Signals (VOS) Methode, steuert das Batterieladeverhalten einer Elektrofahrzeugflotte. Die VOS Methode ermöglicht, dass Elektrofahrzeuge ihre Notwendigkeit des Ladens und die Bereitschaft Energie anzubieten signalisieren. Ein Aggregator sammelt diese Signale und führt anschließend die Steuerung der Energiezufuhr oder -abgabe mit einem minimalen Berechnungsaufwand durch. Ziel ist, das Ladeverhalten der Elektrofahrzeuge so zu steuern, dass sich der daraus ergebende Gesamtenergieverbrauch, einschließlich der nicht steuerbaren Nachfrage sowie der solaren Energieeinspeisung, an ein vorgegebenes Zielprofil annähert. Die Evaluierung der VOS-Methode erfolgt anhand einem Szenario für München (Deutschland). Dieses Szenario basiert auf einer Studie zur Mobilität in Deutschland und auf tatsächlichen Daten zum Energiebedarf und zur Solareinspeisung. Dabei wird die erarbeitete Methode mit einer zentralisierten Optimierung verglichen und gezeigt, dass mit der VOS-Methode vergleichbare Ergebnisse erzielt werden können. Abschließend werden anhand statischer Methoden die Leistungsfähigkeit sowie die Grenzen der VOS-Methode analysiert. In einem Exkurs werden zwei mögliche Erweiterungen vorgestellt: Zum einen die Möglichkeit zur weiteren Reduzierung der Kommunikationsanforderungen und zum anderen Beispiele für alternative Signalentwürfe.

Um die Nachteile von Elektrofahrzeugen, wie begrenzte Reichweiten und lange Ladezeiten, zu kompensieren und somit die Attraktivität und Anzahl von Elektrofahrzeugen zu erhöhen, wird als zweiter Lösungsansatz die intelligente Disposition der Ladeinfrastruktur vorgestellt. Diese intelligente Disposition ermöglicht es, die Fahrtunterbrechungen auf Autobahnen zum Wiederaufladen der Fahrzeugbatterien zu optimieren. Ziel ist, die gesamte Reisedauer für jedes Elektrofahrzeug zu minimieren. Dazu wird ein modifizierter A*-Algorithmus mit definierten Randbedingungen und

einem verteilten Buchungssystem verwendet. Unter Berücksichtigung der voraussichtlichen Auslastungen der Ladestationen wird eine indirekte Koordination der Elektrofahrzeuge erreicht. Dabei werden auch Reisezeit beeinflussende Informationen der Autobahn berücksichtigt. Die Verifizierung erfolgt durch eine Simulation, deren einzelne Fahrten durch eine datenorientierte Methode generiert werden. Die entwickelte Methode wird an einem Fallbeispiel für die A9 von München nach Berlin (Deutschland) evaluiert. Die Ergebnisse bestätigen, dass durch intelligente Disposition die Gesamtreisezeit signifikant reduziert werden kann. Zusätzlich können Veränderungen auf der Autobahn, wie zum Beispiel stockender Verkehr auf einem bestimmten Teilstück, berücksichtigt werden. Über die schnelle Wiederaufladung von Batterien hinaus kann der Ansatz auch für andere Technologien, wie Wasserstoff-Betankung oder Systeme mit Batteriewechsel, verwendet werden.

Acknowledgments

The work towards this doctoral dissertation took place at the Department of Informatics of the Technical University of Munich under the supervision of Prof. Dr. Hans-Arno Jacobsen.

I would like to express my sincere gratitude to my supervisor Prof. Hans-Arno Jacobsen for the continuous support and guidance during my research, and for entrusting me as receiver of part of the hard earned funding from his Alexander von Humboldt Professorship. He gave me a great deal of freedom in terms of the direction of my research and also exercised pressure at those key moments when larger achievements were possible.

I would like to thank the rest of my thesis committee: Prof. Anders Andersen for agreeing to be the second examiner even while officially on sabbatical, and Prof. Nils Thürey for accepting to chair the committee.

This work would not have been possible without the support of the colleagues in our chair. I want to warmly thank the "chair starters" Martin Jergler, Jose Rivera and Christoph Doblander (in order of arrival) not only for their help and for enriching the research with numerous and brilliant discussions, but also for creating such a great working atmosphere during the last four years. My thanks go to Christoph Goebel for his input and support, particularly at the beginning. Also thanks to Anwar Ul Haq for his calm feedback and for being a good officemate.

My thanks also go to students whose thesis I had the chance to tutor. Special thanks go to Julia Händel, whose work on highway fast charging provided important input for parts of this work. Additionally, I would like to thank Hamidreza Mirtaheri and Prof. Gianfranco Chicco for the chance of tutoring a multi-university Master's thesis and coauthoring the resulting paper.

On the non-scientific front, my foremost and infinite thanks go to my beloved Friederike for being my muse, my inspiration, and my inexplicable loyal admirer. She unconditionally supported my decision to pursue a doctoral degree and kept me going on those moments when I was close to change my mind. I want to thank

the youngest family member, our son Bruno, whose recent birth functioned as a turbo-button for finalizing my thesis.

I also want to thank my family for their moral and sometimes even financial support: my mother Sandra and my brothers Carlos and Mauricio who, although far, were always there when I needed them. Mauricio, who was also pursuing his PhD, became an important source of advice. Thanks to my father Jose Victor for his questions. Thanks also to my step father Jose Luis for his numerous visits as family representative. I would like to express my gratitude to my German family: Ingrid, Michael, Daniel, Joachim, Tania, and Marlene; who have made me feel home since the first day in this beautiful country.

I also want to thank my close friends who have been providing their support during these years (alphabetically-listed): Andrea, Carlos, Christoph, Gavin, Hansi, Ina, Lily, Lena, Mario, Michael, Nicole, Saskia, and Vera. Their support took many forms, such as taking care of the restaurant bill to support the student, showing interest on my research and then having to listen what I had to say, personal coaching for mental strength and perseverance, etc. My special thanks to Lily and Gavin for being my language and style consultants for this document.

Although not directly involved in this work, I would also like to express my gratitude to Prof. Risto Wichman and Dr. Stefan Werner from the Aalto University in Finland. They were the first to introduce me into scientific research. When learning about my intention to go back to academia after several years in industry, they provided useful tips and backed my application to this doctoral position.

Contents

Chapter 1

Introduction

Climate change, carbon emission reduction, and independence from fossil-fuels continue to be important issues on the international agenda throughout the past few decades. The numerous efforts aimed at dealing with and realizing these topics have begun to show positive effects. In particular, the share of energy generated from renewable sources has significantly increased [1].

In parallel, there has been an increased tendency towards electrification of products, services, and technology, with electrification of transportation being perhaps the most representative example. Electric vehicles (EV), in particular, allow for emission reduction in urban areas and, due to their use-patterns in urban environments, can potentially operate as flexible electric loads to support the operation of power systems and the integration of renewable energy sources.

This work addresses the use of EVs from two perspectives. First, we look at the EV as a tool for supporting power systems (and therefore the integration of renewable energy sources) by using them as controllable loads and even energy storage. For this we focus on residential environments. Second, we analyze strategies for the efficient use of fast charging infrastructure for long trips which could contribute towards a higher EV adoption. For both perspectives, we put strong focus on the role of ICT technologies in the solution to these problems.

1.1 Motivation

The United Nations Framework Convention on Climate Change (UNFCCC) [2] defines climate change as a *"a change of climate which is attributed directly or indirectly to human activity that alters the composition of the global atmosphere and which is in addition to natural climate variability observed over comparable time periods."* Mitigating climate change involves reducing the sources or enhancing the sinks of greenhouse gases [3]. Carbon dioxide (CO2) represents the largest contributor to greenhouse gas emissions.

In 2010, CO2 emissions from energy accounted for around 60% of global greenhouse emissions [4]. By 2013, around 82% of the world's primary energy supply came from fossil sources. Specifically, heat and electricity generation accounted for 42% of CO2 emissions in 2013, with an increase of 50% in emissions from electricity generation (excluding heat generation) between 2000 and 2013 [4].

Renewable energy sources are a realistic alternative to reduce CO2 emissions and mitigate climate change. In 2014, renewable electricity generation worldwide rose by around 7%, accounting for more than 22% of the total electricity generation. Furthermore, a number of countries have set ambitious renewable integration targets, such as 35% for Germany, 50% for Sweden, and 20% for the European Union by 2020 [5]. Renewable generation, however, incorporates new challenges into how electricity has been traditionally generated, transmitted, and consumed.

To keep the electric grid stable, power supply and demand have to be balanced at all times. To date, this balance is preserved by dispatching generators to match a given demand [6], most of these generators being fossil fueled. As the share of energy from non-dispatchable renewable sources like wind and solar continues to increase, demand-side management and energy storage are becoming more relevant as tools to maintain this balance.

Furthermore, greenhouse gas emissions from the transport sector doubled between 1970 and 2010, faster than any other energy end-use sector [3]. For the majority of transport modes, less than 5% of these emissions are non-CO2 gases [3]. In 2013,

transportation accounted for 23% of global CO2 emissions by sector, with around three quarters attributable to road transport [4].

Transportation electrification offers two important advantages. First, it reduces local carbon emissions and fossil-fuel dependency [7]. Second, it shifts energy needs towards a power system that is increasingly able to leverage energy produced from renewable sources [8, 9]. Electric vehicles (EV), in particular, allow for emission reduction in urban areas [9] and, due to their use-patterns in urban environments, can potentially operate as flexible electric loads to support the operation of power systems and the integration of renewable energy [9, 10, 11, 12].

This potential can only be materialized if the number of EVs is large enough and the required technology and infrastructure are in place. On the one hand, control approaches for coordinated EV charging need to be efficient and realizable with moderate investment. On the other hand, known drawbacks of EVs such as range and charging time need to be addressed.

1.2 Problem Statement

EVs can contribute towards the reduction of CO2 emissions and support the integration of renewable energy sources. Such an ambitious objective is only realizable when there is a large number of EVs and feasible control strategies are implemented. This work concentrates on two main research objectives:

1. *Control when and how individual EVs should charge for supporting the power system towards integrating renewable energy sources, while keeping ICT infrastructure requirements within realistic boundaries.*
2. *Reduce the negative effects of limited range and long charging times of EVs with the help of ICT, particularly for long trips, for reducing the total travel time and therefore enabling a wider adoption of EVs.*

In both cases, the ICT requirements play an important role. The proposed solutions

must be feasible in practice. That is, the infrastructure requirements must be realistic and the solution should be close enough to the theoretical best in order for benefits to exceed investment.

Coordinated EV charging control allows for a higher adaptability to energy supply conditions. This adaptability helps towards integrating renewable energy sources and contributes to the reduction of reserve requirements in power systems. These control strategies become particularly relevant for a large number of EVs. However, their implementation also becomes more challenging as the number of EV increases. Furthermore, the evaluation becomes non-trivial as it is likely to depend on the behavior of EV drivers and the periods when EVs are available for charging.

Centralized optimization methods face the challenge of scalability as the size of the problem increases. Distributed optimization approaches can be used to address scalability limitations, but implementing such solutions could be challenging, mostly due to their iterative nature and high communication overhead. The trade-off between simplicity, scalability, and quality of the solution therefore plays an important role. The quality of the solution is measured in terms of deviation from a given control goal, the scalability in terms of solution time and the simplicity in terms of communication requirements. The VOS approach combines the benefits of a centralized approach regarding simplicity, but distributes part of the computation to the EVs to achieve scalability.

The success of EVs as means to support the power systems depend on their level of penetration. A critical mass needs to be achieved for coordinated control strategies to be effective. To this extent, addressing specific drawbacks that prevent people to choose EVs over fuel-based vehicles is important. Limited range and long charging time are two specific drawbacks of EVs particularly relevant for long trips. Reducing overall travel time on longer trips could contribute towards addressing these drawbacks.

Solving this problem under dynamic conditions such as those in a highway is challenging due to the time-dependent and interdependent nature of the variables involved. The behavior of drivers and traffic on the highway also plays an important role. The trade-off dilemma between centralized and distributed solutions is equally

applicable here. The proposed scheduling approach for fast EV charging on highways aims to reduce the total travel time, measured as the sum of driving, waiting, and charging time for a given trip. This approach applies a local decision-making at EV level but considers CS parameters (such as queue length and waiting times) as the coupling element to coordinate with the EVs. The benefits of our scheduling approach are an efficient use of charging infrastructure and the reduction of travel time.

1.3 Approach

In summary, the objectives of this work are twofold. First, EV charging control in residential environments for supporting the power system. Second, fast EV charging scheduling in highway environments for reducing travel time and facilitating EV adoption. For the former, we propose the Vehicle Originating Signals (VOS) method. For the latter, we propose a dynamic scheduling method for total travel time reduction. In this section, we briefly introduce these approaches.

1.3.1 Vehicle-Originating-Signals for EV Charging Control

To keep the electric grid stable, power supply and demand have to be balanced at all times. Our objective is to facilitate this balance by reducing the difference between a reference power profile and the power consumption of a group of consumers, e.g., a neighborhood served by a section of a distribution network (DN). In other words, we aim to comply with a planned external power supply by compensating for the variations using internal resources.

This planned external power supply is usually the result of a unit commitment process based on expected demand and generator capabilities. Complying to a given planned supply allows operators and utilities to use their resources more efficiently as the need for reserve is lower.

For the internal resources, we consider a scenario with a number of electric vehicles (EV) and solar photovoltaic panels (PV) within the area of control. The EVs can be seen as flexible loads, if they only consume energy, or additionally as storage if they also supply energy back to the grid in what is known as Vehicle-to-Grid (V2G).

The Vehicle-Originating-Signals (VOS) approach for EV real-time charging control, enables an aggregator to control how a fleet of EVs charges in order to follow an arbitrary power profile. This approach takes computational, communication, aggregator, and user requirements into account. The VOS approach can be generalized to different loads and objectives. For the evaluation, we demonstrate how this approach can be used to reduce the variability of demand and distributed solar generation by intelligently charging and discharging EVs.

Several research papers [13, 14, 15, 16, 17] deal with aggregator-based EV charging control, some of them proposing centralized strategies, some proposing distributed approaches. The VOS approach combines the benefits of a centralized approach regarding simplicity, but distributes part of the computation to the EVs. Furthermore, it does not require iterative optimization and could therefore meet the real-time requirements of advanced applications. In addition, we choose a direct control method to ensure certainty in control but, to a certain extent, protect EV users' privacy by limiting information exchange.

1.3.2 Scheduling Fast EV Charging on Highways

Electric vehicles could allow for emission reduction in urban areas and, due to their use-patterns in urban environments, can potentially operate as flexible electric loads to support the operation of power systems and the integration of renewable energy sources. The wide adoption of EVs, however, faces a number of challenges. The limitations on battery energy density and their effects on cost restrict the range or autonomy of EVs to far below that of their fuel-based competitors. The requirements in terms of a new charging infrastructure, particularly if extended beyond places of residence or work, involve significant investment. For example, according to a study in [18], investment in fast-charging infrastructure is unlikely to be profitable at low

EV adoption rates, unless investment cost can be lowered. Additionally, the time required for charging an EV is substantial, with the additional disadvantage that, in general, increasing the charging power negatively influences the battery's lifetime [19]. A higher EV adoption rate can only be reached if sufficient infrastructure is made available.

These major challenges, particularly related to the use of EVs in urban environments, have been the subject of intense research in recent years. We argue that range, infrastructure, and charging-time limitations are major factors in highway environments, an area not as densely researched as the above. The current range of most commercial EV models is not extensive enough to cover long distances. This range decreases further as driving speeds increase. Basic infrastructure, such as electricity and services necessary for the charging infrastructure, are only available on specific points along a highway. Long charging times can potentially cause significant delays not only because of the charging process itself but also because of the potential waiting times resulting from busy charging stations (CS).

Although advances in chemistry, battery, and charging technology play a role in addressing these challenges, we believe that information and communication technologies (ICT) can make a major contribution in efficiently managing the available resources, reducing the required amount of infrastructure for a given service level, and assist in planning and dimensioning fast-charging infrastructure. Therefore, this work proposes a method for scheduling charging stops during highway travel such that the final destination is reached with the lowest possible cost, in our case total travel time. We put special focus on the applicability of this method from the ICT perspective and present our results within the context of a use-case for a 500 km long German highway accompanied by a methodology for generating EV trips based on real data.

As EVs enter the highway, they decide at which CSs to stop and generate a schedule accordingly. This schedule is then continuously updated during the EV's trip to account for changes in CSs and the highway. Unlike other approaches, we focus on total travel time (not only waiting time [20, 21] or infrastructure usage [22]), apply a local decision-making approach at EV level with CS parameters (such as queue

length and waiting times) as the coupling element instead of a global approach [20, 23], and use synthetic trips rather than probabilistic models [22, 20, 21]. The benefits of our scheduling approach are an efficient use of charging infrastructure and shorter travel times, thus contributing to cost reduction and EV adoption.

1.4 Contribution

The main contributions of the VOS approach for EV charging control are:

i. We design the VOS approach: a novel charging control mechanism that aims at matching a given power profile, provides scalability by applying heuristics and partial distribution of computations, and achieves results comparable to those from state-of-the-art optimization solutions in a fraction of the solving time.

ii. We conduct extensive evaluations based on a scenario with real data for electricity demand and solar generation for Munich, Germany, as well as EV driving profiles derived from a German mobility survey.

iii. We compare the performance of our VOS approach to a state-of-the-art central optimization, both in terms of optimality and solving time.

iv. We apply a statistical method to evaluate the performance of the VOS approach in terms of the error's upper bound for a given percentile. This allows for a more insightful evaluation beyond average performance and for making recommendations in terms of parameter selection such as fleet size and load magnitude.

v. We propose an extension to the VOS approach for reducing the communication overhead, which in turn reduces the number of messages by at least 70%.

vi. We propose alternative methods for signal design that allow for earlier charging.

The main contributions our approach for scheduling fast EV charging on highways are:

i. We introduce a scheduling method for planning charging stops on a highway trip, based on an extension of the A* search algorithm that accounts for problem constraints, including EV energy requirements and driving speeds, that enables the reduction of travel times and efficient use of the available charging infrastructure.

ii. We propose a trip generation method that uses data available from highway counters and travel surveys to generate synthetic highway trips that are closer to reality.

iii. We develop a simulation framework for highway traffic that accounts for highway exits/entries, potential charging sites, variable highway speed limitations, and EV-specific characteristics, enabling us to test scheduling methods and account for changes such as traffic congestion.

iv. We implement our approach in a use-case for a German highway connecting Berlin and Munich with the actual highway entries/exits, speed limits, and production EV models, while considering current fuel stations as potential charging sites.

Parts of the content and contributions of this work have been published in:

- V. del Razo and H.-A. Jacobsen. "Smart Charging Schedules for Highway Travel with Electric Vehicles." In: *IEEE Transactions on Transportation Electrification* 2.2 (2016) [24]
- V. del Razo, C. Goebel, and H.-A. Jacobsen. "Vehicle-Originating-Signals for Real-Time Charging Control of Electric Vehicle Fleets." In: *IEEE Transactions on Transportation Electrification* 1.2 (2015), pp. 150–167 [25]
- V. del Razo, C. Goebel, and H.-A. Jacobsen. "Reducing Communication Requirements for Electric Vehicle Charging using Vehicle-Originating-Signals." In: *IEEE SmartGridComm.* 2014, pp. 7–12 [26]
- V. del Razo, C. Goebel, and H.-A. Jacobsen. "On the effects of signal design in electric vehicle charging using vehicle-originating-signals." In: *Computer Science-Research and Development* 31.1 (2016), pp. 49–56 [27]

- V. del Razo, C. Goebel, and H.-A. Jacobsen. "Benchmarking a Car-Originated-Signal Approach for Real-Time Electric Vehicle Charging Control." In: *IEEE PES ISGT*. 2014 [28]

1.5 Organization

The rest of the document is organized as follows. Chapter 2 provides some background on power systems with a focus on key concepts that may not be evident to computer scientists. Chapter 3 presents the related work on the area of electric vehicles with particular emphasis on power systems support and planning long distance trips.

Chapters 4 and 5 elaborate on the VOS method for EV charging control in residential environments. Chapter 4 first presents the model, describes the VOS approach, and introduces the Munich use cases that our evaluation is based on. Then, it introduces a centralized state-of-the-art optimization method and uses it as a baseline to evaluate the performance of the VOS approach. Finally, it presents a statistical analysis of the performance and corresponding findings.

Chapter 5 presents two extensions to the VOS method. First, it introduces a message reduction strategy and corresponding results. Then, it explores alternative signal designs and their corresponding effects. Finally, it presents a discussion of the VOS approach and its different extensions.

Chapter 6 covers the scheduling of fast EV charging on highways. First, it introduces the charging scheduling algorithm for travel time minimization. Then, it describes the simulation framework including a method for data-driven traffic generation. Next, it introduces the use-case for the highway A9 in Germany from Munich to Berlin and corresponding results. Finally, it presents a discussion of EV charging on highways.

Chapter 7 presents the conclusions covering both the VOS approach for EV charging control for residential environments and the fast EV charging scheduling strategy for highway environments.

Chapter 2

Background

The main function of an electric power system is to convert and transport energy. That is, to convert energy from naturally available sources into electricity and transmit this electricity to the location where it is to be consumed. At the consumption point, electrical energy is almost always converted into a different form to be consumed such as light, heat, or mechanical energy. Energy in electrical form can be transported and controlled in a simple and highly efficient and reliable manner [6].

In this chapter, we briefly cover the main concepts and elements in power systems. First, we cover the characteristics, structure, and main elements of electric power systems. Next, we briefly introduce the concepts of renewable energy and distributed generation. Finally, we cover some important concepts in power system operation and control.

2.1 Power System Characteristics and Structure

Electricity can be generated and consumed in direct current (DC) or alternate current (AC) form. DC implies that the current flow is constant in magnitude and flows in one direction. AC implies that the current flow oscillates in magnitude and direction.

Power systems are mostly AC based due to technical and historical reasons. Between the end of the 19th and beginning of the 20th century, AC became the standard for power systems because voltage level transformation was easily achievable through the use of transformers and AC generators and motors were simpler and less expensive to build [6]. Today, due to the technological progress in power electronics, high voltage DC (HVDC) transmission is becoming increasingly attractive for a number of applications, particularly for large amounts of power transmission over long distances.

Some characteristics of electricity supply have a significant effect on how the electric power system is engineered [29]. First, electricity, unlike gas and water, is difficult and expensive to store and there is little control possible on the consumption side. Therefore, balancing electricity supply and demand is one of the major challenges in power systems. Second, electricity generation has a significant environmental impact that increasingly determines what, how and where power plants are installed and operated. Third, generation plants are often far from the loads.

Electric power systems may also vary in size and structure, although most of them share the following characteristics [6].

- They are comprised of three-phase AC system,
- they produce most of the electricity via synchronous generators,
- they transmit power over long distances to widely spread consumers, and
- they operate at constant frequency and voltage.

Large AC power systems are generally three-phase systems. Put simply, this means that each generator provides three voltage sources with a given phase difference between them. This phase difference can be interpreted as some kind of delay between the voltage signals. A three-phase generator is built utilizing three separate conductors for the stator windings. The three-phase principle enables a higher power capability for a given machine size. Additionally, three-phase systems allow for a more efficient transmission and ensure that electric motors always run in the same direction, provided that phases are connected in the same order [29].

Prime movers convert a primary source of energy (e.g., fossil, nuclear, or hydraulic) to mechanical energy. This mechanical energy is converted into electrical energy by (commonly synchronous) generators [6].

The total electrical load usually consists of a base plus a variable element which depends on factors like the time of day, season, weather, etc. Generally, the base load is supplied by the most efficient (lowest operating cost) plant running continuously while the remaining load is met by the less efficient, but less capital-intensive, stations. For hydro systems some generators are only operated during times of peak load. In a power system there is a mix of sources. These include, hydro, coal, oil, renewable, nuclear, and gas. A system operator decides on the power supplied by the different plants in order to achieve an optimal mix, which generally means the most economic operation [29].

A certain proportion of the available generation capacity has to be held as reserve to meet sudden contingencies. A part of this reserve, called the spinning reserve, must be ready to be brought in immediately. This is commonly achieved by operating machines below their maximum capacity. Spinning reserves can be used to cope with errors in prediction of the load or the output of renewable energy sources. A higher proportion of intermittent renewable energy generation, such as solar or wind, increases the required reserve margin [29].

The transmission network in electrical power systems interconnects generating stations and loads. This transmission network consists of the transmission, subtransmission, and distribution systems [6].

The transmission system interconnects major generation sites with main load centers or hubs and operate at the highest voltage levels. Generators usually produce lower voltages (11-35 kV) which are then increased by transformers to the main transmission voltage (230 kV and above) [6].

Higher voltages allow for longer transmission distances with lower losses. However, there is a maximum permissible peak voltage between conductor and ground. Higher voltages require more clearance between the lines and the ground and this relationship is non-linear [29]. Therefore a transmission system usually operates on different

voltage levels.

The subtransmission system connects transmission substations with distribution substations. Some large industrial consumers may be supplied directly from this system. In many power systems, there is no clear separation between transmission and subtransmission systems. When the system expands, higher voltages become necessary and previously transmission-exclusive sections are assigned to subtransmission functions [6].

The distribution systems differ from transmission systems in ways beyond the voltage levels. The number of branches and sources is significantly higher and the general topology is different. Furthermore the way distribution networks are structured and designed depends on whether they are serving rural, suburban, or urban areas [29].

Electricity consumers are generally classified as industrial, commercial, and residential [29]. Industrial loads are lower in quantity but usually power intensive and often consume electricity in three-phase, e.g., three-phase electric motors. Residential and comercial loads generally consume electricity in single phases. The commercial sector refers to shops, schools, offices, and so on.

Although the general form of power systems follows a similar pattern, there are differences in voltage levels, topologies, and operation originating from geographical, historical, and political reasons. In continental European countries, combined generator/transmission utilities (usually covering the whole country and overseen by government control) have been, or are being, separated into generation, transmission, and distribution entities. These entities are individually accountable and allow for private investors to enter the electricity market. Energy is traded under agreed tariffs between national boundaries through interconnects. Due to the dominance of industrial loads with the ability to vary demand and a lower reliance on electricity for heating in private households, daily load variation tends to be lower where compared to the UK, for example. A number of German and Scandinavian cities use combined heat and power (CHP) plants with hot water distribution mains for heating purposes. Transmission voltages are 380-400, 220, and 110 kV and household are supplied at 220-230 V, commonly with a three-phase supply taken into the house [29].

2.2 Renewable Energy and Distributed Energy Generation

Renewable energy sources are an alternative to reduce CO2 emissions. Many of these energy sources come, at least indirectly, from the sun: wind, waves, tides, and solar energy. These renewable sources of energy are intermittent, depend on external factors such as the weather, and cannot be dispatched or controlled in the same way as traditional power generators. In the following, we will briefly cover solar photovoltaic (PV) and wind energy generation.

Photovoltaic conversion occurs in a thin layer of a specific kind of material, such as silicon, where hole-electron pairs are created by incident solar photons. The separation of these holes and electrons at a discontinuity in electrochemical potential creates a potential difference. This technology is space-intensive. For an output in the order of MWs, a very large area is required [29].

Wind energy is produced when the wind causes the rotor of a wind turbine generator to rotate. The power produced depends on the swept area and the cube of the wind speed and is limited by the power coefficient factor of the rotor. At high wind speeds, the output can be controlled by modifying the blade pitch angle. A single large wind turbine can produce around 5 MW [29].

Wind and photovoltaic solar generation produce a lower amount of power compared to traditional sources and have specific geographical requirements. As a result, the generation occurs in a more disperse manner and at lower volumes. This is known as distributed generation (DG).

DG also implies that power may no longer be exclusively fed into the power system via the transmission system. Large conventional power stations feed power into the transmission or subtransmission networks which are designed for bidirectional power transport. However, distribution systems are designed for unidirectional power transport; that is, toward the consumers [30].

2.3 Power System Design and Operation

Power systems are designed and operated to meet the following requirements [6]:

- keep the power quality with regard to constant frequency, constant voltage, and level of reliability,
- meet continuously changing load demand for active and reactive power, and
- supply energy at minimum cost and with minimum ecological impact.

Constant frequency and voltage are not only power quality indicators but also a measurement for the demand-supply balance of active and reactive power respectively.

The allocation of the required power amongst the generators is generally decided before the load appears and is based on a given prediction of the load. In order to meet continuously changing load demand, the system must be able to compensate for the differences between the predicted and the actual load. Synchronous generators in a power system are connected through the transmission system and have the same frequency [29]. If the load is larger than the committed generation, the frequency will decrease and vice versa. By applying frequency control, one can maintain this balance by increasing or decreasing the generation or, more seldom, the consumption of active power. Generation can be controlled by modifying the output of a given generator, usually by controlling the prime movers, or dispatching additional resources.

Voltage stability means that a power system is able to maintain steady acceptable voltages along the system. The main reason for voltage instability is the inability of the power system to meet the demand for reactive power. This is mostly caused by the voltage drop resulting from the power flowing through inductive reactances. Voltage instability is essentially a local phenomenon but with potentially wider impact. Methods for voltage control include sources or sinks of reactive power (e.g., capacitors, reactors, and condensers), line reactance compensators (e.g., series capacitors), and regulating transformers (e.g., tap-changing transformers) [6]. Increased PV solar generation at the distribution network has also significant effects on voltage.

An important tool to analyze the operation, power, voltages, and losses in the power system is the power flow or load flow. The power flow is a network solution tool that provides currents, voltages, and real and reactive power flows at every bus in the system. It represents the electrical response of the transmission or distribution system to a given set of loads and generator power outputs. The most common method for solving the power flow calculation is the Newton–Raphson method [31].

Power systems must also be operated on an economic way. That is, energy must be supplied at the lowest possible cost that allows a certain set of constraints to be met. Generally, generators cannot instantly turn on and produce power, so generation must be planned in advance. Three main concepts relate to the economic operation of power systems: economic dispatch, unit commitment, and optimal power flow; each of them being more comprehensive than the previous.

Real power economic dispatch (ED) aims at minimizing the generators fuel consumption or the overall operating cost of the system. This is done by determining the power output of each generating unit so that the system load demand is met. The main elements of the ED problem are the set of input–output characteristics of each power generating unit. That is, a fuel consumption or an operating cost function [31].

Unit commitment (UC) manages the generation schedule of each unit in a power system for minimizing operating cost and satisfying prevailing constraints. e.g., load demand and system reserve requirements, over a set of time periods. The classical UC problem aims at determining the start-up and shutdown schedules of thermal units to meet the forecast demand over certain time periods. It is a combinatorial optimization problem. The methods for solving the UC problem can be classified into heuristic search, mathematical programming, and hybrid methods [31].

The objective of optimal power flow (OPF) is to find the optimal settings of a given power system network that optimizes objective functions, e.g., generation cost, system losses, voltage deviation, emissions, number of control actions, while satisfying the power flow equations, system security, and equipment operating limits. Control variables include generator real power outputs and voltages, transformer tap changing settings or switched capacitors. The mathematical formulation of the

OPF problem depends on the selected objective function and constraints (i.e., linear, non-linear, integer). The algorithms can be classified into conventional optimization methods, intelligence search methods, and non-quantitative approaches [31].

Chapter 3

Related Work

The effects of increased renewable and distributed generation and their potential solution have been a subject of numerous studies. Similarly, a number of studies related to transportation electrification (either as a challenge factor or a solution alternative) and power systems have been conducted. A survey on transportation electrification in smart grid environments has been conducted by Su et al. [32]. Gungor et al. [33] survey potential smart grid applications and corresponding communication requirements.

Renewable generation and new types of electric loads are particularly challenging for the distribution network level. For example, Woyte et al. [34] studies voltage fluctuations caused by photovoltaic generation. The impact of EVs on the electricity distribution network has also been extensively studied [35, 36, 37].

In this chapter, we first present the related work on EV charging control for supporting the power system. That is, either as means to reduce the effects of EV themselves, to facilitate integration of renewable energy sources, or to provide additional services like storage or regulation. We then cover the previous work in the area of EV charging in long distance trips.

3.1 EV Charging Control for Power Grid Support

The related work in the area of EV charging strategies can be classified based on system architecture (centralized/decentralized) and control method (direct/incentive-based). In centralized architectures, all variables and constraints are known to a central controller, whereas in distributed architectures, there is usually a differentiation between local and global (or coupling) constraints and variables. Local parameters are known to each controlling entity. Global parameters, on the contrary, depend on the overall behavior of the system and need to be communicated to each control entity. In direct control methods, the controlling entity triggers a certain action on the controlled entity. In incentive-based methods, the controlling entity sends a signal for which a certain action by the controlled entity is expected.

As decentralized incentive-based methods, for instance, Gan et al. [38] propose a decentralized algorithm that controls EV charging to fill demand valleys via incentive signals, and Rivera et al. [13] present a framework for incentives-based distributed EV charging control for different objectives. These studies show how the optimization problem can be solved in a distributed fashion. Incentive signals are used to decouple the global constraints from the local problem, where a coordinating entity broadcasts an incentive signal, e.g. a virtual price, and iteratively updates it according to the response of the EVs.

In terms of decentralized, direct control methods, He et al. [39] present a decentralized optimization with direct control to minimize charging costs, Richardson et al. [40] present a local direct control technique for voltage stability in a DN, Rotering et al. [41] present a dynamic programing approach with local controllers fed with energy market information, Martinenas et al. [42] apply linear programming local control to minimize charging costs for a dynamically updated composite price signal that combines real-time hour- and day-ahead prices, and Binetti et al. [14] use an updated power profile for EVs to locally define the charging starting time. These approaches opt for local control, where EVs optimize for their individual objective taking into account global variables like voltage levels or energy prices.

Furthermore, Galus et al. [15] present a decentralized direct control method that

also includes other flexible loads where local managers, which are then connected to an aggregator, are used to hierarchically divide the problem. In a study by Yao et al. [16], a hierarchical decomposition approach is also used. In the high-level, generator units and a number of EV aggregators are jointly dispatched. This results in a low-level problem for each aggregator that is then solved as a mixed integer problem.

Centralized control methods usually apply direct control. For instance, Clement-Nyns et al. [43] aim at minimizing power losses with a centralized, direct control approach, and Goebel et al. [17] evaluate the supply of frequency reserves via centralized and direct EV control. Still, some other combinations are possible. For example, to optimize centrally for the planning phase in order to define either a price or a profile signal, and then apply local optimization for the control [44].

Centralized optimization methods face the challenge of scalability as the size of the problem increases. Distributed optimization approaches can be used to address scalability limitations, but implementing such solutions could be challenging, mostly due to their iterative nature and high communication overhead. Instead, the VOS approach uses heuristics to speed up the solution, distributes the computation by enabling EVs to encode VOS signals, and applies a centralized control. The VOS approach offers a solution where computation and communication overhead are a concern, while some deviation from the results achievable by state-of-the-art solutions is acceptable.

Alternatively, one can address the scalability challenge by optimizing for the aggregated EV load [12, 45]. In the former, EVs are clustered into a single integer variable that can take on values proportional to the number of EVs, whereas in the latter they are grouped by arrival and parking times. EVs can also be grouped for solving the mixed integer low-level problem [16]. Clustering, however, requires a second mechanism to control the individual EVs. The VOS approach controls vehicles individually and such a second mechanism is not required.

There are also incentive-based approaches for social optimality based on stochastic optimization and game theory [46, 47]. Although we don't aim at a social optimum, where there is no solution with a higher benefit for one entity that does not decrease

the benefits of the other parties, the VOS approach achieves a fair resource allocation. It assigns resources based on the individual requirements with respect to the total availability. In Section 5.2, we further explore these concepts for alternative signal designs.

The concept of a single broadcast signal is present in some incentive-based approaches [38, 13]. The idea of broadcasting a set point signal paired with a probability factor is explored by Harris et al. [48]. These concepts allow for the reduction on message requirements from the aggregator to the EVs. In Section 5.1, we build on these concepts for reducing the aggregator-to-EVs message requirements and exploit the modular characteristic of the VOS approach to also reduce the EVs-to-aggregator message requirements.

Similar to Kempton et al. [49], we consider Vehicle-to-Grid (V2G), however, in our case, the economic and market aspects are beyond the scope of the work.

3.2 EVs and Long Distance Trips

Research on EV charging has focused on its relationship with the power systems infrastructure, mostly in urban or suburban environments. Highway-related problems of EV charging have not been as densely studied.

EV highway-related work has focused on infrastructure planning and charging strategies. A number of studies have been focusing on placement of CS infrastructure along a highway. Some studies conclude that driving range is a major factor for defining CS infrastructure location, with facility cost and population coverage also playing an important role [50, 51]. Sathaye et al. [52] introduce a continuous optimization approach for locating charging stations on highway corridors with a case study for Texas. Furthermore, other studies take existing infrastructure into consideration and limit potential CS locations to existing rest areas or fuel stations [53, 22]. Different charging power rates are analyzed concluding that fast-charging is necessary to achieve a reasonable level of service and minimize the cost [54]. Bae et al. [55] aim at modeling charging demand using a fluid dynamic traffic model for

arrival rates at different CS and a M/M/s queue model for the demand within the CS with focus on infrastructure planning and energy demand. In contrast, our work considers fast-charging infrastructure located on existing rest areas or fuel stations and uses data-based synthetic highway trips for generating the charging demand.

In terms of modeling and charging strategies, Gong et al. [56] use a gas-kinetic model to optimize power management with dynamic programing. This work focuses on hybrid vehicles and fuel consumption. Rahman et al. [57] also focus on hybrid vehicles and fuel consumption where a method based on Satisfiability Modulo Theories (SMT) and a price-based navigation technique for load balancing are presented. A dynamic allocation technique using a centralized control platform that focuses on maximizing infrastructure utilization has also been presented [22]. Our approach considers only battery-based EVs and focuses on travel time, not on consumption or infrastructure utilization.

Yang et al. [20] compare global vs. local information strategies for a highway in Taiwan with 6 CSs and an event-based model. They conclude that having global information about CS workload helps to reduce waiting times. Qin et al. [21] also aim at minimizing waiting time. They show that a theoretical lower-bound is achieved when the charging demand of all CSs is balanced and propose a distributed strategy based on CS reservation which follows certain success statistics. We also make use of a CS reservation system but account for changes via dynamic updates.

A balanced CS demand is also considered the optimal strategy and a two-level approach is proposed by Gusrialdi et al. [23]. The higher-level distributed scheduling algorithm optimizes the operation of the charging network while the lower level cooperative control law allows individual EVs to decide whether or not to charge based on neighboring EVs. The approach requires communication between EVs to cooperate, is based on a stochastic model for CS arrivals, and is applied to an example with four CSs. In our work, the objectives are local to each EV but EVs loosely interact with each other through estimates of CS occupancy levels as coupling variables.

Pourazarm et al. [58] address the scheduling problem as a path-finding problem within a graph of CS nodes. They use dynamic programming and, when dealing

with multi-vehicle routing, apply a grouping technique based on flows. Similarly, Storandt et al. [59] uses a graph model and considers the problem as a constrained shortest path problem. The work concentrates more on urban environments where the number of paths can be very large and the number of CS visits is given as a constraint. The authors propose a pre-processing approach for saving computations. We also formulate the problem as a shortest path problem but use a modified A* algorithm focusing on total travel time.

Highway traffic modeling is a complex field with several approaches available depending on the level of detail provided and the information available [60, 61]. In our simulation framework, we do not apply complex inter-vehicular dependencies or gas-kinetic-based flow simulations. However, we foresee the use of more robust and mature traffic simulation systems as an input for our framework in the form of time-variant highway speeds.

Our approach differs from previous work in several ways. First, we use a close-to-reality evaluation in a real highway scenario with data-based traffic generation, full length highway, and a large number of CSs. Second, we consider the total travel time reduction as the objective function, accounting for driving and charging times in addition to waiting time. Last, we consider a local EV-centered approach with limited computation and communication requirements, which indirectly accounts for other EVs through a CS reservation system.

From the evaluation perspective, our work is based on data-based generated trips whereas related work either allocates EVs randomly along the highway [22], or uses a stochastic (mostly Poisson-based) model [20, 21, 23]. Similar to Bodet et al. [22], we consider CS sites at rest and fuel stations along the highway and use a German highway as a use-case. We also consider different types of EVs and variable speeds along the highway.

From the scheduling perspective, we focus on time reduction. However, our focus on total travel time reduction, not only waiting time, is advantageous under varying highway conditions. Similar to Pourazarm et al. [58], we adjust charging time to energy requirements. Time-variant driving speed, mostly limited by highway speeds, is also taken into account.

Finally, our work focuses on applicability. We do not use centralized control and focus on individual EV optimization. Communication only takes place between specific CSs and the EV without the need to provide all trip information. Although we do not aim at a global optimization (e.g., [20, 23]), we indirectly account for the behavior of other EVs by using the CS reservation information as a coupling variable. Similar to other studies [58, 59], our model is based on a graph abstraction and shortest-path search but we focus on algorithms with complexities achievable by existing in-car navigation technologies.

Chapter 4

EV Charging Control with VOS

In this chapter we present the EV charging control problem for supporting the power system and the proposed solution. This solution, the Vehicle-Originating-Signals (VOS) approach for EV real-time charging control, enables an aggregator to control how a fleet of EVs charges in order to follow an arbitrary power profile. The solution takes into account computational, communication, aggregator, and user requirements. Section 4.1 presents the model and describes the VOS approach. Section 4.2 introduces the Munich use cases that our evaluation is based on. Section 4.3, introduces a centralized state-of-the-art optimization method and uses it as a baseline evaluate the performance of the VOS approach. Finally, Section 4.4 presents a statistical analysis of the performance and corresponding findings.

4.1 Model

In this section we introduce the VOS approach. We present the power-matching problem and model. We also discuss the implications of solving this problem with state-of-the-art optimization techniques and cover the assumptions made at system level. Finally, we describe the VOS approach in detail including the roles of EVs and the aggregator.

4.1.1 Power-Matching EV Charging Control

Figure 4.1.1 illustrates the scenario assumed in the following. For a given area of the distribution network and the loads and distributed generation connected to it, the goal of the aggregator is to control the charging and discharging behavior of EVs such that the aggregated power profile matches a target power profile, $P_O(k)$, as closely as possible. The aggregated power profile, $P_{agg}(k)$, is defined as the difference between the demand and the local generation within the defined area, i.e., the total power demanded from the grid at time step k. That is:

$$P_{agg}(k) = P_D(k) - P_S(k) + \sum_{i=1}^{N} P_{EV}^i(k) \tag{4.1.1}$$

where for a given time step k, $P_D(k)$ represents the inflexible demand, $P_S(k)$ denotes the produced solar power, and $P_{EV}^i(k)$ is the power consumed by the i^{th} EV. P_{EV}^i can be negative, meaning that the EV is supplying energy back to the grid (V2G).

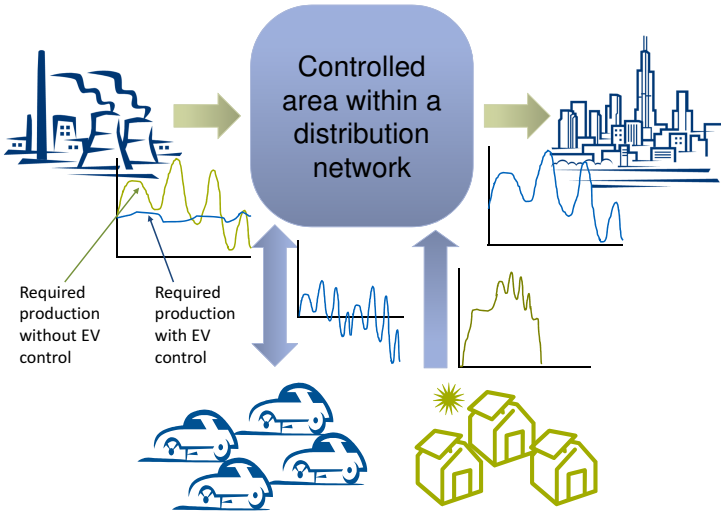

Figure 4.1.1: Model overview

Matching a given target profile is an alternative to dispatching generators to meet the demand. Dispatching generators according to the given demand requires that a certain capacity is kept as reserve and that every new configuration is guaranteed to

meet the constraints of all generators, the transmission, and the distribution grid. By controlling demand to meet a given $P_O(k)$, which has been planned to meet all these constraints, one could enable operators and utilities to use their existing capacity more efficiently and to reduce their operational requirements.

Since we concentrate on a limited section of a distribution network, it is reasonable to assume that the internal generation and loads can be aggregated into a single node.

Our objective is to minimize $|P_O(k) - P_{agg}(k)|$ for all k subject to the set of constraints of each vehicle $\mathbb{X}_{EV^i}$ and the limitations of the electricity distribution network $\mathbb{X}_{DN}$. Using (4.1.1) we can express this problem formally as follows:

$$\begin{aligned} \min_{P^i_{EV}(k)} & \left(P_O(k) + P_S(k) - P_D(k) - \sum_{i=1}^{N} P^i_{EV}(k) \right)^2, \quad \forall\ k \in T \\ \text{subject to} & \\ & P^i_{EV}(k) \in \mathbb{X}_{DN}, \quad \forall\ k \in T \\ & P^i_{EV}(k) \in \mathbb{X}_{EV^i}, \quad \forall\ k \in T, i \in N \end{aligned} \tag{4.1.2}$$

Assuming that the constraints are linear, (4.1.2) is a convex optimization problem that can be solved with state-of-the-art optimization techniques. However, the complexity of this problem increases at least at a polynomial rate of its dimensions [62], which in turn increase with the number of EVs and constraints.

For example, let n be the number of EVs and m the number of constraints. Consider only two constraints per EV, $\sqrt{m}$ iterations (reasonable for interior-point methods [62]) and a complexity of nm^3 per iteration. That results in 11.3 $n^4\sqrt{n}$ for n EVs and $357,770.9\ n^4\sqrt{n}$ for $10n$ EVs, over 31 thousand times higher.

Therefore, we argue that this approach is no longer feasible for large EV fleets, especially if the goal is on-line or real-time control.[1] Furthermore, the linearity of

[1] By real-time, we mean that these are not planning or day ahead decisions, but control decisions that have to be made on the spot with currently available information and before the next control interval starts.

the constrains is not necessarily guaranteed, e.g., EVs may charge at defined power levels and not at infinitesimal fractions of it, like a given power rating or a set of power levels, resulting in discrete variables. Discrete variables lead to an integer programming problem that is significantly more computationally intensive. The VOS approach is an alternative to deal with this issue.

We make three assumptions at the model level. First, we assume that the length of a time step k is significantly larger than the communication delays between elements (milliseconds vs. seconds or minutes) and are therefore not taken into account. Control with delays up to a few seconds is sufficient to cover a wide range of power system control problems [63, 64].

Second, we consider a maximum charging rate P_{EV}^{max}, common to all chargers, i.e., fast charging is not taken into consideration. We see fast charging as a premium service that may be excluded from the control scheme.

Finally, we assume no losses when (dis)charging the battery. This assumption is justified since a charger's efficiency is relatively high, and it is irrelevant for the method since it would only affect the total consumed power and therefore slightly increase the reference $P_O(k)$.

4.1.2 Vehicle-Originating-Signals Approach

In the Vehicle-Originating-Signals (VOS) approach, an aggregator directly controls a fleet of EVs, as illustrated in Figure 4.1.2. At each time step, every connected EV computes a *Need-for-Charge* (NfC) and a *Willingness-to-Supply* (WtS) signal, and sends them to the aggregator. The aggregator collects these signals and returns charging instructions to the EVs. The NfC and WtS signals coexist, meaning that, at a given time, an EV may be willing to either charge or discharge with a given NfC or WtS. The aggregator decides to call on one of these options depending on the resources available and the signal values of other EVs.

This approach has two immediate advantages. First, the NfC and WtS signals

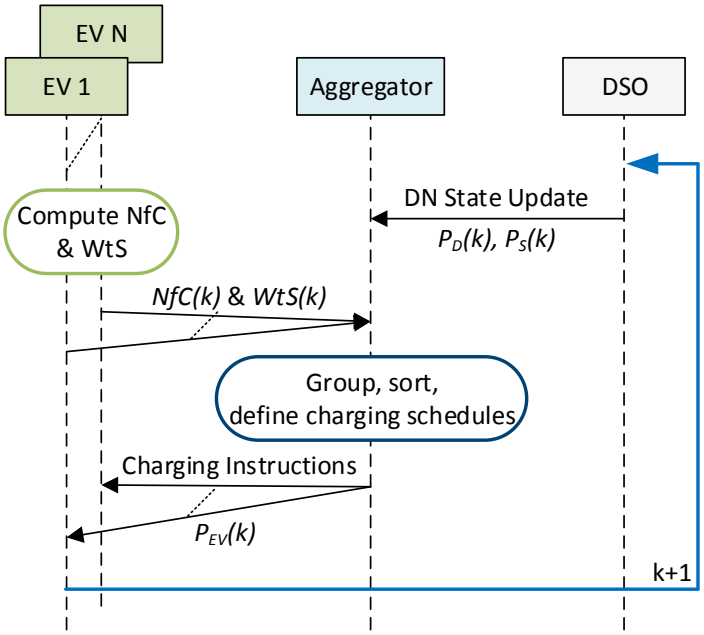

Figure 4.1.2: VOS process overview

are computed by every EV, resulting in high distribution of computation and relatively high preservation of the EV owner's data privacy.[2] Second, by reducing the information exchange to two scalars per time step, we have relatively low communication overhead, especially if compared with distributed iterative methods. Moreover, since the NfC and WtS are computed values, the number of messages can be reduced. This is further explored in Section 5.1.

EV Need for Charge Signal

The NfC is defined as a function of the remaining connection time k_{av}^i and the time required k_{req}^i to reach the desired state of charge (SOC) in percent. A threshold policy makes sure that the EV constraints are fully satisfied. The thresholds are scalars without units.

[2]Only two derived metrics (NfC and WtS) are revealed to the aggregator as opposed to, e.g., parking times, SOC or vehicle objectives and constraints.

For every EV i and time step k, based on its target charge level SOC^i_{tar}, battery capacity E^i_{max}, current energy in the battery E^i_{bat}, allowed charging rate limit per time step E^i_{rate}, and departure time k^i_{dep}, we define the required and available number of steps k^i_{req} and k^i_{av} as:

$$k^i_{req} = \frac{SOC^i_{tar} E^i_{max} - E^i_{bat}}{E^i_{rate}} \tag{4.1.3}$$

$$k^i_{av} = k^i_{dep} - k \tag{4.1.4}$$

where k^i_{req} can take non-integer values. The departure time k^i_{dep} can be either a time set by the user or an expected departure time resulting from a statistical calculation. In the use case in Section 4.2, we assume it is given. Also, E^i_{max} is specific to EV i, therefore, different battery capacities to account for different models or battery degradation over time are also possible.

We then define the thresholds $C_{QoS} > C_{tar} > C_{full}$, where C_{QoS} indicates that the EV *must* charge to reach SOC^i_{tar}, C_{tar} indicates that the EV has reached SOC^i_{tar}, and C_{full} indicates that the EV's battery is fully charged.

We define the NfC as:

$$\mathrm{NfC}^i(k) = \begin{cases} C_{QoS}, & \text{if } C_{QoS} \leq \mathrm{NfC}^i_{temp} \\ \mathrm{NfC}^i_{temp}, & \text{if } C_{tar} \leq \mathrm{NfC}^i_{temp} < C_{QoS} \\ C_{tar}, & \text{if } \mathrm{NfC}^i_{temp} < C_{tar} \\ C_{full}, & \text{if } E^i_{bat} = E^i_{max} \end{cases} \tag{4.1.5}$$

where

$$\mathrm{NfC}^i_{temp} = C_{QoS} \frac{k^i_{req}}{k^i_{av}} \tag{4.1.6}$$

EV Willingness to Supply Signal

For the computation of the WtS, we consider the thresholds C_{maxS} indicating the maximum willingness, and C_{noS} indicating that this EV is not willing to supply at all, where $C_{maxS} \gg C_{noS}$. For a given EV i and time step k, the WtS is a function of the available time k^i_{av}, the departure time k^i_{dep}, and the current SOC^i. To set the WtS within its thresholds, we scale it by C_{maxS} and shift it by C_{noS}, resulting in:

$$\mathrm{WtS}^i(k) = \begin{cases} C_{noS}, & \text{if } E^i_{bat} \leq E^i_{min} \text{or } k^i_{av} \leq k^i_{req} \\ C_{maxS} SOC^i \frac{k^i_{av}}{k^i_{dep}} + C_{noS}, & \text{otherwise} \end{cases} \tag{4.1.7}$$

The Aggregator

At each time step, the aggregator receives the NfC and WtS signals from the EVs, defines a charging strategy and instructs the EVs to charge accordingly. The process is described in Algorithm 4.1.1.

To be realizable in real-time, EVs and aggregator must complete this process in sufficiently less time than the duration of one time step k. Each EV needs to compute two scalars and implement the charge/discharge action. Since this is done separately by each EV, its role in the solving time is negligible. The aggregator, however, performs up to two sort operations and processes each EV's signal. Therefore, the solving time depends on the number of EVs and its upper bound is proportional to the fleet size N. In Section 4.3, we show that this relationship is linear.

Although this approach does not ensure the best feasible solution for the sum of $|P_O(k) - P_{agg}(k)|$ over time, this process does minimize $|P_O(k) - P_{agg}(k)|$ on every time step k. Furthermore, we can provide conditions for an upper bound as follows.

Let N_k be the set of EVs plugged in time step k. Let N^Q_k, N^T_k, and N^F_k be the subset of N_k of EVs with $\mathrm{NfC}(k) = C_{QoS}$, C_{tar}, and C_{full}, respectively. Finally, let N^S_k be the subset of EVs with $\mathrm{WtS}(k) = C_{noS}$. Using these definitions, the following conditions can be formulated:

$$P_{EV}^{max} N_k^Q \leq (P_O(k) - P_D(k) + P_S(k)) \tag{4.1.8}$$

$$0 \leq (P_O(k) - P_D(k) + P_S(k)) \leq \tag{4.1.9}$$

$$P_{EV}^{max}(N_k - N_k^T - N_k^F) + \sum_i^{N_k^T} \min(P_{EV}^{max}, E_{max}^i - E_{bat}^i)$$

$$-P_{EV}^{max}(N_k - N_k^Q - N_k^S) \leq (P_O(k) - P_D(k) + P_S(k)) \leq 0 \tag{4.1.10}$$

Let RES_P be the resolution or smallest possible increment of P_{EV}, which can be at most P_{EV}^{max}. The resolution RES_P is an upper bound to $|P_O(k) - P_{agg}(k)|$ if, either conditions (4.1.8) and (4.1.9), or conditions (4.1.8) and (4.1.10) hold. In other words, $P_{agg}(k)$ converges to $P_O(k)$ as long as the power requirements of those EVs with $\text{NfC} = C_{QoS}$ do not exceed $P_O(k) - P_D(k) + P_S(k)$ and if there are enough EV resources to consume or supply this amount of energy. The choice of $P_O(k)$ must take these feasibility constraints into account.

Algorithm 4.1.1

Algorithm 4.1.1: Aggregator

1. $P_{agg}(k) \leftarrow P_D(k) - P_S(k)$
2. **Sort** EVs by NfC in descending order
3. **While** $P_{agg}(k) < P_{agg}^{max}$ and NfC $= C_{QoS}$
   - Charge EVs with NfC $= C_{QoS}$
4. **If** $P_{agg}(k) \leq P_O(k)$
   (a) $S \leftarrow$ **Select** EVs with $C_{full} <$ NfC $< C_{QoS}$
   (b) Charge EVs
   - Continuous case:
     (Allocate available power to EVs proportional to NfC)
     For EV i in S:

$$P_{EV}^i \leftarrow \min\left(P_{EV}^{max}, \frac{\text{NfC}^i}{\sum^S \text{NfC}^i}\left[P_O(k) - P_{agg}(k)\right]\right)$$

$$P_{agg}(k) \leftarrow P_{agg}(k) + \sum^S P_{EV}^i(k)$$

   - Integer case:
     (Allocate available power to EVs with highest NfC)
     For EV i in S:
     If $P_O(k) \leq P_{agg}(k)$, **Break**
     $P_{EV}^i \leftarrow P_{EV}^{max}$
     $P_{agg}(k) \leftarrow P_{agg}(k) + P_{EV}^{max}$
5. **Else** (meaning $P_O(k) < P_{agg}(k)$)
   (a) **Sort** remaining EVs by WtS in descending order
   (b) $S \leftarrow$ **Select** EVs with WtS $> C_{noS}$
   (c) Discharge EVs
   - Continuous case:
     (Allocate required power to EVs proportional to WtS)
     For EV i in S:

$$P_{EV}^i \leftarrow \min\left(P_{EV}^{max}, \frac{\text{NfC}^i}{\sum^S \text{NfC}^i}\left[P_O(k) - P_{agg}(k)\right]\right)$$

$$P_{agg}(k) \leftarrow P_{agg}(k) + \sum^S P_{EV}^i(k)$$

   - Integer case:
     (Allocate required power to EVs with highest WtS)
     For EV i in S:
     If $P_{agg}(k) \leq P_O(k)$, **Break**
     $P_{EV}^i \leftarrow -P_{EV}^{max}$
     $P_{agg}(k) \leftarrow P_{agg}(k) - P_{EV}^{max}$

4.2 Munich Scenario

In this section we introduce the scenario that is used for the evaluations of this work. The VOS approach can be used to make the aggregated demand follow arbitrary target profiles. Our main use case focuses on a *constant* power profile $P_O(k) = P_O$, which results in load leveling, where the target P_O is ideally the average of $P_{agg}(k)$ over time. In addition, we define two supplementary use cases with a variable $P_O(k)$ to illustrate the validity of our approach under these conditions.

A constant power profile has two desirable effects. First, renewable energy is consumed locally, assuming the renewable generation capacity is below the desired P_O. Second, generation can be planned more efficiently since the aggregated demand of the controlled area is less variable over time. In other words, non-renewable resources operate at constant levels for long periods. This results in fewer ramping events and lower requirements for reserved capacity, which brings environmental and economical advantages. Yet, in a more realistic scenario, one would need to account for transmission-level renewable generation to achieve the same effect. That is, the target power profile would be the sum of the planned output of non-renewable generation plus the renewable generation at the transmission level. This is not within the scope of our work.

The evaluation presented in this work is based on actual data provided by Munich's distribution system operator (DSO) [65] and the official mobility survey conducted by the German government [66].

The Munich DSO supplies yearly information on a 15 min granularity. We take the load and distributed intake (reflecting local solar generation) data for the low voltage level and select a 24 hour period starting on a given date at noon, such that the considered time period spans an entire night. Then, we scale the load profile by F_{demand} to obtain a demand magnitude manageable by the intended EV fleet size, e.g., 3% of Munich's demand for fleet sizes of 1,000-20,000 EVs. Finally, we use the same factor for scaling the solar generation data and multiply the resulting solar profile by F_{solar} to mimic a higher solar penetration.

The mobility survey includes data for all of Germany. We filter data from major cities (>500k inhabitants) in order to get a data set valid for Munich and large enough to be representative. Additionally, we apply a set of quality assurance rules to ensure that: the interviewed person is the driver, the used vehicle belongs to the household, and the average reported speeds are lower than 120 km/h. For workdays (Monday-Thursday), that amounts to around 1,800 trips from 500 households. In our experiments, we select entries for workdays and up to three vehicles per household to build N vehicle driving profiles. These profiles include parking times, driving times, and driving distances. Driving distances are used to calculate the EVs consumption while driving and the corresponding battery SOC at arrival.

If the size of the fleet N we want to generate is higher than three times the number of trips available, we introduce a random Gaussian noise to the starting time and trip duration and adjust the remaining parameters, e.g., arrival time, parking time, SOC at arrival, etc., accordingly. This noise has mean zero, a standard deviation of 15 minutes, and is restricted to a maximum of 1 hour. By adding this random noise, we are able to generate driving profiles for large fleets with a lower probability of repeated profiles.

We run simulations for varying fleet sizes, keeping the rest of the parameters constant. We use a time step $\Delta t = 15$min that matches the granularity of our data. For the simulation, we consider a homogeneous fleet of EVs with $SOC_{tar} = 85\%$, battery maximum and minimum capacities of $E_{max} = 16$kWh and $E_{min} = 1$kWh, and charging power $P_{EV} = 4$kW. A homogeneous fleet allows us to isolate the driving profiles as the main random events without loosing generality. Different SOC^i_{tar} or E^i_{max} influence the fleet's power requirements and therefore the target P_O, not the validity of the method.

Furthermore, we assume that the EVs charge only at home and are plugged in only once (during the longest parking period). The last assumption implies a more realistic scenario where users only plug in the EV once their driving day is over rather than every time they park at home.

The ideal value for P_O is the average of $P_{agg}(k)$ over the day. $P_{agg}(k)$ depends on the EV power requirements, which correspondingly depend on driving and parking times.

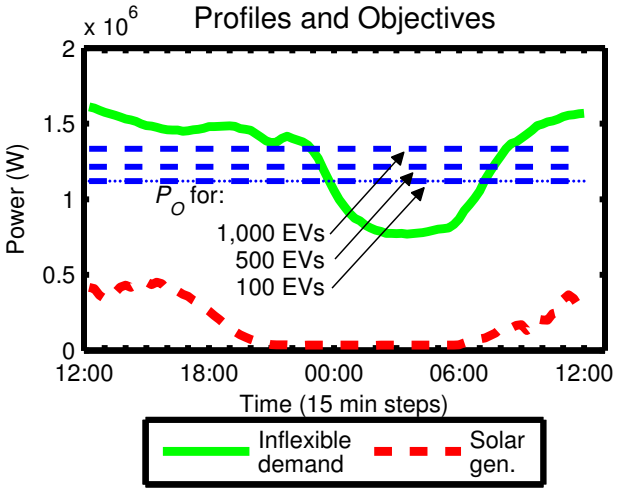

Figure 4.2.1: Demand, solar and target power profiles

Since these values are not known in advance, an estimate of these requirements is needed.

For the EV power requirements estimate, we first define the realistic SOC^i_{tar} from a sample fleet. This SOC^i_{tar} is either the maximum achievable SOC considering the connection time or the general target (85% in our case). To this value we then add two thirds of the difference between the target and the full SOC, calculate the required energy based on the initial SOC and average it over time. The result is the average power requirement per time interval for an EV in the fleet. The power requirements of a given fleet are estimated by multiplying this average times the fleet size. In practice, the EV consumption would come from actual measurements and statistical or empirical studies. Figure 4.2.1 shows the inflexible demand, solar generation and target power P_O for different EV fleet sizes.

For the evaluation of the VOS approach for variable power profiles in Section 4.4, we make some modifications to the scenario presented above. First, we define a demand-following and a valley-filling case. The demand-following case aims at keeping the same behavior of the inflexible demand. The valley-filling case aims at shifting more of the load towards the regions with lower inflexible demand. Then, we combine EV power requirement estimate with the solar generation to calculate the expected average additional power requirements. Finally, we allocate these additional power

requirements along the inflexible demand curve to produce the target $P_O(k)$. For the demand-following case, we distribute the power requirements uniformly. In other words, $P_O(k)$ is a shifted version of the inflexible demand. For the valley-filling case, we allocate the additional power requirements so that more power is consumed during the valley period and less during the peak period.

4.3 Benchmarking the VOS approach

In this section the VOS approach is compared with a a state-of-the-art centralized optimization in terms of error performance and solving time. We describe the optimization used for the benchmark followed by the corresponding results.

4.3.1 Benchmark

We formulate the problem as a centralized optimization with a quadratic objective function. Additionally, we define a continuous and a mixed-integer optimization to account for different types of decision variables $P_{EV}^{i,k}$. For each case, we also consider complete and partial EV information availability upon solution time.

We use Matlab[67] and Yalmip[68] to model the problem. We do not expect any tool-specific bias since we only measure the solver's solving time and use Gurobi[69], a state-of-the-art solver, to solve the optimization problem.

In the notation below, we use indexes i, k to refer to EV and time step, respectively. The optimization problem is defined as:

$$\min_{P_{EV}^{i,k}} \left\| P_O^k + P_S^k - P_D^k - \sum_{i=1}^{N} P_{EV}^{i,k} \right\|_2^2 \tag{4.3.1}$$

s.t.

$$-D_P^{i,k} P_{EV}^{max} \leq P_{EV}^{i,k} \leq D_P^{i,k} P_{EV}^{max} \tag{4.3.2}$$

$$\text{diag}(SOC^i)E^i_{max} \leq E^i_o + \sum_{k=1}^{T} P^{i,k}_{EV}\Delta t \leq E^i_{max} \tag{4.3.3}$$

$$E^i_{min} \leq E^i_o + B^{k,k}P^{i,k}_{EV}\Delta t \leq E^i_{max} \tag{4.3.4}$$

$$P^k_{agg} = P^k_D - P^k_S + \sum_{i=1}^{N} P^{i,k}_{EV} \tag{4.3.5}$$

$$0 \leq P^k_{agg} \leq P^{max}_G \tag{4.3.6}$$

where P^k_O is a vector containing the constant P_O on every element. $D^{i,k}_P$ is the driving profile matrix containing ones for each EV i connected at time step k. P^{max}_{EV} is the maximum (dis)charging rate assumed equal for all EVs. Vectors E^i_{min}, E^i_{max} and E^i_o are the minimum/maximum allowed and initial state of charge of EV i's battery. The vector SOC^i indicates the target state of charge of EV i, and Δt is the time step size. $B^{k,k}$ is a lower triangular matrix that, combined with the charging profile matrix $P^{i,k}_{EV}$, indicates the state of battery charge at every time step.

We want to minimize the deviation of the aggregated power profile from a reference profile (4.3.1) subject to a maximum (dis)charging power per EV, per time step (4.3.2), ensuring that the EV's battery is at least at a certain SOC when departing (4.3.3), where batteries should remain within their allowed energy levels at all times (4.3.4), and the total power consumption does not exceed a given threshold (4.3.5-4.3.6).

Equations (4.3.1-4.3.6) refer to the continuous problem. To convert this into the mixed-integer case, one has to change (4.3.2) so that $P^{i,k}_{EV}$ can only take the values $\{-P^{max}_{EV}, 0, P^{max}_{EV}\}$.

Clairvoyant Benchmark

In the complete information or clairvoyant case, we assume that all the required information for the considered period T is known ex-ante. This information includes P_D, P_S, and driving profiles for the entire EV fleet. Therefore, we only need to perform the optimization once, and the result is valid for every time step k until T. This benchmark yields the best possible solution in terms of performance.

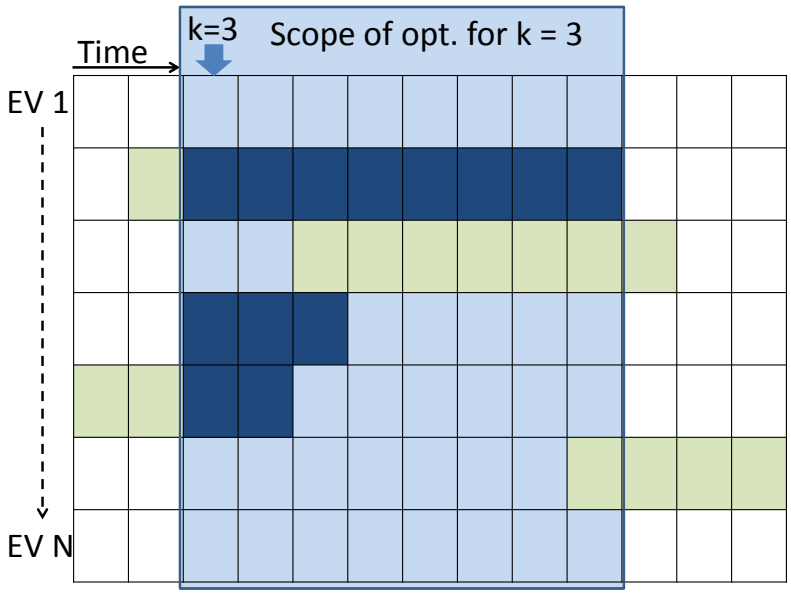

Figure 4.3.1: Building the EV profile set for the receding horizon approach

Receding Horizon Benchmark

In the partial information or receding horizon case, we assume that only P_S and P_D are known for the entire period under consideration. Departure times, however, are only known for those EVs that are connected at the corresponding time (cf., [39]). The optimization problem is solved at every time step k and the result is only applied in that time step. This benchmark represents a more realistic scenario in terms of known information, but also the worst case in terms of solving time.

Figure 4.3.1 illustrates how the EV information is built for every time step. As a reference, the clairvoyant approach would use the entire matrix. We are optimizing for $k = 3$ and therefore only consider the information of the EVs connected at this time step (three EVs) and optimize for the shaded period covering up to the last known EV departure. The optimization problems are in general smaller but need to be solved in every time step.

For the evaluation, we concentrate on two metrics: (i) the error with respect to

the objective, measured as the normalized[3] mean squared error (MSE) of $P_{agg}(k)$ with respect to P_O, and (ii) the solving time measured strictly only for the solver excluding data acquisition, modeling, and parsing.

We use July 5th, 2012 as starting date, scale the demand by $F_{demand} = 0.3\%$ to a peak value of 1.6 MW, and a solar penetration $F_{solar} = 5$. We run the simulations for fleet sizes of $N = 100, 200, ..., 1000$. For each N, we generate the scenario once and use the same data for all cases. That is, for the continuous and integer problems for: our approach, the clairvoyant, and the receding horizon optimization benchmarks (6 runs per fleet size).

Regarding the settings of the mixed-integer solver, we limit the solving time to 250 min in the clairvoyant case and define a relative optimality gap of 0.05 and a time limit of 15 min in the receding horizon case. Normally, a lower time limit increases the deviation from the optimal result and a smaller relative gap increases the solving time.

4.3.2 Results

The results are divided into: (i) the aggregated power profiles for 600 EVs, (ii) a performance comparison in terms of objective fulfillment and solving time, and (iii) a trade-off analysis between objective fulfillment and solving time for different fleet sizes.

Figure 4.3.2 shows the aggregated power profiles for a fleet of 600 EVs in Watts (W) for the studied day. The graphs show the resulting $P_{agg}(k)$ for the continuous and integer versions of the two benchmarks and the VOS approach, respectively. They additionally show the pre-aggregated $P_D(k) - P_S(k)$ profile to put the results into perspective. There is an expected smoother profile for the continuous case with respect to the integer one, since continuous values can be calculated to the desired objective while integer ones need to be combined. Additionally, the receding-horizon benchmark deviates more from the desired flat profile, particularly at the beginning

[3] Normalized MSE $= \frac{1}{T}\sum(\frac{P_O - P_{agg}(k)}{P_O})^2$

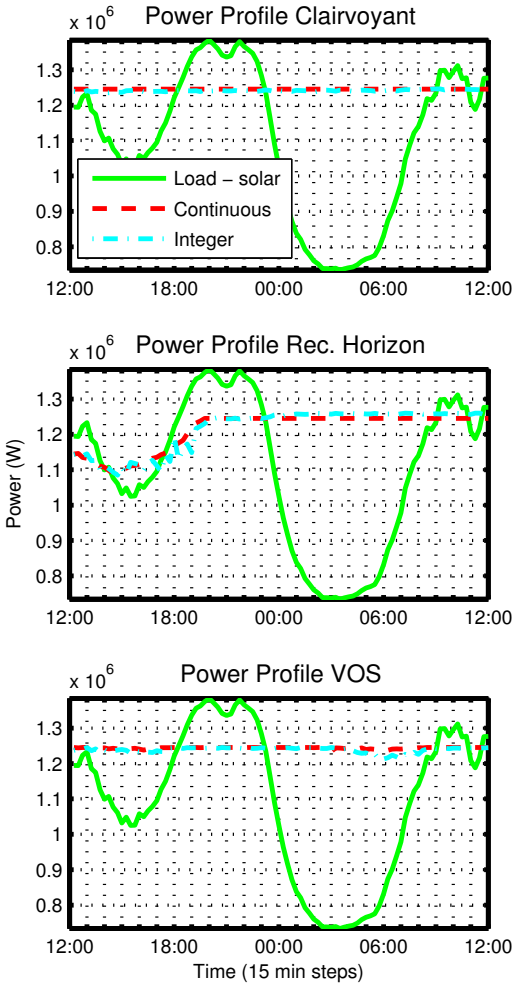

Figure 4.3.2: Power profiles for 600 EVs

of the observation period, and possibly incurring in ramps that are hard to follow by the system operator. This effect is caused by the lack of future driving profile information, which is also more pronounced at the beginning.

Figure 4.3.3a illustrates the performance in terms of distance to goal (normalized MSE) and solving time (seconds) for different EV fleet sizes. The scale of the y-axis is logarithmic for both measurements. The bars in the solving time figures show the standard deviation, maximum and minimum values.

As expected, the clairvoyant optimization for the continuous case shows a better performance in terms of objective fulfillment, because the driving information is known for the entire control period and the continuous variables can be adjusted more precisely and faster. However, in the integer case, we see a reduced performance due to the limited time available for optimization.

Another relevant finding is that our approach performs consistently better than the receding horizon optimization as the number of EVs increases. On the one hand, this demonstrates the scalability of our approach and its effectiveness. On the other hand, it points out the main limitation of our approach: lower performance for small fleet sizes. Yet, for a fleet size of 300 EVs, the normalized MSE of our approach for the integer case is already 2.83×10^{-3}. That is an error of 5% or 60kW for a target $P_O = 1.17$MW, which one can consider acceptable if the solving time is put into perspective. Average errors below 1% are possible with fleets of 600 EVs and larger.

The advantages of our approach become clear when observing the differences between solving times. The VOS approach performs several orders of magnitude better than both benchmarks. Furthermore, the solving time for our approach is similar for the continuous and integer cases, whereas it is several orders of magnitude different for the benchmarks. Additionally, the increase in solving time as the number of EVs increases is moderate and its variance remains low. These findings emphasize the flexibility and scalability characteristics of our approach.

Figure 4.3.3b summarizes the findings in a trade-off analysis. It shows the normalized MSE on the y-axis and the solving time on the x-axis. The closer to the lower left corner, the better the method. The performance of our approach is consistent,

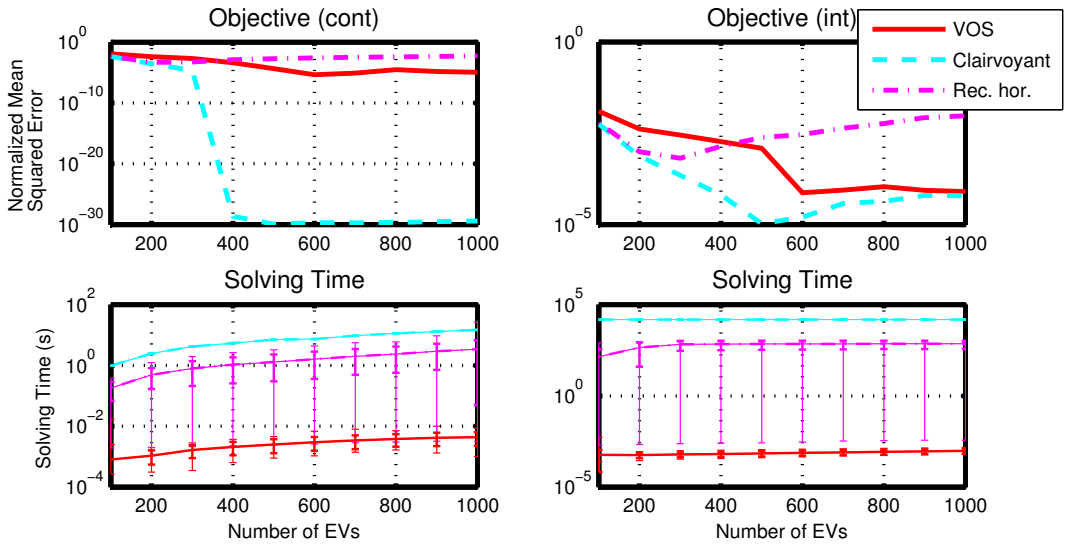

(a)

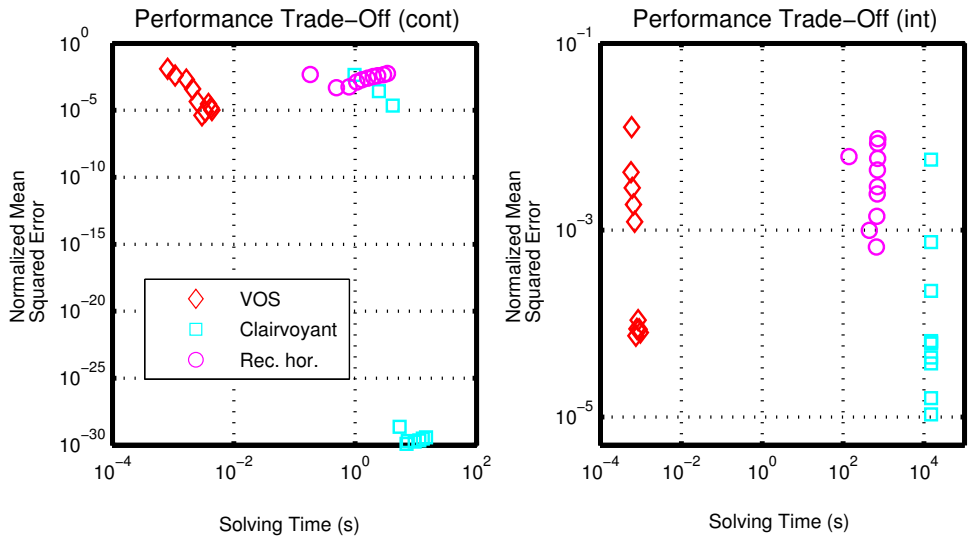

(b)

Figure 4.3.3: Performance: (a) goal and solving time, and (b) trade-off

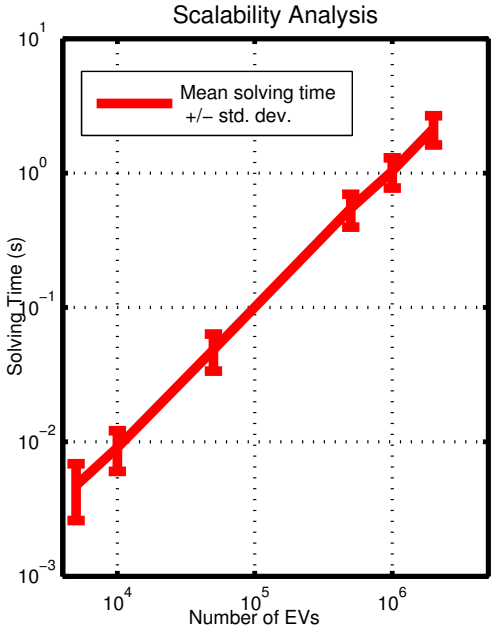

Figure 4.3.4: Scalability of VOS approach for up to 2 million EVs

especially, once a sufficiently large fleet (over 400 EVs) is used. Thus, our approach provides an attractive trade-off between computation time and objective fulfillment.

Figure 4.3.4 shows the mean solving time for fleets from five thousand to two million EVs and the standard deviation of this solving time within one experiment, that is, for the different time steps. The solving time increases linearly with the size of the problem at a rate of less than 1 second per 1 million EVs, or less than a microsecond for each additional EV. Furthermore, the standard deviation also grows proportionally to the size of the problem. Since, in our experiments, we process every EV sequentially, we believe that the solving time can be further improved with parallel processing.

4.4 Reliability Analysis of the VOS Approach

Measuring the MSE is useful for comparing the VOS approach against the benchmark. In practice, however, it is desired that the error remains below a certain level for most of the cases. From the electric utility perspective, peaks in demand represent additional capacity even if the average is low. In this section, we present a method for analyzing the reliability of the VOS approach in terms of percentiles, followed by an evaluation for the scenario described in Section 4.2.

4.4.1 Reliability Analysis

The performance of the VOS approach depends on the EV fleet size and the magnitude of the load. Our reliability analysis has the following objectives: (i) identify the largest error to expect with a given probability, (ii) find the range of the EV fleet size that yields the best results, (iii) quantify the influence of external factors, such as varying demand and weather, on the performance, and (iv) evaluate the approach for a variable profile $P_O(k)$.

We run Monte Carlo simulations for the scenario described in Section 4.2. We use $F_{demand} = 3\%$ and fleet sizes of $N = 4,000 - 19,000$ in steps of 500 EVs. For each N, we run 100 simulations, keeping the same values except for the generated driving profiles. This allows us to eliminate biases resulting from specific driving profile combinations. The number of simulations was chosen by running 600 simulations for the smallest N and choosing the point where the error's accumulated mean varies less than 1×10^{-6} and its standard deviation remains almost constant as shown in Figure 4.4.1.

We consider the integer problem, i.e., $P^i_{EV}(k) \in \{-P^{max}_{EV}, 0, P^{max}_{EV}\}$. We measure the absolute error $|P_O - P_{agg}(k)|$ for every run and time step. Then, we organize the measurements by EV fleet size and calculate the percentile of the error. For the evaluation, we report the 80-, 95-, 99- and 99.9-percentiles. In the following, we refer to the process described above as one Monte Carlo run (MCrun).

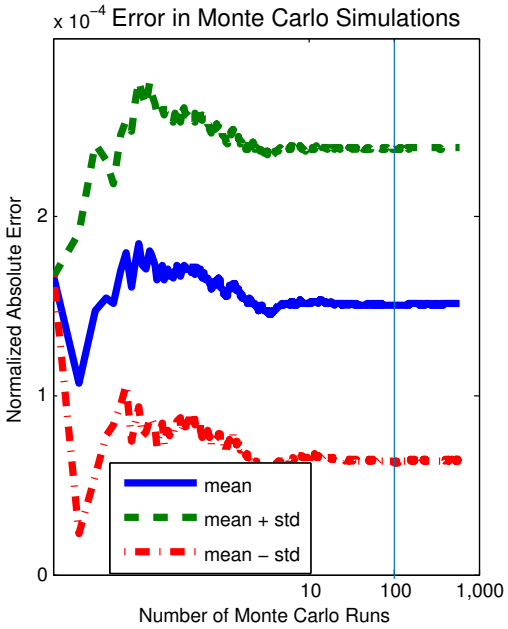

Figure 4.4.1: Monte Carlo error analysis

The evaluation is performed as described in Table 4.4.1. Except for Experiment 4, the method can be generalized for any objective function and it is not limited to our load leveling example.

Table 4.4.1: Reliability analysis experiments

Experiment	Description
1. Performance, Fleet Size and Solar Penetration	We use July 5th, 2012 as in the benchmark and $F_{solar} = 1$. This returns the relationship between the fleet size and performance for these specific conditions. Then, we increase F_{solar} =2,3,4,5 with one MCrun/step. This gives us an insight of the influence of an increased solar penetration on the performance.
2. Seasonal Influences	We use random weekdays for a given season for each of the 100 repetitions, but use the same dates for the different values of N within an MCrun and one MCrun per season. The load and solar generation are taken exactly for the generated date, and the driving profiles are produced for the corresponding season and day type. This gives us some information on the influence of seasonal factor (demand and solar generation variations) and at the same time eliminates day-specific biases.
3. Fleet Size vs. Demand Ratio	We use July 5th, 2012, a fixed N to F_{demand} ratio of 8000 to 3% of Munich's load (around 16MW peak), and N = 400, 800, 4,000, 8,000, 16,000, 32,000, 64,000, 128,000 in one MCrun. This gives us insight into whether the performance is dependent on the $N : F_{demand}$ ratio. In other words, whether we can increase the load proportionally to the fleet size and get equivalent results.
4. Prediction Accuracy	We vary P_O by factors of 0.95, 0.99, 1.01, and 1.05 with one MCrun/step. Since the calculation of P_O depends on the expected values for P_D, P_S, and $\sum P_{EV}^i$, this evaluation indicates the sensitivity of the VOS approach with respect to prediction errors for this specific use case.
5. Variable Power Profiles	We use a variable $P_O(k)$ instead of a constant P_O. We evaluate two use cases as described in Section 4.2. The first is a demand-following profile that follows the shape of the inflexible demand but uniformly shifted according to the additional energy requirements. The second is a valley-filling profile that follows the shape of the inflexible demand but increases the share of additional energy requirements during the lower consumption times.

4.4.2 Results

The results in the following are illustrated with percentile graphs. These graphs display the number of EVs on the x-axis, the normalized absolute error on the y-axis, and the 80-, 95-, 99- and 99.9-percentiles. These percentiles show the maximum magnitude of the error for the given percentage.

Performance, Fleet Size and Solar Penetration

Figure 4.4.2 illustrates the results from experiments 1 and 2 of the reliability analysis. Figure 4.4.2a shows the percentile analysis considering the given date and current solar generation capacity in Munich. The remaining figures reflect the influence of an increased solar generation capacity of up to five times the current one.

The choice of an EV fleet size depends on the requirements agreed upon between the aggregator and the utilities. The factors influencing this choice are the maximum allowed error and the probability that errors fall within this allowed maximum. For example, with current solar generation, we could achieve relative errors below 1% for 80% of the cases with a fleet of 5,000 EVs. However, if the requirement is a 99% reliability, we can only commit to errors below 5% with a fleet of at least 9,000 EVs.

There is a clear tendency of a better performance the larger the fleet size, especially for higher percentiles. However, the 80-percentile tends to increase with the fleet size, indicating higher error values but a more homogeneous behavior.

This tendency is better illustrated in Figure 4.4.3. As the size of the fleet increases, the proportion of the inflexible demand in the aggregated load decreases. Therefore, the peaks from the inflexible demand have less influence on the aggregated load, resulting in fewer outliers. However, the influence of the EV energy requirements increases, which in turn causes generally higher errors.

The results in Figure 4.4.2 also show that an increase in solar penetration has a positive effect: better results can be achieved with smaller fleets. On the one hand,

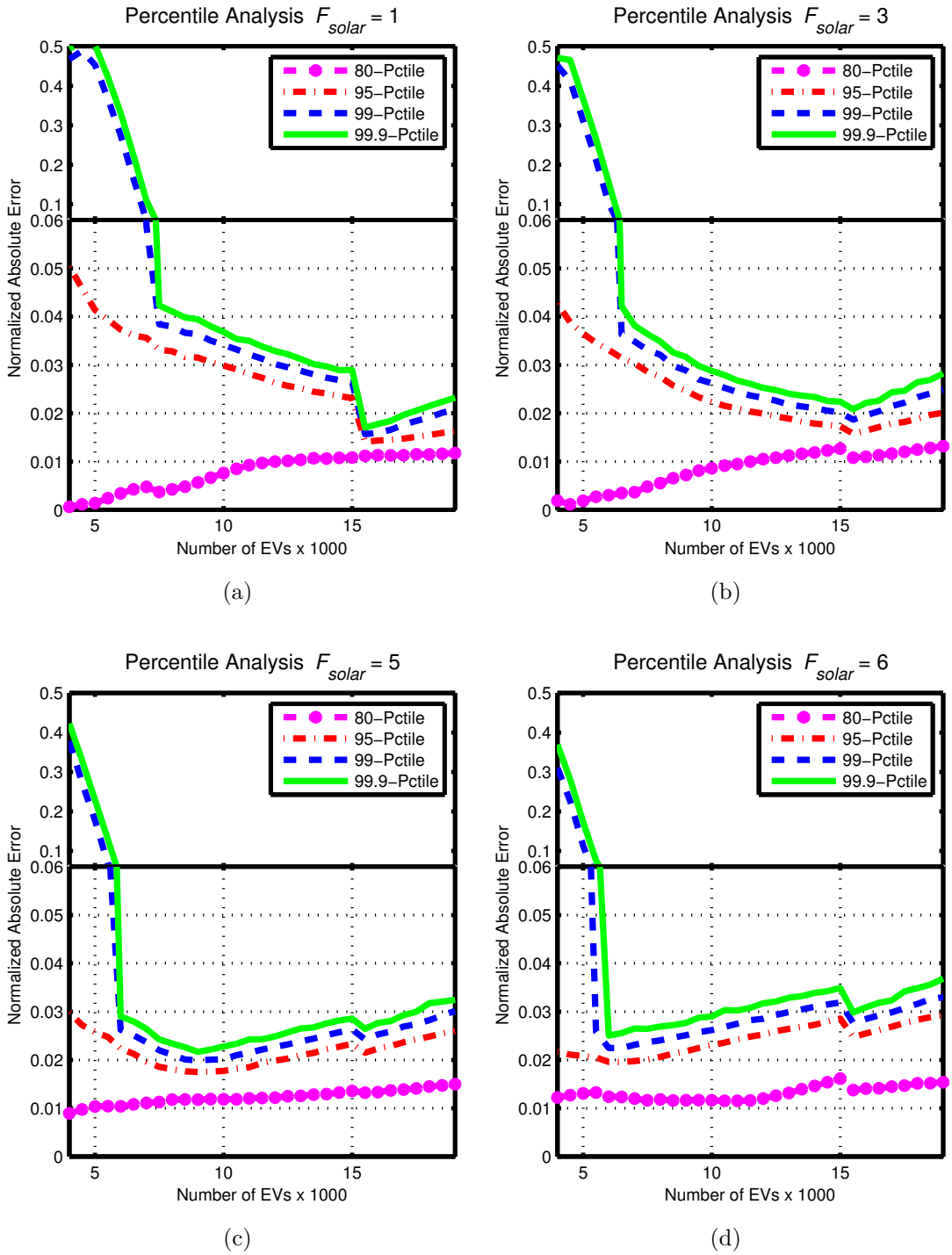

Figure 4.4.2: Percentile analysis for (a) 1x; (b) 3x; (c) 5x; and (d) 6x the current solar penetration

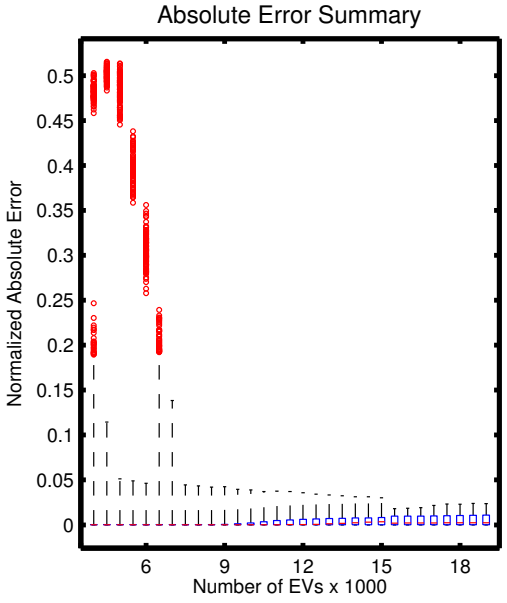

Figure 4.4.3: Box plot: normalized absolute error with current solar generation

the target P_O decreases as the solar penetration increases. On the other hand, solar energy tends to be generated also during high demand periods (i.e., during the day) which in practice reduces the magnitude of the peaks. Although this experiment focuses on one specific day, we observed a similar behavior for different days and seasons. This suggests that using the VOS approach for load leveling could potentially facilitate solar integration.

From the applicability perspective, these findings are also relevant. As the solar penetration continues to increase, aggregators do not need to worry about negative effects from increased penetration. On the contrary, they could increase their service capacity while keeping the same infrastructure and expenses.

Seasonal Influences

Figure 4.4.4 illustrates the results for Experiment 4 of the reliability analysis. Figure 4.4.4a - 4.4.4d show the performance of the VOS approach for different seasons. Although there are some variations from season to season, we observe a relatively consistent performance throughout the year. Since this evaluation covers the entire year, it could be seen as the tool for aggregators to decide on the fleet size or load magnitude to commit to.

Figure 4.4.5b shows a similar evaluation but done throughout the whole year. In other words, it would be equivalent to merging all seasonal evaluations but with one fourth of the samples. As such, it gives an overview of the performance for an entire year.

Contrary to the evaluation yielding to Figure 4.4.5b, where the driving profiles where generated according to the season of the corresponding random date, Figure 4.4.5a illustrates the performance when no seasonal filter is applied. We observe a significant deterioration in the overall performance. This could indicate a correlation between power consumption and driving patterns between seasons. Furthermore, it emphasizes the importance of accurate driving models and data, especially for feasibility studies.

Finally, we also evaluate the VOS approach for weekends instead of weekdays. The results are illustrated in Figure 4.4.6. From the aggregator's perspective, this evaluation indicates whether a given performance is maintained for different day types. The way we see it, aggregators would define parameters based on weekday evaluations since they account for most of the operation time. Still, they would verify that there is no major performance deterioration during weekends. In our results, there are no negative effects in performance. That said, we have significantly less data for weekends as we have for weekdays, so the results in Figure 4.4.6 could be challenged.

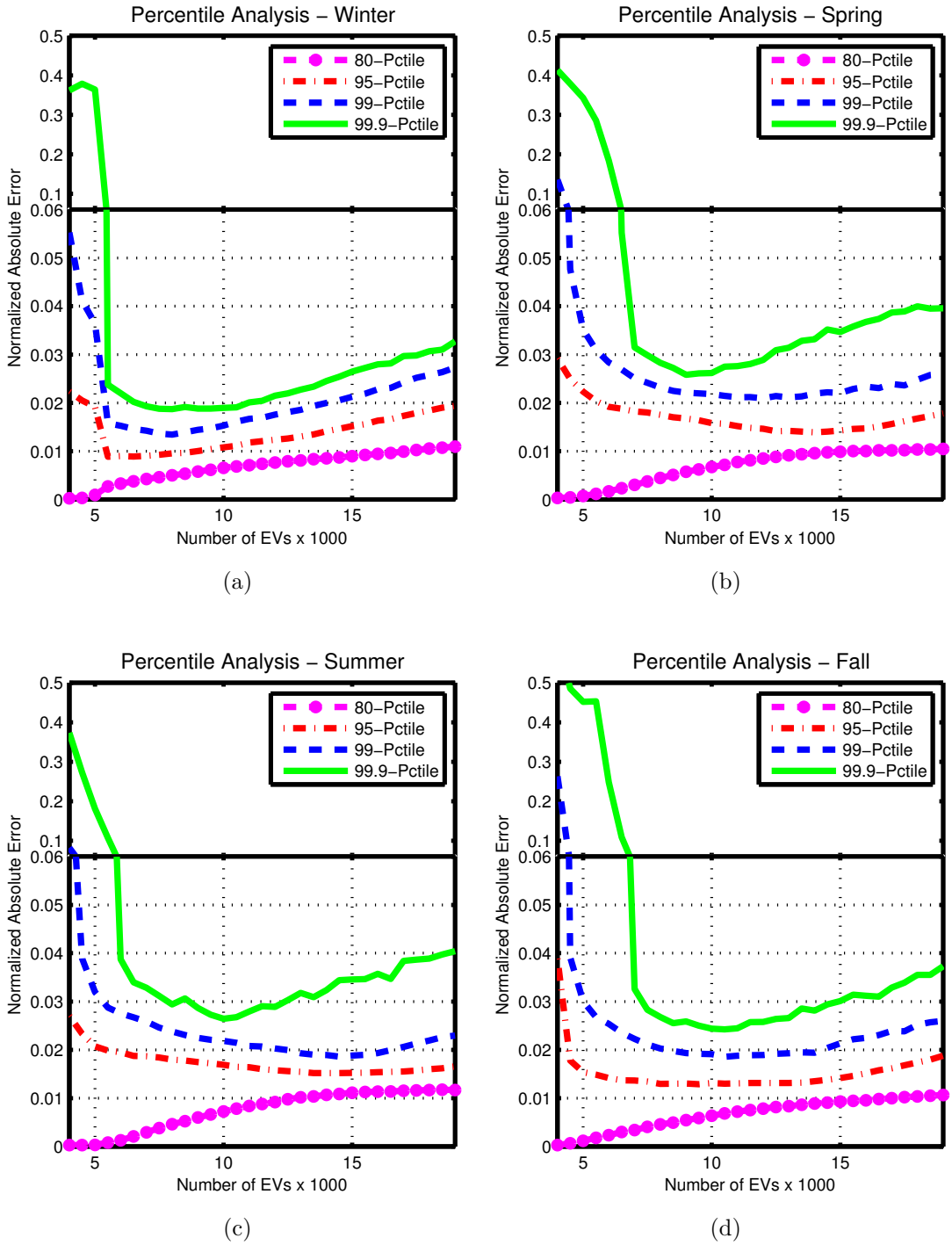

Figure 4.4.4: Percentile analysis for (a) winter; (b) spring; (c) summer; (d) fall

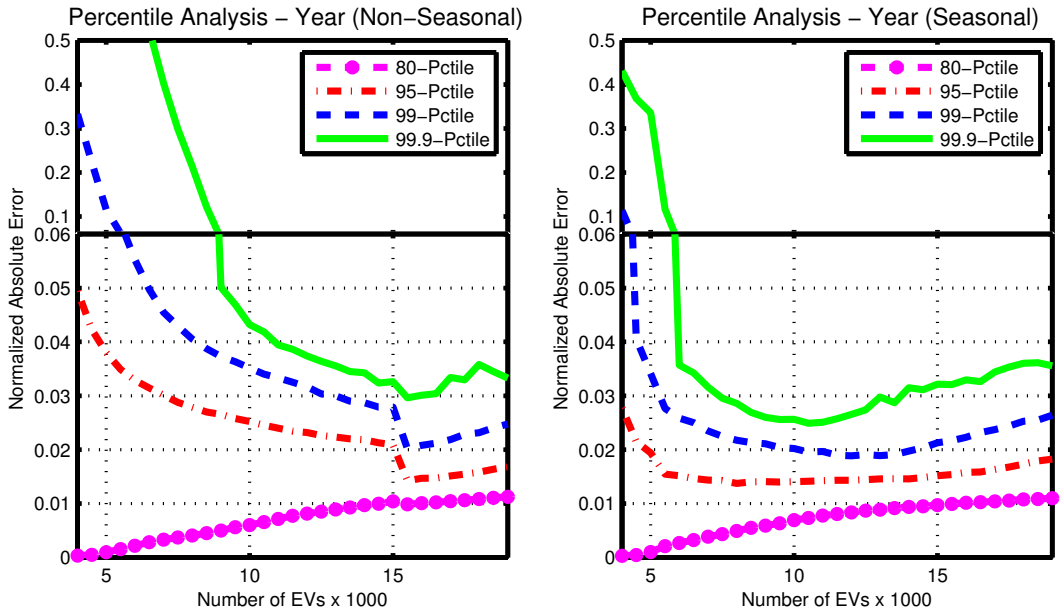

(a) (b)

Figure 4.4.5: Effects of seasonal driving profiles

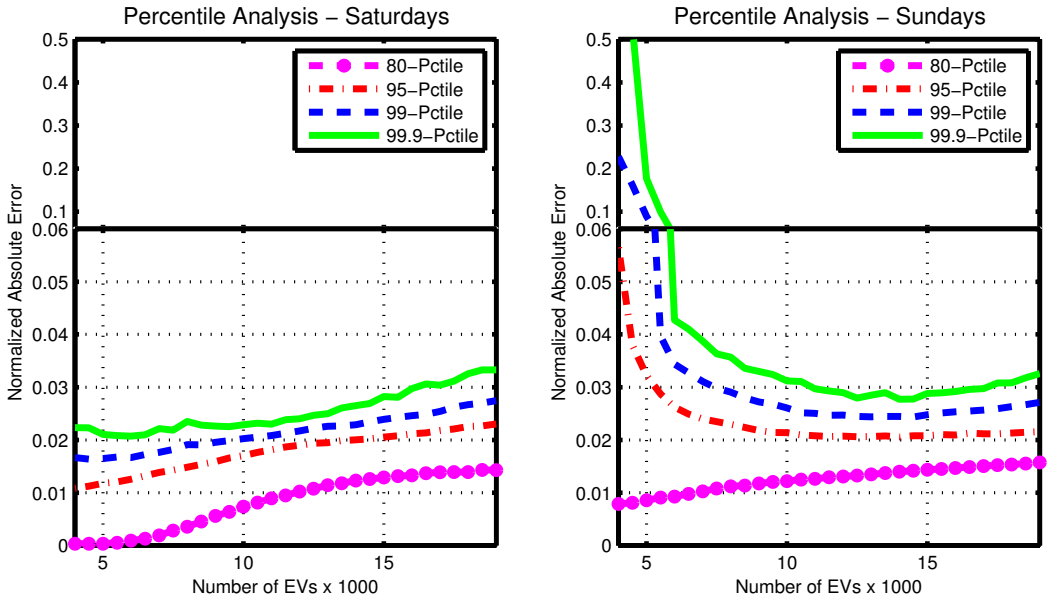

(a) (b)

Figure 4.4.6: Percentile analysis for weekends

Fleet Size vs. Demand Ratio

Figure 4.4.7 shows the results for Experiment 3 in the reliability analysis. The objective of this analysis is to evaluate whether a given result can be generalized to an arbitrary fleet or load size.

The performance remains constant for fleets of 16 thousand EVs and higher. It also remains constant for 4 and 8 thousand EVs. In addition to the jump from 8 to 16 thousands, in our experiments we also see a decrease between Ns in the hundreds and in the thousands, yet constant within the range of its order of magnitude.

This effect is likely to be related to a precision effect. The lowest step in power is related to the P_{EV} of a single EV. For example, the impact of 250 EVs would amount to 1MW. That is an error of around 6% for a fleet size of 8,000 and 3% for a fleet size of 16,000, which is consistent with the results for the 99-percentile. For fleets of 100 - 1,000 EVs, the influence of the lowest step with respect to P_O is larger than for fleets of 1,000 - 10,000 EVs. After a certain fleet size is reached, this effect is no longer noticeable.

Our experiments thus indicate that this result can be extrapolated to an arbitrary fleet or load size within a range of at least one order of magnitude. This has positive implications for aggregators as their service providing capacity would increase linearly to the fleet size.

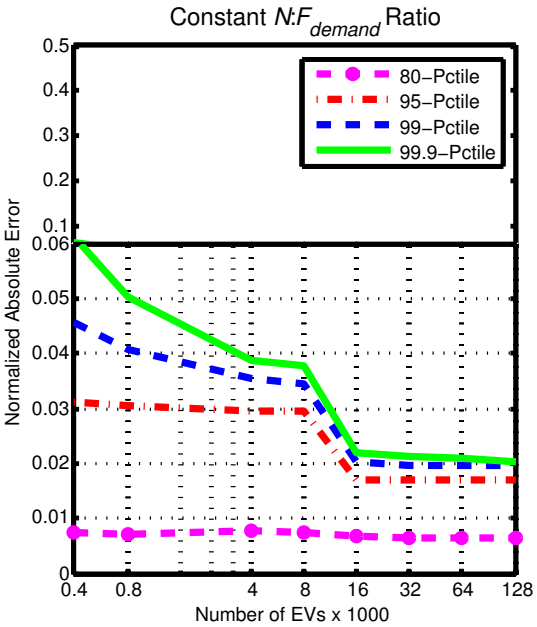

Figure 4.4.7: Percentiles for a fleet-size-to-demand ratio of 8000:3%

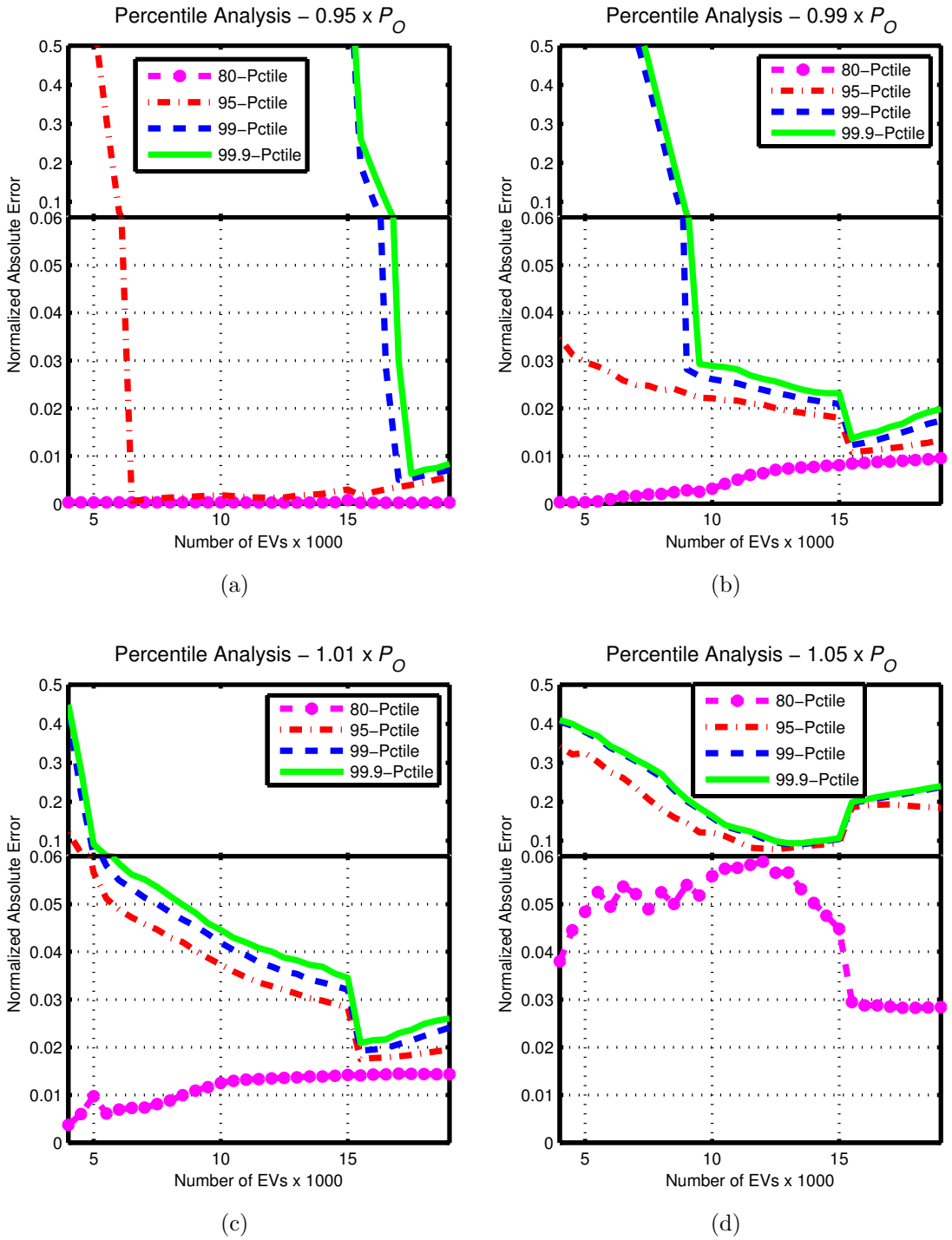

Figure 4.4.8: Percentile analysis for P'_O = (a) $0.95P_O$, (b) $0.99P_O$, (c) $1.01P_O$, and (d) $1.05P_O$

Prediction Accuracy

Figure 4.4.8 illustrates the results for Experiment 4 of the reliability analysis. Unlike the previous evaluations, the relevance and interpretation of these findings are specific to the objective of choice. In our case, we aim at power leveling, so the magnitude chosen as objective P_O must ensure that the power supply/demand balance is met. The evaluation indicates the impact of errors in the prediction of the total energy or the average power demand.

The sensitivity towards an error in the objective P_O is relatively high. Already at 1% (Figure 4.4.8b and 4.4.8c), we see different performance compared with Figure 4.4.2a. This could indicate a significant challenge for pursuing a load leveling objective. Yet, it can be argued that errors in predicting averages are in principle lower than those for predicting time series. Figure 4.4.8a and 4.4.8d show the performance for prediction errors of 5%. The results suggest that for this scenario it is better to underestimate P_O rather than overestimate it.

The sensitivity towards variations in P_O is not specific to the VOS approach, but to the requirement of defining an objective P_O ex-ante. One alternative to minimize errors in prediction would be to update P_O for shorter time periods, e.g., hourly or every 15 minutes. Another alternative is to use the result of an aggregated optimization, e.g., a unit commitment like in [12] and [45] to define a specific target P_O and then use the VOS approach to reach this target.

From the aggregator's perspective, these findings could help in the formulation of commitments depending on the availability of predictions and their quality.

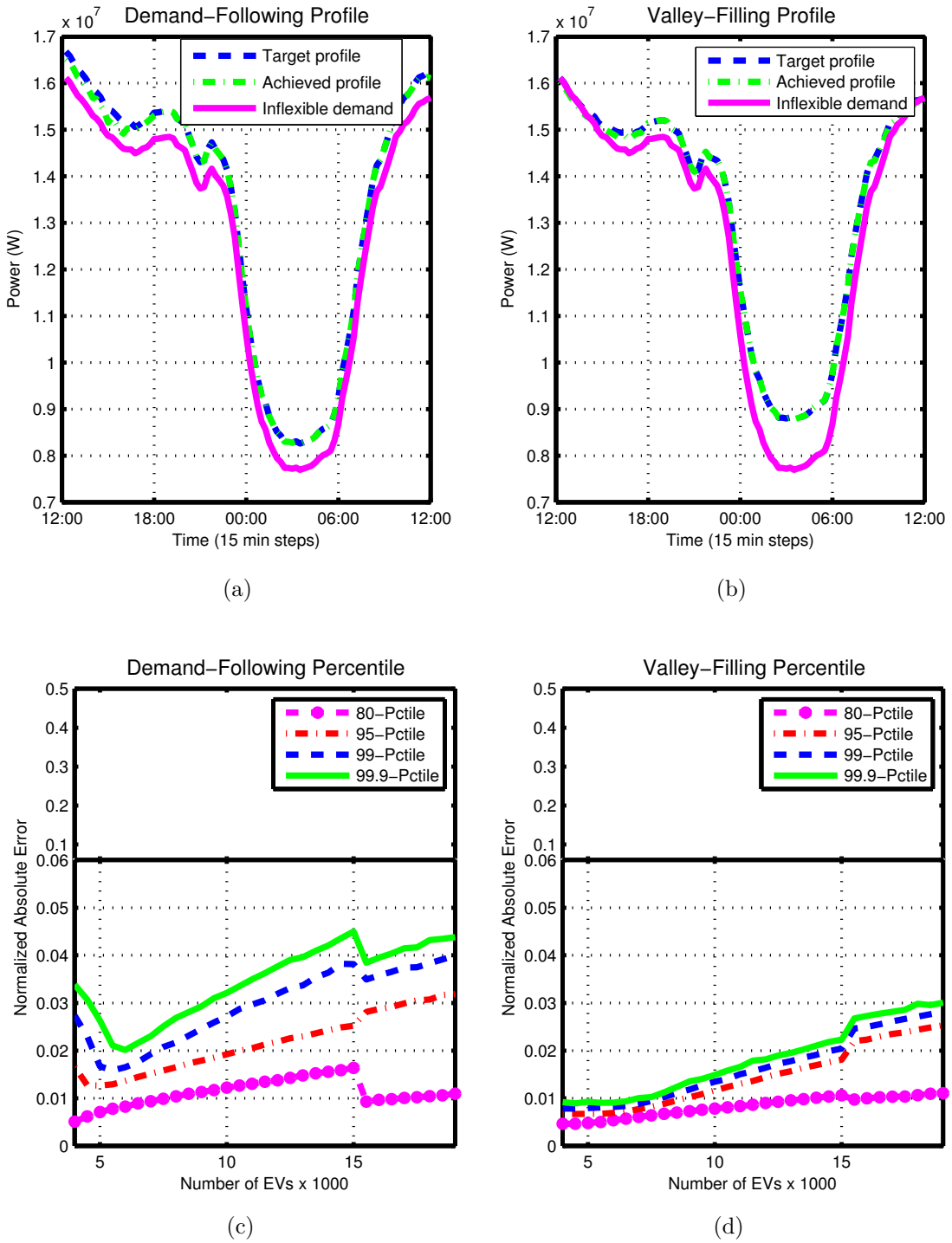

Figure 4.4.9: Demand following and valley filling profile and percentile analysis

Variable Power Profiles

Figure 4.4.9 show the results for the demand-following and valley-filling use cases respectively. In Figure 4.4.9a and Figure 4.4.9b, we see the target and achieved profiles for a fleet of 4,000 EVs. The difference in the target profiles $P_O(k)$ is mostly visible in the period between 00:00 and 06:00, where the valley-filling profile is higher. As we get closer to 12:00 in both sides, the valley-filling profile is very close to the inflexible demand while the demand-following profile keeps the same shift along the entire day.

The VOS approach succesfully matches the power profile in both cases. Furthermore, the percentile analysis in Figure 4.4.9c and Figure 4.4.9d show that low errors can be achieved also for larger fleets. In our use cases, we are able to match the valley-filling profile better than the demand following one. The valley occurs at night when more EVs are parked.

These results show that the VOS approach is also suitable for variable power profiles. In general, the VOS approach distributes the available resources in order to meet a certain target. This target $P_O(k)$, however, has to be feasible, and, although the VOS approach does not test this feasibility, it does minimize the deviation from it. In practice, the feasibility of $P_O(k)$ would be addressed by the entity setting this target, e.g., the DSO.

Chapter 5

Extensions to VOS

This chapter presents two extensions to the VOS method and closes with a general discussion. Section 5.1 introduces a message reduction strategy and corresponding results. Section 5.2 explores alternative signal designs and their corresponding effects. Finally, Section 5.3 presents a discussion on the VOS approach and its different extensions.

5.1 Reducing VOS Message Requirements

The VOS approach enables vehicles to compute signals reflecting their need for charge and willingness to supply power, and an aggregator to collect these signals and implement the control in a computationally efficient manner. However, it still requires messages to be exchanged at every time step. For example, for performing control in 15 minutes intervals, we need to send and receive messages every 15 minutes. This load becomes more significant as the number of EVs and the granularity of the control intervals (i.e., milliseconds or seconds instead of minutes) increase. Since signal computation and control are decoupled, it is possible to reduce this requirement, independently of the length of the control interval.

The concept of a single broadcast signal is present in incentive-based approaches like [38] and [13]. The idea of broadcasting a set point signal is also explored in [48]. These concepts allow for the reduction on message requirements from the aggregator to the EVs. In this section, we build on these concepts to reduce the aggregator-to-EVs message requirements. Furthermore, we exploit the modular characteristic of the VOS approach to reduce the EVs-to-aggregator ones.

5.1.1 EV-to-Aggregator Messages

In the original VOS approach, a message containing the values of the NfC and WtS signals is sent in every time step. From (4.1.5) and (4.1.7), we identify that these signals only depend on local information. Furthermore, the only value that is externally influenced is the energy level of the EV's battery E^i_{bat} which depends on the charging power P^i_{EV} assigned by the aggregator.

Since the range of values for P_{EV} is known, it is possible to calculate a set of possible future values for NfC and WtS in terms of P_{EV}. This set of possible values can be sent to the aggregator in a single (and larger) message with a lifetime of several time steps. On every time step, the aggregator can then choose the NfC and WtS values for each EV depending on the calculated P^i_{EV}, instead of receiving a new message.

Figure 5.1.1 illustrates how an EV builds the set of possible NfC values. Messages are sent at the time step $k = \tau$ and have a message lifetime of T_M time steps. For a given EV, τ is equal to the arrival time step k_{in} for the first message. The EV then computes the possible NfC values based on the possible values of P_{EV}.

As k increases, the set of possible NfC values forms a complete V-ary tree [70], where V indicates the number of values that P_{EV} is allowed to take. The height of the tree h_M is $T_M - 1$ except when the EV departs before the end of the message lifetime or $k^i_{dep} < \tau_i + T_M$ resulting in $h_M = k^i_{dep} - \tau_i - 1$.

There is, however, a significant trade-off between the reduction of the number of messages and the message size. For our V-ary tree, the total number of nodes (i.e.,

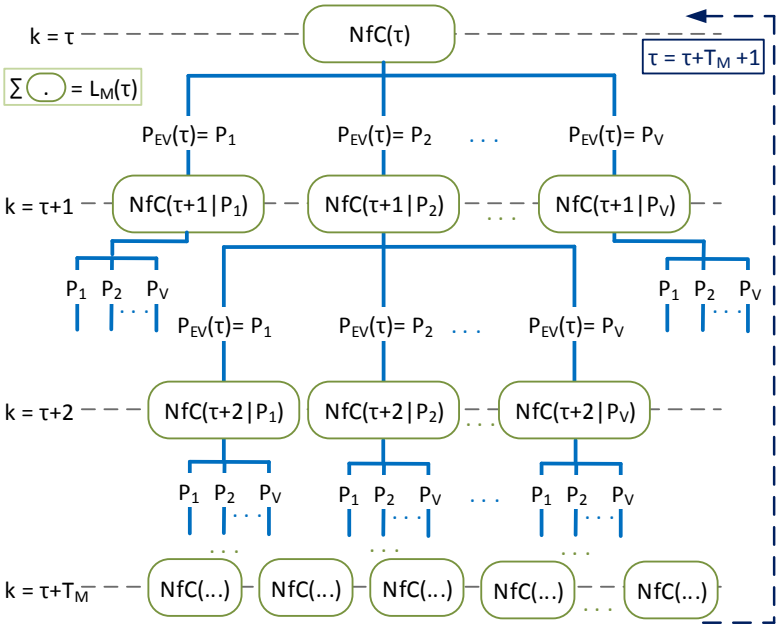

Figure 5.1.1: The NfC value set

NfC values) is [70]:

$$L_M^i(\tau_i) = \frac{V^{h_M(\tau_i)+1} - 1}{V - 1} \tag{5.1.1}$$

where:

$$h_M(\tau_i) + 1 = \min(T_M, k_{dep}^i - \tau_i) \tag{5.1.2}$$

The lower bound in terms of the number of messages can be achieved if the message lifetime $T_M \to \infty$. In this case, every EV sends only one message which is valid for the entire plug-in period. The message size depends on the length of this plug-in period and therefore varies from EV to EV.

From (5.1.1), we can see that the size of the message depends also on V. This means

that P_{EV} can only take on a discrete number of values so this approach cannot be applied for a strictly continuous P_{EV}. However, it is possible to approximate this for a continuous approach by increasing the granularity of P_{EV} at the cost of increasing V. For a granularity of $\frac{P_{EV}^{max}}{P_{EV}^{step}}$, we would have:

$$V = 1 + \frac{2}{P_{EV}^{step}} \tag{5.1.3}$$

E.g., if we want a granularity of one tenth of P_{EV}^{max}, then $V = 21$.

The lower bound in terms of message size is therefore achieved when $P_{EV}^{step} = 1$ so $P_{EV}^{i}(k)$ can take on the values $\{-P_{EV}^{max}, 0, P_{EV}^{max}\}$ and $V = 3$, i.e., we have a tertiary tree. The other lower bound for the message size holds when $T_M = 0$ but that means sending messages every time step which is against our objective.

A second tree could be built for the WtS signal. However, since both values depend on the same P_{EV}, this is solved more efficiently by integrating both values into the tree. That is, each node of the tree contains a value for NfC and WtS. This also would enable a more efficient data compression and lower overhead. For example, one would need a single pointer for both values and one could compress both values into a single frame.

Since our tree is full and complete, we don't have a significant overhead in terms of structures. A serialized list could be sent by the EV and ordered by the aggregator based on a predefined sequence. Therefore, we approximate the new message size as $L_M^i(\tau_i)$ times the original (one NfC and WtS) message size.

Still, the message size grows exponentially and this method should be applied with caution. Table 5.1.1 presents message size values in terms of number of nodes for $V = 3, 10$ and $T_M = 4, 10$ to give some intuition on the actual cost of this approach.

Table 5.1.1: Number of nodes for different V and T_M

	T_M	
V	4	10
3	40	29,524
10	1,111	$1.1\text{x}10^9$

To strictly minimize the number of messages, we also want to avoid large messages that need to be fragmented before being sent. In addition, we want to include as much information as possible within this single unit. We therefore use the concept of maximum transmission unit (MTU) in communication networks to define a target message size that ensures no fragmentation and maximum information exchange.

We define the net MTU as the payload size without transmission overhead, i.e., $\text{MTU}_{nett} = \text{MTU} - \text{OH}_{nw}$. The number of nodes would be $L_M^{tar} = \frac{\text{MTU}_{nett}}{S_{node}}$, where S_{node} is the node size in bytes, and depends on the protocol and compression applied. L_M^{tar} is only an intermediate value and can take any real value.

From (5.1.1) and (5.1.2), we define the tree's target height which in turn defines the target message lifetime T_M^{tar} as:

$$h_M^{tar} = \frac{\log\left((V-1)L_M^{tar}+1\right)}{\log V} - 1 \tag{5.1.4}$$

$$T_M^{tar} = \left\lfloor h_M^{tar}+1 \right\rfloor = \left\lfloor \frac{\log\left((V-1)L_M^{tar}+1\right)}{\log V} \right\rfloor \tag{5.1.5}$$

The actual number of nodes sent is:

$$L_M^{tar*} = \frac{V^{T_M^{tar}}-1}{V-1} \tag{5.1.6}$$

For example, an Ethernet network has MTU = 1500 bytes, which is also a common default value for DSL and 3G routers. For an overhead of 10% (reasonable when considering higher level protocols) and $S_{node} = 8$, corresponding to two (NfC and WtS) floating point values of 4 bytes each, we have $\text{MTU}_{nett} = 1,350$ which for $V = 3$ can fit up to $L_M^{tar} = 168.75$ nodes, allowing for a message with lifetime $T_M^{tar} = 5$ time steps and $L_M^{tar*} = 121$ tuples of NfC/WtS values.

5.1.2 Aggregator-to-EV Messages

The VOS approach implements a direct control by sending a charging instruction to every EV. These instructions depend on the EV's NfC and WtS values and the available resources at the time. If we consider the integer case, meaning that $P^i_{EV}(k)$ can take the values $\{-P^{max}_{EV}, 0, P^{max}_{EV}\}$, the aggregator assigns resources based on a highest-first approach. That means that the NfC of the last EV that was instructed to charge can be seen as a set point: all EVs with higher NfC charged and all EVs with lower NfC did not.

One can potentially reduce the control messages to a single broadcast signal containing the set point values for the NfC and WtS. For this to yield the same results, however, each EV must have unique values for NfC and WtS, and since these only depend on local EV information, we cannot ensure uniqueness. We therefore propose a solution in which the set point values for NfC and WtS are coupled to a probability rate to steer those EVs having NfC or WtS values equal to the set point. In other words, for the NfC case, those EVs with higher NfC than the set point charge, those with a lower do not and those with an NfC equal to the set point charge with probability $p(\text{NfC})$.

The aggregator's algorithm is modified as shown in Algorithm 5.1.1. The EV receives the broadcast signal and checks first the NfC set point. It charges if (i) its NfC is larger, or (ii) its NfC is equal and a random function returns true. If the EV does not charge, it checks the WtS set point and discharges if (i) its WtS is larger, or (ii) its WtS is equal and a random function returns true. This random function returns true if the output of a uniform random number generator of range [0,1] is less than or equal to the set point's probability rate coupled to the NfC or WtS, respectively.

The use of a probability factor implies an increase in uncertainty. This uncertainty, however, exists only for those cases where there are more vehicles with the same values as the set points. The probability of having more than one EV with the same NfC or WtS values increases with the number of EVs. Nevertheless, the impact of this uncertainty also decreases as the fleet size increases. The more EVs, the likelier it is that the practical distribution matches the theoretical one.

Algorithm 5.1.1

Algorithm 5.1.1: Aggregator with broadcasting

1. $P_{agg}(k) \leftarrow P_D(k) - P_S(k)$
2. **Sort** EVs by NfC in descending order (index i^*)
3. **While** $P_{agg}(k) < P_{agg}^{max}$ & $NfC = C_{QoS}$
   (a) $P_{agg}(k) \leftarrow P_{agg}(k) + P_{EV}^{max}$
   (b) i^*++
4. **While** $P_{agg}(k) \leq P_O(k)$ & $C_{full} <$ NfC $< C_{QoS}$
   (a) $P_{agg}(k) \leftarrow P_{agg}(k) + P_{EV}^{max}$
   (b) i^*++
5. NfC_Set_Point $\leftarrow$ NfC(i^*)
6. **Calculate Probability Rate**
   (a) $a \leftarrow$ **Count** NfC = NfC_Set_Point **in** Sortedlist (0:i^*-1)
   (b) $b \leftarrow$ **Count** NfC = NfC_Set_Point **in** Sortedlist (0:end)
   (c) NfC_Probability_Rate $\leftarrow a/b$
7. **Sort** remaining EVs by WtS in descending order (index i^{**})
8. **While** $P_{agg}(k) > P_O(k)$ & WtS $> C_{noS}$)
   (a) $P_{agg}(k) \leftarrow P_{agg}(k) - P_{EV}^{max}$
   (b) i^{**}++
9. WtS_Set_Point $\leftarrow$ WtS(i^{**})
10. **Calculate Probability Rate**
    (a) $a \leftarrow$ **Count** WtS = WtS_Set_Point **in** Sortedlist (0:i^{**}-1)
    (b) $b \leftarrow$ **Count** WtS = WtS_Set_Point **in** Sortedlist (0:end)
    (c) WtS_Probability_Rate $\leftarrow a/b$
11. **Broadcast**
    - NfC_Set_Point, NfC_Probability_Rate
    - WtS_Set_Point, WtS_Probability_Rate

5.1.3 Combined Approach

It is possible to combine the two approaches above to enable further reduction in the number of messages. This, however, requires some adjustments. The EV-aggregator message reduction is based on the principle that future NfC/WtS values can be accurately predicted for a given charging action. However, the aggregator-EV message reduction introduces a degree of uncertainty that challenges this predictability principle. The EV does not know beforehand if and when a case with NfC/WtS equal to the set point will occur, nor the action that would be taken accordingly. The aggregator knows how many EVs are under this condition and, of those, how many are expected to take action, but it does not know which EV takes what action.

This challenge can be addressed by introducing a retransmission protocol. Whenever an EV encounters a set point value equal to its NfC or WtS, it schedules a message transmission for the next time step. That is:

Algorithm 5.1.2

Algorithm 5.1.2: Retransmission modification

If NfC(k) = NfC_Set_Point OR WtS(k) = WtS_Set_Point:
$\tau \leftarrow k + 1$.

The trade-off here is the number of triggered retransmissions. A retransmission is triggered if either the NfC or the WtS are equal to the set point, so the number of retransmitted messages M_{rtx} depends on how often this happens. Yet, M_{rtx} is the upper bound for the cost of combining both approaches. Since the message lifetime T_M remains the same, the new message spans over $\tau_{new} + T_M$, so no message needs to be sent at $\tau_{old} + T_M + 1$. The closer the retransmission is to the original transmission, the higher the cost of retransmission, and the higher the amount of transmitted data that is later discarded.

For example, an EV sends its NfC/WtS tree upon connection, receives a broadcast signal with the set point equal to its NfC and the random function results in a charging action "charge." The aggregator has no way of knowing what charging action

Table 5.1.2: EV-to-aggregator message reduction results

Signal size (bits)	MTU per mes.	Mes. life time T_M	Reduction in total	Mes. per EV (mean)	Reduction in mean	Mes. per EV (3-qtile)	Reduction in 3-qtile
32	1	5	79.4%	12.9	79.4%	16	79.2%
32	2	6	82.7%	10.8	82.7%	13	83.1%
32	3	6	82.7%	10.8	82.7%	13	83.1%
16	1	6	82.7%	10.8	82.7%	11	83.1%
16	2	7	85.0%	9.4	85.0%	11	85.7%
16	3	7	85.0%	9.4	85.0%	11	85.7%
8	1	7	85.0%	9.4	85.0%	11	85.7%
8	2	7	85.0%	9.4	85.0%	11	85.7%
8	3	8	86.8%	8.2	86.8%	10	87.0%

the EV took so it cannot choose the next NfC value from the tree. The EV needs to retransmit a tree in the next time step, which, since happening shortly after the first transmission, results in more messages and a large amount of data sent but not used.

5.1.4 Results

We compare the traditional VOS and the message-efficient VOS approach by running one MCrun for each of them, following the same experimental setup as described in Section 4.4. We use random weekdays in spring for each of the 100 repetitions, but use the same dates for the different values of N within an MCrun and for the two approaches. The load and solar generation are taken exactly for the generated date and the driving profiles are produced for spring weekdays. Although our use case is based on 15 minutes control intervals, the results are relative to k and T_M, and are therefore valid for shorter intervals.

EV-to-Aggregator Messages

Table 5.1.2 summarizes the results for the EV-to-Aggregator message reduction method. We analyze the MCrun for 4,000 EVs, that is 100 simulations each with 96 time steps. We report results for different sizes of NfC/WtS signals and number of MTUs per message. We assume it is possible to format the NfC/WtS to different

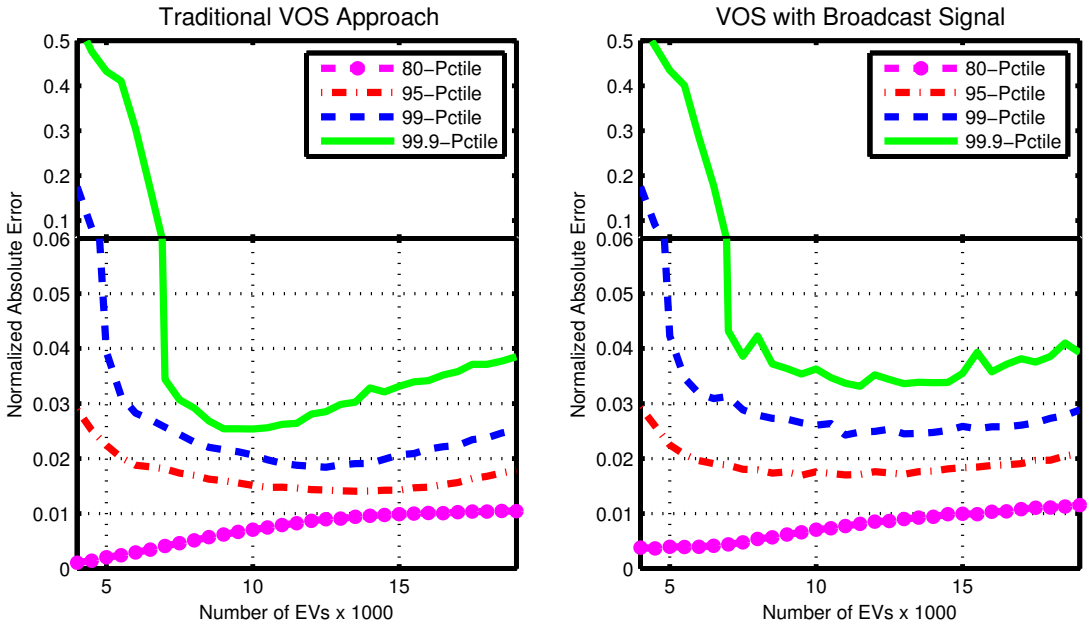

Figure 5.1.2: Percentile performance for aggregator-to-EV message reduction

bit sizes (8-32) and consider up to three 1500 bytes-large MTUs per message with an effective payload of 90%. The message lifetime is calculated based on (5.1.5). Reductions are reported as $1 - \text{result/reference}$, where the references are the total, mean, and 3rd quartile of the messages sent by EVs in the traditional VOS.

We achieve savings of at least close to 80%. We can improve reduction by allowing messages larger than one MTU (fragmentation) or compressing the data. The second alternative should be preferred as it also reduces number of packets and therefore the network usage.

Aggregator-to-EV Messages

Figure 5.1.2 presents the results for the message reduction at the aggregator level. These graphs display the 80-, 95-, 99- and 99.9-percentiles with the number of EVs on the x-axis and the normalized absolute error on the y-axis, for the original VOS and the broadcast signal approach.

Table 5.1.3: Combined approach message reduction results

Reduction vs.	Mean	Minimum	Maximum
EV-only approach	56.5%	48.4%	70.1%
Agg-only approach	47.5%	37.8%	64.0%
Traditional VOS	73.7%	68.9%	82.0%

The results for up to a fleet size of 7 thousand EVs are very similar for both approaches. Less EVs result in less occurrences of signals with the exact same values. The 80-percentile remains mostly unaffected while the higher percentiles show a negative impact on performance, until around 16 thousand EVs. For very large fleets, the cases of exactly equal signal values are higher but also the randomization tends to the desired uniform shape. The impact, however, is below 0.01 for the highest percentile and quite minimal for the rest.

The benefits of this approach become significantly higher as the fleet size increases. Since we only broadcast one message, independently of the fleet size, this approach saves 3,999 messages per time step for a 4,000 EV fleet and 19,999 for an EV fleet of 20,000 EVs.

Combined Approach

Table 5.1.3 presents the results for the combined approach. We analyze the MCrun for 4,000 EVs and compare the results against the two message-efficient alternatives applied separately and the traditional VOS approach. We consider the case with $T_M = 5$. We count the total number of messages sent for each of the 100 simulations, calculate reductions per run and report mean, maximum, and minimum. Reductions are reported as $1 - \text{result/reference}$, where the references are the total number of messages sent by EVs and aggregator in one run.

In all cases, we achieve significant reductions which suggests that it is worth to combine both approaches. The most important factor influencing the reduction is the number of retransmissions. In our experiments, we experienced on average around 87 thousand retransmission per run. That is around 21 messages per vehicle or almost twice the average of the EV-reduction approach. These number of retransmissions

are biased to our data source. Since we have a limited number of samples to produce driving profiles, we generate a number of similar profiles for larger fleets. Similar profiles produce similar VOS signals which increase the probability of retransmission. We therefore believe that the reduction in a real world scenario is potentially higher.

5.2 Alternative Signal Design

In this section we explore the use of alternative signal designs for the NfC. We take the original design of the NfC signal and experiment with its curvature. This can be seen as modifying the risk affinity of the EVs, i.e., a linear function would be more risk balanced and a concave function would be more risk averse. We analyze the effects of these alternative signals in terms of the algorithm's performance and the benefits for the EVs. Particularly, we explore the magnitude and probability of errors with respect to a reference power profile and the energy available in the batteries relative to the remaining parking time.

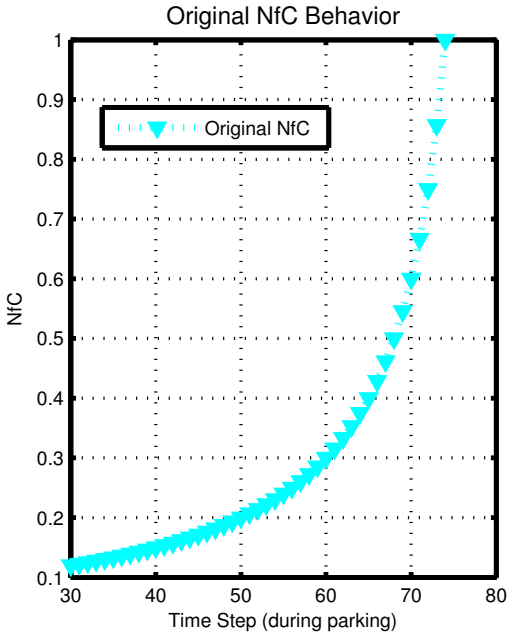

Figure 5.2.1: Original NfC signal

5.2.1 Alternative NfC Signals

In the traditional VOS approach, the NfC is computed by every EV on every time step based on (4.1.5). From (4.1.3-4.1.6), we observe that, if the energy level E^i_{bat} does not change, the NfC signal shows a $1/k$ behavior in the interval between C_{tar}

and C_{QoS}. Figure 5.2.1 shows the NfC behavior of an EV parked during the interval $k = [30, 80]$ and $E^i_{bat} = 10$kWh. For the NfC signal we use $C_{tar} = 0.1$ and $C_{QoS} = 1$.

We consider the NfC signal to be a utility function. Since the concavity of a utility function indicates its level of risk aversion [71], we can say that the original NfC is a risk-affine function. The value of NfC initially increases slowly and accelerates as the deadline or departure time approaches. A concave NfC function would increase faster at the beginning and slower towards the end, showing a greedy behavior.

Since the threshold policy implemented in the VOS approach ensures that the EV charging requirements are met before departure, the risk plays no role for EVs leaving according to schedule. The risk, however, may play a role for EVs leaving before the planned deadline, since with the current risk strategy they would be more likely to charge towards the end of the parking period.

From the aggregator's perspective, one could expect that a risk-affine strategy for the NfC brings more flexibility to the aggregator and contributes towards improved performance. Yet, extremely risky functions may cause also very fast growth of the NfC towards the end of the parking periods, which could have a negative effect on the algorithm's performance.

We define six alternative NfC signal designs for this study:

- NfC_{linear} - a linear approximation of the original NfC
- NfC_{safe} - a concave version based on the original NfC
- $\text{NfC}_{dynamic}$ - a function with varying convexity,
- NfC_{pow2} - convex function built from the square of the linear approximation
- NfC_{pow4} - convex function built from the 4th power of the linear approximation
- NfC_{pow8} - convex function built from the 8th power of the linear approximation

The first three signal designs provide insights on the effects of risk reduction on the algorithm's performance and the benefits for EVs. The last three signal designs

provide information on whether the algorithm's performance can be improved by increasing the risk. In the following we describe the signal design process.

The NfC is calculated by every EV on every time step. Since it depends on both the current battery level and the ratio between required and available times, its parameters constantly change. Therefore, for every EV and every time step, we generate an NfC function with the parameters valid at the given time. First, we calculate the current NfC value based on the original algorithm as in (4.1.5). Then, we use (4.1.5) and the arrival and departure times to generate the curve for the original NfC with the current parameters. Next, we identify the time interval and end points where the NfC takes values between C_{tar} and C_{QoS}. Finally, we identify the value pairs for the end points of the above interval ($k_{nfc.min}$, NfC_{min}) and ($k_{nfc.max}$, NfC_{max}).

To generate NfC_{linear} we produce a linear function crossing the end points. If we take a line to be $y = mx + b$, or $\text{NfC}_{linear} = mk + b$, we have:

$$m = \frac{\text{NfC}_{max} - \text{NfC}_{min}}{k_{nfc.max} - k_{nfc.min}} \tag{5.2.1}$$

$$b = \text{NfC}_{max} - m \cdot k_{nfc.max} \tag{5.2.2}$$

To generate NfC_{safe}, we reflect the original NfC on NfC_{linear}, resulting in:

$$\text{NfC}_{safe} = m \cdot \left(k_{dep} - \frac{k_{req}}{\text{NfC}_{linear}} \right) + b \tag{5.2.3}$$

The $\text{NfC}_{dynamic}$ is a linear combination of $\text{NfC}_{original}$ and NfC_{linear}, weighted by a safety factor F_{safety}. That is:

$$\begin{aligned} \text{NfC}_{dynamic} = {} & F_{safety} \cdot \text{NfC}_{safe} \\ & + (1 - F_{safety}) \cdot \text{NfC}_{original} \end{aligned} \tag{5.2.4}$$

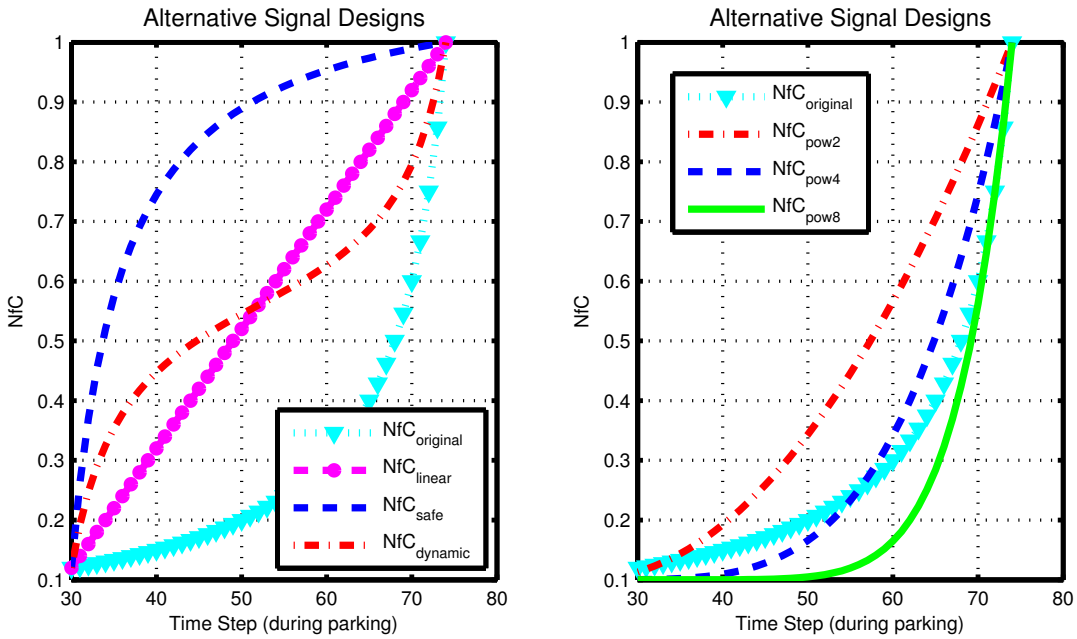

(a) (b)

Figure 5.2.2: Signal designs: (a) linear, safe, and dynamic NfC signal designs; and (b) pow2, pow4, and pow8 NfC signal designs

F_{safety} can take fixed or dynamic values between 0 and 1. An example of a dynamic value is:

$$F_{safety} = \text{NfC}_{linear} / \max(\text{NfC}_{linear}) \tag{5.2.5}$$

Figure 5.2.2a shows the original, linear, safe and dynamic versions of the NfC signal for an EV parked during the interval $k = [30, 80]$ and $E^i_{bat} = 10$kWh. For the NfC signal we use $C_{tar} = 0.1$ and $C_{QoS} = 1$ and $F_{safety} = 0.5$.

To generate NfC_{pow2}, NfC_{pow4} and NfC_{pow8}, we take the NfC_{linear} and increase it to the corresponding power. This results in a set of functions with similar parameters but different levels of convexity. Figure 5.2.2b shows these functions for the same EV mentioned above.

Although we use different NfC signal designs, in this paper we consider the case

where all EVs follow the same signal design within a given scenario. In other words, a game theoretic analysis, where different EVs can follow different risk strategies, is out of the scope of this work.

5.2.2 Results

We compare the original NfC design and the proposed designs by running one MCrun for each of them, following the experimental setup described in Section 4.4. Additionally, we evaluate the progress of the batteries' SOC during the parking period. To do so, we normalize all parking periods to a 10-interval period and extrapolate or average values accordingly. We then evaluate the SOC relative to the target SOC^i_{tar} on each interval. That is, if an EV had a target of 85% and by half of its parking period has reached 95%, the relative SOC for this period would be close to 1.12. This allows for an homogeneous evaluation for all EVs.

Algorithm Performance

Figure 5.2.3 summarizes the results for algorithm performance. We see a decrement in performance when using the NfC_{safe} design. In the safe design, EVs tend to behave more greedy and therefore reduce the flexibility of the aggregator. The NfC_{linear} and $\text{NfC}_{dynamic}$ designs offer very similar performance to that of the original design. We identified a slightly better performance of the dynamic design for fleets below 8 thousand EVs. Figure 5.2.4 illustrates how NfC_{pow2} to NfC_{pow8} designs show a significantly inferior performance.

These results suggest that a lower risk strategy with a linear or dynamic design does not have a significant impact on the performance. Furthermore, a higher risk strategy based on power versions of the linear design have a negative effect on performance. Since all EVs follow the same strategy and the aggregator always favors EVs with higher NfC, independently from how much higher the value is, a lower risk strategy provides comparable performance as long as the threshold values are not constantly being met.

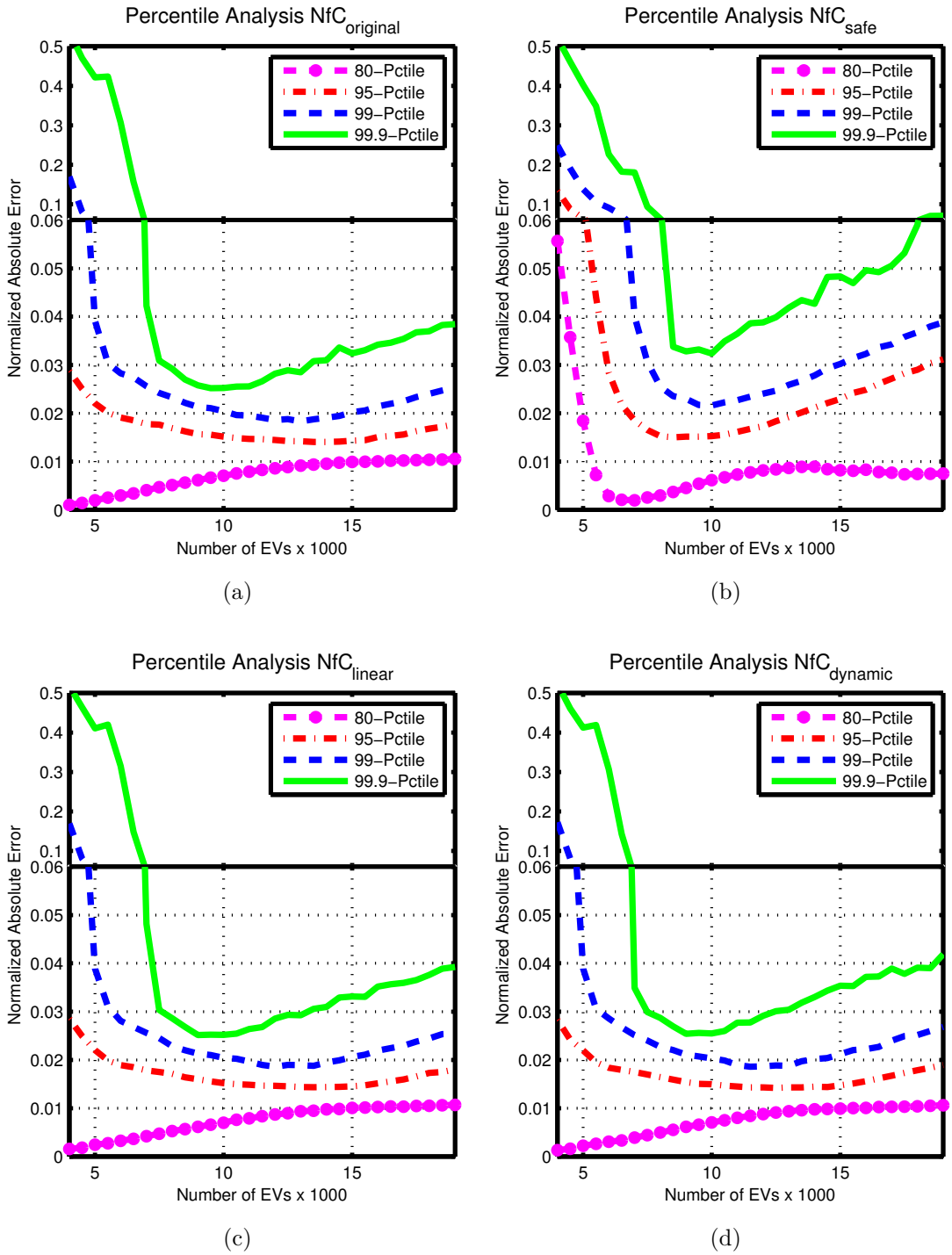

Figure 5.2.3: Original (a), safe (b), linear (c), and dynamic (d) NfC signal designs

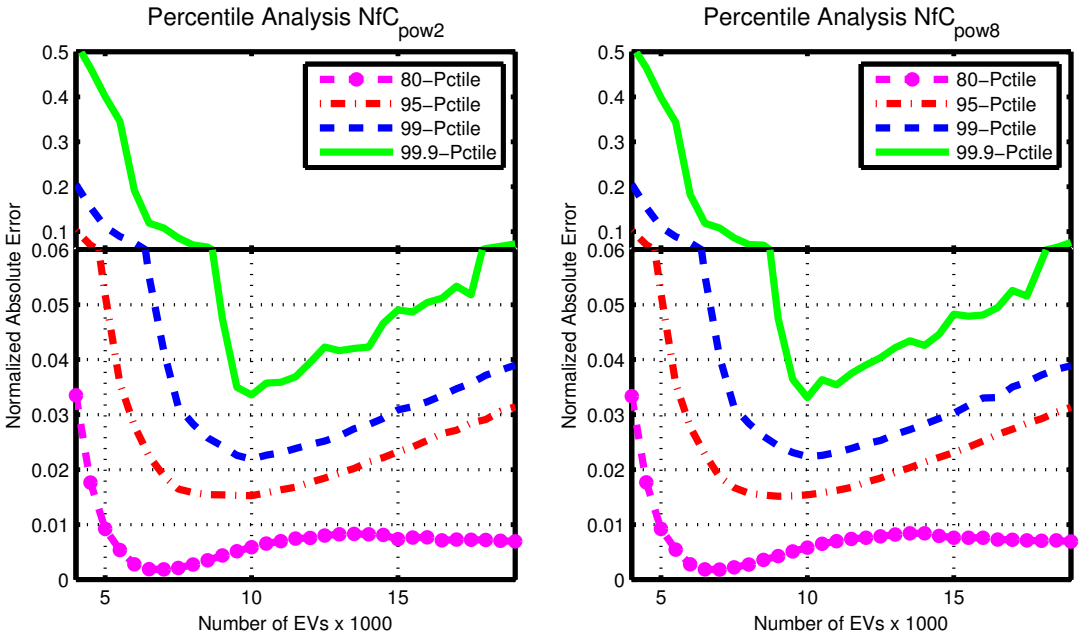

(a) (b)

Figure 5.2.4: Pow2 (a) and pow8 (b) NfC signal designs

EV Intermediate SOC

It is desired that, while keeping the performance, EV batteries charge as early as possible. In this way, they would be less affected in case of an early departure. Figure 5.2.5 shows the relative SOC for 25% and 1% of the EVs with the lowest relative SOC during their parking period. The results show that the lower 1% do benefit from a linear or dynamic risk strategy with a difference up to over 10% of additional SOC. Furthermore, a safe risk strategy has negative results which indicates that following a greedy strategy is decremental for both common and individual objectives. For the lower 25% the negative impact of the safe approach is more significant. Furthermore, the original NfC design performs slightly better than the linear and dynamic one at the beginning of the parking period. Our experiments also showed than on average there is little difference between the different strategies.

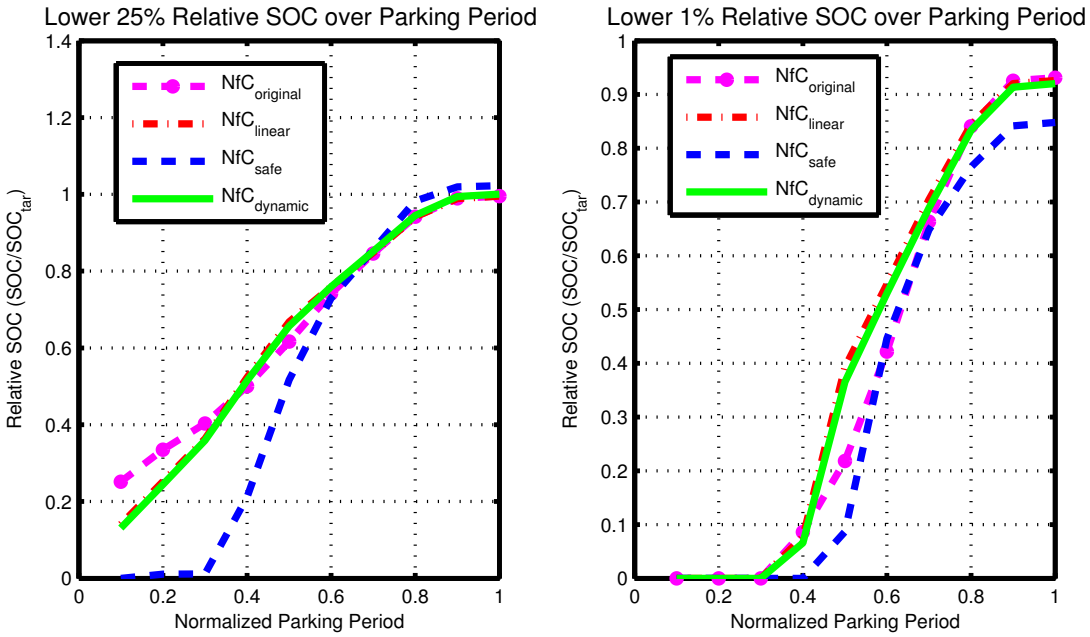

Figure 5.2.5: Lower 25% (a) and 1% (b) relative SOC values over a parking period

5.3 Discussion of VOS

This work presents the VOS approach and four main studies around it. First, a benchmark of the VOS approach against a centralized optimization alternative. Second, a reliability analysis, where we determine the upper bound of the error with a given probability. Third, a method for reducing the communication overhead of the VOS approach in terms of number of messages. Fourth, an alternative signal study with focus on global and individual performance.

Our benchmark analysis shows that the VOS approach offers a very attractive trade-off between computational complexity and performance. Furthermore, our experiments show good scalability with a linearly increasing solving time of less than one second per one million EVs. Although the benchmarks could be made more competitive by better tuning of the solvers, their solving time remains in the best case polynomial while the VOS approach shows a linear solving time, which could be further improved through parallelization.

Nevertheless, a combination of the VOS approach with an optimization approach could in some cases be appropriate. Offline optimization methods could be used for defining accurate objectives like day or hour ahead estimations, when solving time is not a major concern,. Optimization methods, where the aggregated EV behavior can be efficiently calculated regardless of the fleet size, could define grouped or clustered resources to be then individually allocated by the VOS approach.

Beyond its computational advantages, we would like to emphasize the flexibility of our approach. First, it decouples constraints and objectives so that EVs can readily change their priorities and objectives (e.g., battery lifetime maximization) without affecting the aggregator's design and vice versa. Second, it has low dependency on forecast accuracy since decisions are made only based on current information. Third, although it solves the problem only for the current time step, it does take into account future states of the EVs since this information is integrated in the NfC/WtS signals. Last, it preserves the EV owners' data privacy since only calculated scalars are sent.

To capitalize on the computational and flexibility benefits of the VOS approach, we need to demonstrate its applicability. The reliability analysis provides promising insights regarding this applicability. Through the reliability analysis, we quantify performance in terms of accuracy and respective probability. This analysis also allows us to determine the influence of P_D, P_S, and the fleet size on performance. Furthermore, it shows that the VOS approach works under different seasonal and weather conditions. This reliability metric could also be used to identify the crucial parameters of the VOS approach. In practice, it is a method that would allow an aggregator to define its commitments based on the fleet size or vice versa.

Our results show that the required fleet size to achieve a certain performance may decrease as the solar generation capacity increases. This has two positive consequences. First, it shows that the VOS approach could be a good method for facilitating distributed renewable energy integration using EVs. Second, it provides a future-proof alternative to aggregators as the solar penetration continues to increase.

Moreover, we also establish a relationship between the fleet size, the load, and the performance that enables aggregators to safely update their commitments proportional to the addition of new EVs to the fleet. For our Munich load leveling scenario, 6-10 thousand EVs for 3% of Munich's load provided good results. In other words, such a fleet size could level the load of an area with around 40 thousand inhabitants[1] with errors under 3% in 99.9% of the cases. This still requires 15% to 25% of the population to drive an EV. Such a level of penetration is only foreseeable in the long term.

The VOS approach can be made more message-efficient. The introduced modifications allow us to significantly reduce the number of exchanged messages, enabling a more efficient use of communication resources with negligible influence on performance and preserve the computational efficiency, modularity, and privacy-preserving characteristics of the approach. By exploiting this modularity, we split the problem into EV-to-aggregator and aggregator-to-EV message reduction.

EV-to-aggregator messages are reduced by around 80% by transmitting tree structures

[1]Proportion of load (F_{demand}) vs. served population [65]

containing future possible values in a single message, with the trade-off of an increased message size. To keep this size within applicable limits, we restrict it to one or a few MTUs resulting in message sizes within the kilobyte range. Since the MTU of a given path varies depending on the type of network and even varies with network utilization, one improvement could consider dynamically adjusting the message lifetime to the reported MTU (e.g., path MTU discovery) at a given time.

Aggregator-to-EV messages are reduced by broadcasting a single control signal as opposed to individual ones. This single message contains a pair of set point values and probability factors for NfC and WtS. Savings of over 99.9% are possible with a minor impact on performance.

Combining both approaches is possible but requires a retransmission protocol. Results show overall savings of more than 70% in comparison with the traditional VOS approach and improvements of at least 50% with respect to the two methods applied individually.

The message-efficient modification makes sense when the time steps or control periods become shorter, i.e., messages are exchanged on a seconds or shorter basis. For time steps in the minutes range, the benefits are limited. Larger time steps require less frequent communication but would tend to group message exchanges into smaller periods. This results in peaks of transmitted data, which may become critical when using the EV message reduction method, since messages increase in size. This issue can be addressed with protocols that distribute the load over a longer time frame.

One benefit of our modular approach is the possibility of an alternative signal design. Since the signal design is decoupled from the control, it is possible to modify it in order to reach a particular objective. Alternative signal designs could either improve the performance in terms of following a given power profile or increase the benefits to the EVs in terms of battery levels along the parking period. Results show that increased risk strategies may have a negative influence on performance as opposed to an expected positive one. Furthermore, the risk-moderate strategies studied, i.e., the linear and dynamic NfC designs, do not have a significant influence on the performance and provide an additional benefit to EVs: higher SOC levels at an earlier stage. In other words, too high risk aversion (i.e., greedy behavior) or too

high risk affinity have a decremental effect on both performance and individual EVs.

One limitation of the VOS approach is its performance for small EV fleets. We don't see this as a strong limitation since the advantages of our approach become more significant as the size of the problem increases. For small fleets, state-of-the-art optimization remains probably the best choice.

Although this is not a limitation of the approach, this work assumes that EVs also supply energy back to the grid (V2G). For this to be feasible, the economic benefits of doing so should be higher than the costs resulting from the increased use of the battery. Although we do not elaborate on this economic analysis, we believe that the WtS signal could be used as metric for assigning rewards.

Future work includes more elaborate and alternative designs for NfC and WtS signals with different objectives, both for EVs and the aggregator, e.g., for improved battery life or better aggregated performance. Including a DN topology, its corresponding power flow, and a set of aggregators allocated to certain neighborhoods could also provide new insights. In addition, different reference profiles and other renewable sources could be explored. For example, one could consider the predicted generation including wind as a reference profile and use the VOS approach to compensate, in addition to the local variations, for the difference between predicted and actual wind generation. Moreover, one could look into the extension of the approach to other flexible loads like heating, ventilation and air conditioning. From the game theoretic perspective, an interesting direction for future work could be the analysis of EVs following different strategies within the same fleet. Alternatively, new signal designs based on known economic utility functions could also be explored.

Chapter 6

EV Charging in Highway Environments

Electric vehicles may allow for emission reduction in urban areas and, due to their use-patterns in urban environments, can potentially operate as flexible electric loads to support the operation of power systems and the integration of renewable energy sources. However, this requires having a large number of electric vehicles and the wide adoption of EVs is challenging due to limitations in driving range and charging infrastructure. Range and infrastructure limitations are major factors in highway environments. ICT may be used to address these limitations to some extent.

This chapter presents a method for scheduling charging stops during highway travel such that the final destination is reached as early as possible. Section 6.1 introduces the charging scheduling algorithm for travel time minimization. Section 6.2 describes the simulation framework including the method for data-driven traffic generation. Section 6.3 introduces the use-case for the highway A9 in Germany from Munich to Berlin and corresponding results. Finally, 6.4 present a discussion.

6.1 Active Scheduling of Fast-Charging Stops

In this section, we introduce our active scheduling approach. First, we describe the objective, model, and notation. Then, we introduce our modified A* shortest path algorithm for constrained searches. Next, we briefly discuss the specific graph abstraction used for the constrained A* algorithm. Last, we present the complete process for schedule calculation and maintenance. The units of measurement referred to in the following are seconds for time, km for distance, km/h for speed, kW for power, and kWh for energy, unless otherwise specified.

6.1.1 Driving, Charging, and Scheduling Model

The proposed model comprises three main components: EVs, a highway or highway path, and CSs. An EV enters the highway and, if its trip is longer than its range, will stop at least once at a CS. The choice of charging stops depends on the strategy an EV follows; for example, an EV could choose to charge at the last reachable CS.

The charging strategy we propose aims at an intelligent choice of charging stops to minimize overall travel time. This strategy requires real-time information. The strategy assumes there is a communication infrastructure that allows for CS and EVs to communicate with each other and for EVs to receive highway-related information. None of these assumptions are beyond the capacity of existing technologies. Vehicles can be connected via mobile communication technologies for vehicles and persons (e.g., 2G - 4G). Existing fuel stations already have access to communication services, for example, for processing credit card payments.

When an EV enters the highway, it first surveys the CSs available on its route and their current states. The EV then calculates a desired set of charging stops and charging times and makes a booking for the corresponding CSs including expected arrival time. The EV's charging schedule may be adapted if highway or CS conditions change.

Along a given highway of length HL, there is a set of entries/exits $\mathbb{EX}$ and charging

stations $\mathbb{CS}$. Elements in $\mathbb{EX}$ are potential start and destination points for EVs, while elements in $\mathbb{CS}$ are potential charging stops. Exits and charging stations are characterized, among others, by their position on the highway. Additionally, a highway has a speed profile that defines the maximum driving speed as a function of time and position on the highway $V_{\mathrm{HW}}(s, k)$.

A position s on the highway can take values $[0, \mathrm{HL}]$ and can be given in two formats: absolute (highway kilometer) and relative to the driving direction (kilometer from origin point). That is, the absolute position increases in one direction and decreases in the opposite one, whereas the position relative to the driving direction always increases. In the following, we use s as a relative position unless denoted as s^{abs}.

A charging station $\mathrm{CS}_c \in \mathbb{CS}$ is characterized by the supported charger types and corresponding number of charging poles (CP) N_P^c. For each charger type, the CS has a queue $Q^c(k)$ representing those EVs in the CS waiting for a free CP, where $\mathrm{FP}^c(k)$ represents the number of free CPs. Each CS maintains its own booking system which includes estimated arrival and required charging time. Based on this booking system, a CP can estimate a queue length $\mathrm{Q}_{est}^c(k)$ for a given k in the future.

Individual characteristics of an EV are its trip, state, type, and schedule. The trip of the i^{th} EV is described by starting position S_{start}^i, starting time T_{start}^i, and destination position S_{end}^i. The EV's state at time k is characterized by the distance traveled $d_i(k)$, its position on the highway $s_i(k)$, the driving speed $v_i(k)$, a preferred speed $V_{pr}^i(k)$, the traveled, driven, waited, and charged times $t_{trav}^i(k)$, $t_{driv}^i(k)$, $t_{wait}^i(k)$, $t_{chrg}^i(k)$, respectively, and the state of charge (in percent) of the battery $SOC^i(k)$. The EV's state evolves in time steps of length Δt. The EV's type is characterized by model, maximum speed V_{max}^i, battery capacity E_{max}^i, minimum allowed battery level E_{min}^i, fast-charging power P_{FC}^i, a charging rate function in terms of time, charging power, and SOC $E_{chg}^i(\Delta t, P, SOC)$, and a consumption function in terms of speed and distance $E_{con}^i(\Delta d, v)$. Type parameters depend on the brand and model of the EV. The schedule $\mathbb{SD}^i$ is a set of tuples containing a planned CS to stop at, and the target SOC $(\mathrm{CS}_c, SOC_{tar}^{(i,c)})$ to continue the trip.

The state of an EV is updated depending on its driving flag DF^i, where

$$DF^i = \begin{cases} idl & : \text{EV not on highway} \\ drv & : \text{EV moving along the highway} \\ wai & : \text{EV arriving/at a CS but not charging} \\ chg & : \text{EV at a CS and charging} \end{cases} \tag{6.1.1}$$

such that

$$idl \rightharpoonup drv, \text{ when current } k \text{ reaches } T^i_{start} \tag{6.1.2}$$

$$drv \rightharpoonup wai, \text{ when EV enters a CS} \tag{6.1.3}$$

$$wai \rightharpoonup chg, \text{ when } \mathrm{FP}^c(k) > 0 \tag{6.1.4}$$

$$chg \rightharpoonup drv, \text{ when } SOC^i(k) \geq SOC^{(i,c)}_{tar} \tag{6.1.5}$$

$$drv \rightharpoonup idl, \text{ when } s^i(k) \text{ reaches } S^i_{end} \tag{6.1.6}$$

The state change in (6.1.3) occurs if the CS matching the EV's current position is included in the EV's schedule $\mathbb{SD}^i$. Equation (6.1.4) implies that a charging pole becomes available. Equation (6.1.5) indicates that the target SOC has been reached. Equation 6.1.6 implies that the EV has reached its final destination.

The distance traveled, position, and corresponding initial values of an EV are defined as:

$$d_i(k + \Delta t) = d_i(k) + \Delta d^i(k), \tag{6.1.7}$$
$$\text{with } \; d_i(0, \cdots, T^i_{start}) = 0$$

$$s_i(k + \Delta t) = s_i(k) + \Delta d^i(k), \tag{6.1.8}$$
$$\text{with } \; s_i(0, \cdots, T^i_{start}) = S^i_{start}$$

where:

$$\Delta d^i(k) = v_i(k) \cdot \Delta t_{(hr)} \tag{6.1.9}$$

$$v_i(k) = \begin{cases} \max\left(V^i_{pr}(k), V_{\text{HW}}(s_i(k), k)\right), & \text{if DF}^i = drv \\ 0, & \text{otherwise} \end{cases} \tag{6.1.10}$$

$V^i_{pr}(k)$ is given and $\Delta t_{(hr)}$ stands for the value converted into hours. Equation (6.1.10) implies that EVs will travel at their preferred speed unless the highway speed limit is lower.

Updates to the different time measurements are expressed as

$$\Delta t^i_{trav}(k) = \begin{cases} \Delta t, & \text{if DF}^i \neq idl \\ 0, & \text{otherwise} \end{cases} \tag{6.1.11}$$

$$\Delta t^i_{driv}(k) = \begin{cases} \Delta t, & \text{if DF}^i = drv \\ 0, & \text{otherwise} \end{cases} \tag{6.1.12}$$

$$\Delta t^i_{wait}(k) = \begin{cases} \Delta t, & \text{if DF}^i = wai \\ 0, & \text{otherwise} \end{cases} \tag{6.1.13}$$

$$\Delta t^i_{chrg}(k) = \begin{cases} \Delta t, & \text{if DF}^i = chg \\ 0, & \text{otherwise} \end{cases} \tag{6.1.14}$$

Finally, updates to the SOC of an EV is expressed as

$$SOC^i(k + \Delta t) = \begin{cases} SOC^i(k) - \Delta SOC^-_{(i,k)}, & \text{if DF}^i = drv \\ SOC^i(k) + \Delta SOC^+_{(i,k)}, & \text{if DF}^i = chg \\ SOC^i(k), & \text{otherwise,} \end{cases} \tag{6.1.15}$$

where:

$$\Delta SOC^-_{(i,k)} = \frac{E^i_{con}(\Delta d^i(k), v^i(k))}{E^i_{max}} \tag{6.1.16}$$

$$\Delta SOC^+_{(i,k)} = E^i_{chg}\left(\Delta t, P^i_{FC}, SOC^i(k)\right) \tag{6.1.17}$$

Equations (6.1.15 - 6.1.17) imply that EVs consume energy while driving, depending on the driving distance and speed, and gain energy depending on charging power

and current SOC. $E^i_{con}(\cdot)$ and $E^i_{chg}(\cdot)$ are EV-specific functions. $E^i_{con}(\cdot)$ indicates the consumption of a given EV as a function of traveled distance and speed while $E^i_{chg}(\cdot)$ indicates the energy gain as a function of time, charging power, and current SOC. Although our evaluation does not cover battery aging or driving style (e.g., [72]), one could update the definition of $E^i_{con}(\cdot)$ and $E^i_{chg}(\cdot)$ to account for these factors.

The objective of our scheduling strategy is to find a schedule $\mathbb{SD}^i$ such that the total travel time, including driving, waiting, and charging time, is minimized. The strategy has to fulfill the constraints of the individual EV and the highway.

$$\min_{\mathbb{SD}^i} \sum^{\hat{k}} \left(\Delta t^i_{driv}(\hat{k}) + \Delta t^i_{wait}(\hat{k}) + \Delta t^i_{chrg}(\hat{k}) \right), \quad \left\{ \hat{k} \mid S^i_{start} \leq s^i(\hat{k}) \leq S^i_{end} \right\} \tag{6.1.18}$$

s.t.

$$E^i_{min} \leq SOC^i(k) \cdot E^i_{max} \leq E^i_{max}, \forall\ k$$

The interpretation of (6.1.18) is as follows: for a given EV, choose a schedule such that the sum of driving, waiting and charging times along the duration of the trip are minimized, subject to the energy limitations of the EV. Although the problem formulation (6.1.18) may appear simple, its solution is not as simple. All quantities are time-dependent and are influenced by external factors. Equations (6.1.11 - 6.1.15) indicate that SOC and times depend on the vehicle state. The vehicle's state depends on position and time. Position depends on speed while driving, which depends on highway conditions. The portion of t^i_{wait} for a stop on a given CS depends on the length of the queue at that CS which correspondingly depends not only on the arrival time of the given EV, but also on when other EVs arrive.

One alternative for solving this problem is to use existing shortest path algorithms considering travel time as the weight or cost. However, existing shortest path algorithms, such as Dijkstra and A* search, normally do not account for constraints. Therefore, we introduce an enhanced A* shortest path search algorithm that accounts

for the constraints in this problem.

6.1.2 Constrained A* Path Search for Fast-Charging Schedules

The A* algorithm is widely used for shortest path searches and is based on a directed graph data-structure abstraction [73, 74]. Similar to Dijkstra's algorithm, it incrementally explores neighbors and accumulated weights to choose a path with the lowest weight. The A* algorithm includes a heuristic function to estimate the minimum remaining cost or distance at every node which can be used to accelerate the computation.

The main reasons for choosing A* as our base algorithm are threefold. First, neighbor exploration allows us to test for constraint fulfillment at every step and exclude non-feasible alternatives at an early stage. Second, the use of a heuristic function to calculate the minimum remaining cost is convenient because the earliest an EV can arrive at its destination is limited by distance and speed. Third, A* is a widely used algorithm with efficient implementations available for a variety of systems [75, 76], including embedded systems, which is relevant for the applicability of the proposed solution.

The conventional A* algorithm keeps track of the variable it aims to minimize along the entire search. In our case, that would be the traveled time $\hat{t}^i_{trav}$. We introduce a modification where we maintain a second variable, the available energy in the EV $\hat{E}^i$. Each time a neighboring node is explored, we test that the resulting value of $\hat{E}^i$ remains within $[E^i_{min}, E^i_{max}]$. If this is not the case, the corresponding potential path is avoided. This can be done, as in our case, by not queuing the neighbor into the queue of potential nodes, or alternatively assigning an extremely high cost to the corresponding path.

The constrained A* shortest path algorithm receives as input a graph describing all possible paths, the source and destination nodes, and the EV_i, including state and type. The specific implementation of the A* algorithm is based on [75]. The

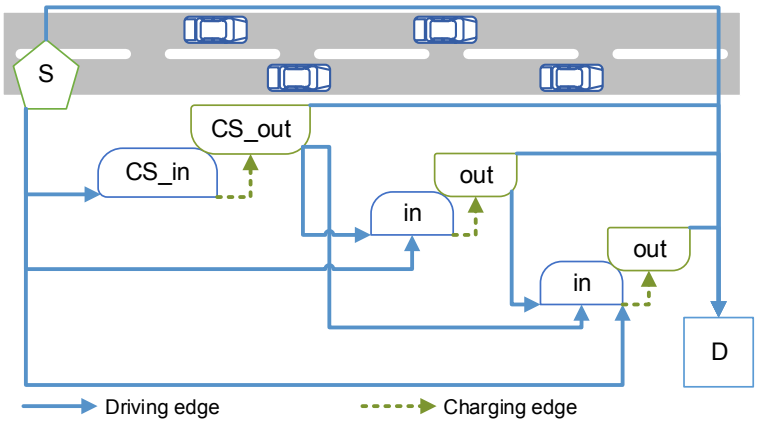

Figure 6.1.1: Graph abstraction

algorithm is described in the following.

The function **get_h_time(·)** is the heuristic function describing the minimum remaining time from a given node to the destination. In our case, it is a function of distance and speed. For an always underestimating heuristic, and resulting certainty that the found path is the shortest, one can use the EV's preferred speed V^i_{pr}. Less strict heuristic functions can be used to accelerate the algorithm.

The function **get_costs(·)** returns an estimation of both time cost and energy consumption between two nodes (or the graph's edge) and a feasibility statement. The edge is feasible only if the cumulated energy minus the consumption for that edge is within $[E^i_{min}, E^i_{max}]$. The time costs result from driving, waiting, and charging. Driving time is calculated based on the expected speeds along the route between nodes. Charging and waiting times depend on the predicted demand of a specific charging station. Energy consumption is positive during driving and negative while charging.

Algorithm 6.1.1

Algorithm 6.1.1: Constrained A* Shortest Path

```
function constrained_search(graph, src, dst, ev) returns path:

PriorityQueue queue,
Dict enqueued, explored

queue.push((0, src, 0, graph[src]['current_energy'], None))
while queue:

    o, this_node, time, cum_energy, parent ← queue.pop

    # If target reached, traverse path:

    if this_node == target:

        path ← [this_node]
        node ← parent
        while node is not None:
            path.append(node)
            node ← explored[node]
        path.reverse()
        return path

    if this_node in explored: continue

    explored[curnode] ← parent

    for neighbors in graph[this_node]:

        if neighbor in explored: continue
        e_cons, t_cost, feasible ← graph.get_costs(this_node, neighbor, cum_energy,
        ev)
        if not feasible: continue
        # Update accumulated values:
        e_ncost ← cum_energy - e_cons
        t_ncost ← time + t_cost
        # Compare with so-far-best:
        if neighbor in enqueued
            t_qcost, h_time ← enqueued[neighbor]
            if t_qcost ≤ t_ncost: continue
        else:
            h_time ← graph.get_h_time(neighbor, dst, ev)
        # Enqueue new so-far-best values:
        enqueued[neighbor] ←  t_ncost, h_time
        queue.push((t_ncost + h_time, neighbor, t_ncost, e_ncost, this_node))
```

6.1.3 Graph Abstraction for EV Charging Stops

Figure 6.1.1 illustrates the graphs abstraction of our approach. We have four type of nodes: one source node, one destination node, and a number of **CS_in** and **CS_out** node pairs (each of these node pairs represents a CS). By defining CSs as pairs of in/out nodes, we are able to differentiate between two types of edges: driving edges and charging edges.

A driving edge connects either the source node or a **CS_out** node to either a **CS_in** or the destination node. A driving edge cannot connect the **CS_out** node to the **CS_in** node of the same CS. If a driving edge ends on a **CS_in** node, the EV stops to charge. The costs of a driving node are the driving time and positive energy consumption. Both values depend on the driving speed which may be time-dependent and estimated based on current available data.

The speed and resulting cost and consumption calculations can be averaged over the entire distance between the two nodes or over blocks of shorter distances at a trade-off between precision and computation complexity. In our case, we opt for the more precise approach.

A charging edge connects a **CS_in** node to the **CS_out** node of the same CS. The time cost is a combination of waiting and charging time and is estimated by the corresponding CS on request. The waiting time depends on the expected length at the time of arrival which is calculated based on the existing bookings at the time of the request. The charging time depends on the estimated cumulated energy, charging power, and target SOC. Charging power is EV specific but a constant from the EV perspective. The target SOC is fixed to an ideal level, likely to be EV specific, but currently at 80% for existing commercial vehicles. A second process described in Section 6.1.4 adjusts this target SOC to the requirements of the chosen route.

To build the graph, an EV scheduler defines the source node as its current position and initializes the estimated cumulated energy to its actual energy level. Then, the scheduler submits a request for a list of available CSs between the current position and the destination and connects the nodes with edges, according to the

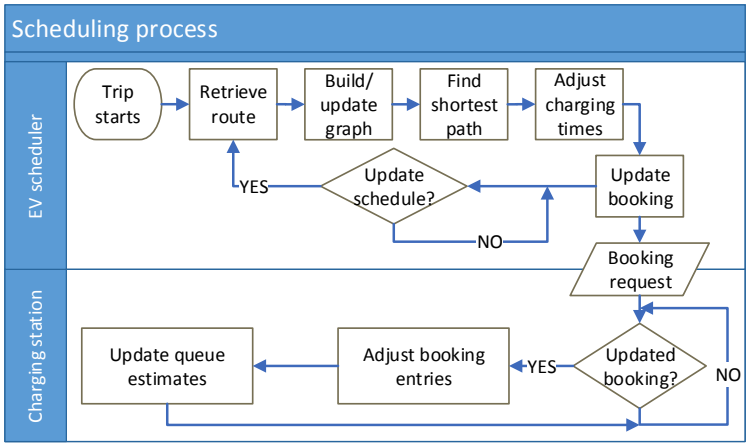

Figure 6.1.2: Scheduling process

logic described above. The graph can be updated by removing those edges ending in nodes located behind the current EV position, which, if done incrementally, incurs a marginal computational burden.

6.1.4 Schedule Generation Algorithm

Figure 6.1.2 summarizes the scheduling process for each EV. Upon initiating a trip or entering a highway, the EV retrieves its route. Next, it produces a graph abstraction and uses it to find the shortest path as described in Sections 6.1.2 and 6.1.3. Then, the charging times at each chosen stop are adjusted and the corresponding booking request is sent to the CS. The EV then continues the trip as planned unless an update schedule event is received, in which case, the process above is repeated. Upon receipt of a booking request, a CS will update its booking entries and process its corresponding queue estimates.

The route contains the destination, a list of CSs available on the way, and the highway information including speeds and traffic notifications. This information can come, for example, from the map or navigation system used by the EV. Most of the information, such as CSs on the route and posted speed limits, are static. Traffic information may change during a given trip.

Once the target charging stops are defined by the shortest path algorithm, the EV computes the target SOC ($SOC_{tar}^{(i,c)}$) for each stop. In the previous step, the path is calculated assuming a fixed target SOC, usually 80%. However, the distance between two planned stops might require less energy. Therefore, for each stop, the target SOC is calculated based on the energy required to reach the next planned stop, or the destination if it is the last stop. This calculation uses the EV's consumption function $E_{con}^{i}(\cdot)$ and desired driving speed V_{pr}^{i}, i.e., the worst case, and adds a certain margin on top.

The decision for calculating the target SOC on a second step is justified as follows. First, the A* algorithm requires a comparable value for weight of a given edge. This weight is measured in time and the time cost at a charging edge depends on the target SOC. Second, the A* is greedy in nature, that is, it evaluates the neighbors before moving to the next node. Calculating the required energy requires already knowing the next planned stop, which is not available when evaluating a given edge.

One could produce multiple node pairs connected with edges representing discrete values of different target SOCs. Alternatively, one could create functions for every possible path and try to apply an optimization technique to solve for target SOCs at each stop. The first option would increase the graph size significantly while the second option would result in several optimization problems with dynamics involved. Either option would challenge both the space and computational limits of embedded devices where ideally such a service would be installed.

Once the charging times have been adjusted, the EV has defined its schedule with a set of planned stops containing expected arrival time and target SOC. This information is then shared with each of the involved CSs in the form of booking requests.

Upon receipt of a booking request, each CS updates its planned bookings and recomputes its expected queues. A CS recomputes its expected queues by emulating the planned bookings and producing queue lengths for time windows of pre-defined length. The queue length at a given time window depends on the queue length at the previous time window, the arrivals at the current time window, the number of charging poles, and an average charging time.

The CSs become the coupling element on the system as they indirectly reflect the plans of other EVs. In other words, an EV planning to stop at a given CS bases its decision on the expected queue length, which correspondingly depends on the decision of other EVs. Individual EV decisions, therefore, depend on decisions made by other EVs.

In order to maintain up-to-date planned schedules, EVs need to recompute their path. If this is not done, the EV is at a disadvantage with respect to those EVs that have computed their path more recently. This action can be event-triggered. An event can be, for example, an increase in queue lengths of a CS over a certain threshold or a timer elapse.

The manner in which these events are triggered needs to be carefully considered. For example, triggering a re-schedule immediately after any EV has updated a booking may result in an unstable circumstance whereby all EVs cyclically react to each others' actions.

Since an EV is constantly updating its schedules, it is also indirectly adapting to what other EVs are doing. Although there is no guarantee that an equilibrium can be achieved, two statements hold true for our approach. First, an EV will only modify its path if there is a better path available. Second, any computed path remains feasible, independent of the actions of other EVs. In other words, an EV will follow a path that was, in the worst case, the shortest path possible the last time it checked, and, even if there may be a better path available, the chosen path remains compliant with the particular EV's constraints.

In terms of complexity, the determination of a the schedule benefits from its distributed computation and the underlying A* algorithm. Since the schedule is generated at EV level, its computation time does not directly depend on the number of EVs and remains constant as the number of EVs increases. The most computationally intensive task from the EV perspective is the modified A* shortest path search which only adds a constant time operation to the original A* algorithm. Computations performed by the CS do increase in complexity as the number of EVs increase. However, this complexity is proportional to the number of EVs served by each station and not the total number of EVs. In Section 6.3.2, we provide

experimental evidence for the performance and scalability of the approach.

6.2 Highway EV Traffic Simulation Framework

In this section, we introduce the highway EV traffic simulation framework used for our experiments. This traffic simulation network does not pretend to compete with comprehensive simulation tools like [77, 78]. However, it offers a simplified, modular, and adaptive alternative for studying different charging strategies for EVs along a highway. First, it produces highway trips based on highway-specific data and trip length statistics, producing trips that are closer to reality using publicly available data. Second, the EV traffic simulation framework allows for the insertion of highway specific parameters, such as exits, position of CS, and speed limits. Third, the framework can process time- and segment-specific speeds from external data sources to reproduce the current state of the highway like heavy traffic. Last, it enables the comparison of different scheduling strategies, accepting virtually any algorithm with a very simple interface.

6.2.1 Data-based EV Traffic Generation

The proposed method for generating EV highway trips is based on a combination of diverse data sources. In the following we describe the method and its application to German highways.

Traffic on highways varies by time of day, position, day of the week, season, and a long list of other factors. In many countries, counters at specific points on the highway provide insight on these variations. German highways are highly instrumented and hourly counts for each counter are accessible either as a statistical summary or as detailed entries upon request [79].

Lengths of trips also play an important role and this information cannot be inferred from the counter data. Therefore, a second source that provides this information is

needed. For the German case, a mobility survey includes a specific section regarding long distance trips [66]. This information allows us to classify trips by the size (population) of the place of origin.

Finally, the type of personal vehicle (e.g., size, energy consumption, category) may be of interest. Although the mobility survey [66] also surveys information on vehicle type, the relationship between type of vehicle and long distance trips is not addressed. Information on vehicle type is commonly available from data for car registrations, for example in Germany [80].

The first step for generating a trip is defining a potential counter where the EV in question was counted and the time this happened. This information is retrieved from the counter data in form of spatial and temporal distributions. The spatial distribution comprises the number of counts on a given station with respect to the total counts. Each counter has its own temporal distribution consisting of counts on a given hour with respect to the daily counts.

The spatial and temporal distributions can either be produced based on statistics and curves, such as those provided in [79], or produced from raw data with the hourly counts of an entire year. The proposed framework supports the raw data alternative including very flexible filtering alternatives for specific days, day of the week, month, and season.

Once a potential counter and hour of the day have been defined, the tool offers two alternatives for generating trips: vehicle was counted at the beginning of its trip, or vehicle was counted at a random point during its trip.

For the first alternative, we locate the closest exit to the position of the counter, and based on the size of cities close to this exit, we randomly sample a distance from the travel survey. We then adjust the distance to the closest available exit and choose the starting time randomly within the given hour.

The second alternative is more complex. First, we define a random proportion of the trip already covered when the EV was counted. Next, we sample a distance from the accumulated trip distribution of the travel survey and find the closest potential

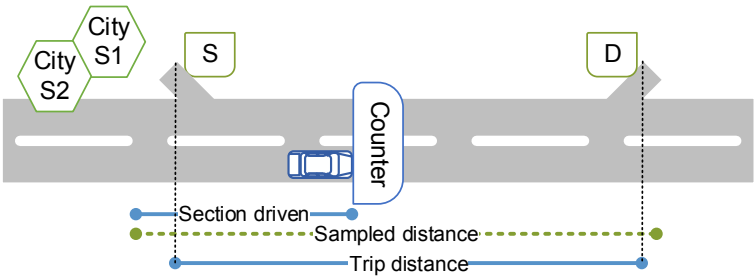

Figure 6.2.1: Trip generation with variable start point

exit corresponding to the already traveled distance. Then, we validate that such a trip length exists in the travel survey for the category of cities close to that exit and repeat the process if the validation fails. Last, we adjust the distance according to the closest exit and choose a start time within the hour interval. This alternative is illustrated in Figure 6.2.1

After start position, end positions, and starting time for a given trip have been defined, we choose an EV type based on the vehicle-type distribution. This process is repeated for all EVs in the simulation.

A validation of this method shows a comparable behavior between the generated trips and the counter data. An exact match is not possible because counter data also include commuter and local trips, which are not represented in our synthetic trips.

6.2.2 Simulation Tool

The architecture of the simulation tool is illustrated in Figure 6.2.2. The three main components are the EVs, the highway, and the CS. There is, in general, a many-to-one relationship between EVs and a highway as well as between CSs and a highway. The design supports multiple highways although this functionality has not been verified. The simulation tool is discrete-time-based, whereby the time steps can be set in seconds.

A CS component consists of a number of charging poles grouped into pole types (e.g.,

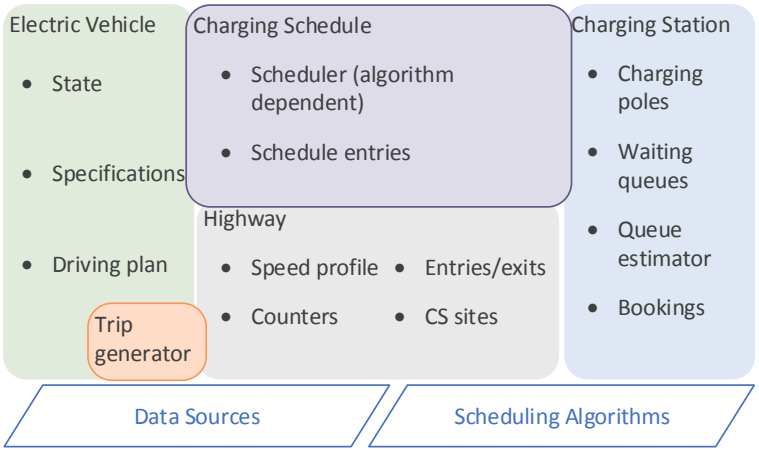

Figure 6.2.2: Simulation tool architecture

Tesla super charger and standard fast-charging poles) and a waiting queue per pole type. Each queue has a queue estimator that, based on the bookings of a given CS, updates estimated queue lengths along a given period (e.g., a day) for pre-defined intervals (e.g., 30 min). The results of this queue estimator are used by the charging schedule to evaluate potential waiting time at a given arrival time. CS are located on the highway at specific CS sites.

In addition to a number of CS sites, the highway consists of a speed profile, entires or exits, and counting stations. Counting stations are only used to maintain traffic statistics. Entries and exits are assumed to be a single point on the highway and always bidirectional, i.e., EVs can enter or leave the highway at this point. Similar to CS sites, entries and exits are characterized by their position on the highway and the driving direction in which they are located (although they are mostly located in both driving directions).

The speed profile of a highway consists of two sub-components: a static speed profile and a traffic notice profile. The static speed profile is a set of entries describing fixed speed limits along the highway and is position-dependent. The traffic notice profile is a set of entries describing temporal speed limits that can be updated during runtime. This type of entry is used to describe a time-dependent restriction (such as evening speed limits for noise reduction), externally set speed limits (such as those on

variable speed boards managed by a transportation authority), and traffic congestion. The speed profile is used by EVs to set their driving speeds along the highway and by the charging schedule to estimate driving times and energy consumption along the planned route.

An EV consists of state, specifications, and a driving plan. The state component takes care of updating the simulation-dependent parameters of the EV such as time, position, and current SOC. The specifications are used to calculate vehicle-specific allowed speeds, charging rate, and speed-dependent energy consumption while driving. The driving plan executes the charging stops following the charging schedule.

A charging schedule component is responsible for planning and managing the charging stops for an EV. It resides in the EV but interacts with the highway and CS components. The scheduler applies an algorithm to define a charging strategy and uses the EV's current state and specifications to estimate future states along the highway. As explained above, the scheduler influences the EV's driving plan and makes use of the highway speed profile and the CS queue estimations. The scheduler produces schedule entries which are also shared with the corresponding CS to update its bookings. This component is flexible and can be used to realize virtually any scheduling strategy with two constraints: the scheduler should implement the **generate_schedule** and **update_schedule** functions, and the resulting schedule entries must follow a specific format. The strategy presented in Section 6.1 is implemented with the charging schedule component.

The trip generator applies the data-based traffic generation described in Section 6.2.1. Other data sources include highway details (such as exits and speed limits), geographical information (cities and population), and CS details (position, number of poles, and pole types).

6.3 Evaluation

We apply our scheduling method and simulation framework to a use-case based on the German highway A9 from Munich to Berlin. First, we describe the use-case and the experimental setup. Then, we present the corresponding results.

6.3.1 Use Case

The A9 connects Berlin and Munich. Our study is concerned with the driving direction Munich to Berlin. The highway has 36 traffic counters [79], 79 exits/entries, and 45 CS locations. The exact position of exits, counters, CS locations, and the driving speed limits are based on [81] and manual inspection in Google Maps. The 45 CS locations reflect existing fuel stations along and near the highway plus existing or planned Tesla Super Charger locations [82]. The number of charging poles on each Tesla CS location follows the information in [82]. For the remaining CS, we consider four 50kW fast-charging ports per location. Some of these CS locations are only accessible in one driving direction.

To model the time it takes to reach a CS location from the highway, a penalty time is associated to each CS location. In our case, we select one time-step (5 min) for CSs located directly on the highway and 2 time-steps (10 min) for those located nearby but not directly on the highway.

We consider four types of EVs. Three are based on commercial specifications: Nissan Leaf, BMW i3, and Tesla S, and one is defined as a generic model. The generic model consumes 0.15 kWh per km. For the other three EV types, the consumption curves are produced by fitting curves to data available from [83, 84, 85, 86]. The EV types are uniformly distributed and we define a preferred driving speed of 120 km/h for all EVs. The EV-specific parameters are described in Table 6.3.1.

Table 6.3.1: EV parameters for evaluation

Parameter	Tesla S	BMW i3	Nissan Leaf	Generic
Battery capacity (kWh)	85	18	24	16
Maximum speed (km/h)	223	160	135	130
Charging power (kW)	120	50	50	50
Time (min) to $SOC_{tar} = 80\%$	40	30	30	30

The consumption curves are defined by the following functions.

$$E_{con}^{Tesla}(d, v) = \frac{7.41v^5 - 266v^4 + 51,590v^3 + 679v^2 + 29.83v - 0.061}{v^4 + 458.1v^3 - 1647v^2 - 758.8v + 490.3} \cdot d \quad (6.3.1)$$

$$E_{con}^{BMW}(d, v) = (0.00625v^2 + 0.725v + 50) \cdot d \quad (6.3.2)$$

$$E_{con}^{Leaf}(d, v) = (0.008837v^2 + 0.1393v + 63.26) \cdot d \quad (6.3.3)$$

In [87], a more detailed description of these functions is provided.

We generate trips for a period of 24 hrs but continue to run the simulation for another 24 hrs to allow all EVs to reach their destination. The time step is 5 minutes and the queue estimator for the CS generates estimates for 15 minute windows.

We use the same generated set of trips and EVs to run the simulation for two strategies: last in range (LiR) and active scheduling (AS). In the LiR strategy, EVs will charge at the last CS they are able to reach. The AS strategy implements the method proposed in Section 6.1

We run experiments as described in Table 6.3.2.

Table 6.3.2: A9 fast charging scenarios

Experiment	Description
1. LiR vs. AS	We compare the two strategies under the same experimental conditions assuming that the speed profile remains constant along the entire simulation.
2. AS under varying traffic conditions	We run the AS strategy in two modalities: i. schedule generation only on initiation of the trip, and ii. continuous schedule update. We then insert a traffic notice with 50 km/h speed limit for the segment between km 250 and km 350, between 15:00 and 16:00, inserted during runtime at 15:00. This experiment evaluates the adaptive capacity of the AS.
3. Uniform trip generation	We compare LiR and AS for trips starting in Munich and ending in Berlin with a uniform random starting time within 24 hours. This experiment gives us some insights about the global benefit of local EV decision making.
4. Potential as planning methodology	We compare LiR and AS but with an infinite number of charging poles on this station. This experiment gives some insight on the number and location of required charging poles if we were to achieve zero waiting times.

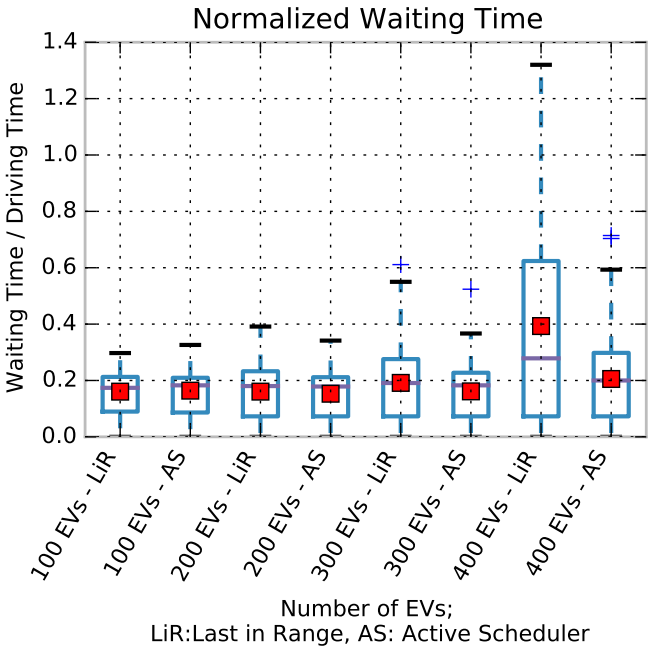

(a)

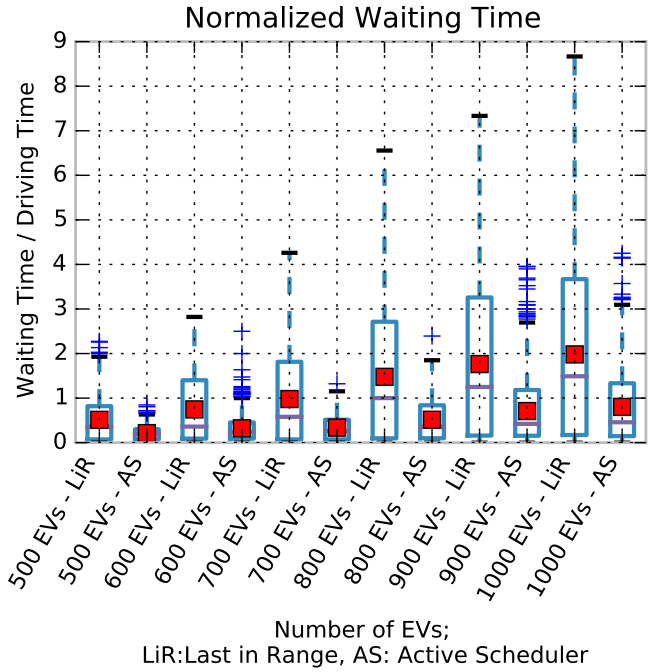

(b)

Figure 6.3.1: Normalized waiting time for different daily number of EVs

6.3.2 Results

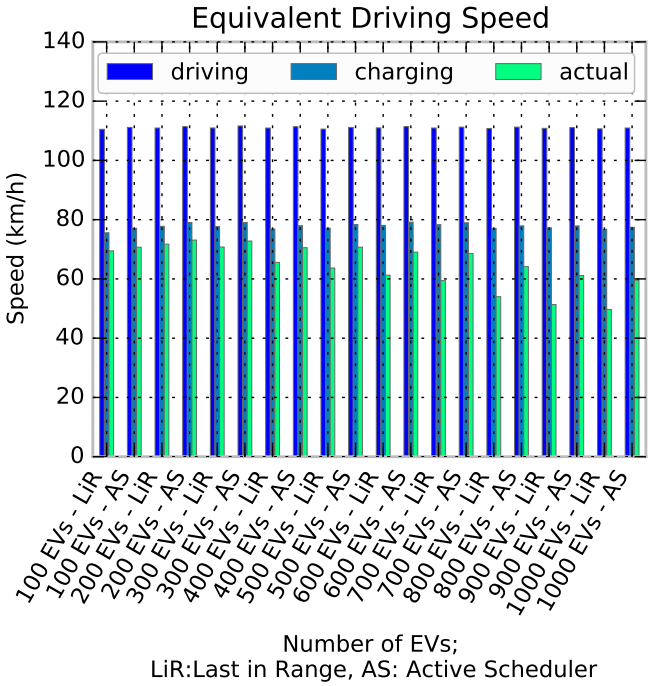

Figure 6.3.2: Mean equivalent driving speeds for different daily number of EVs

LiR vs. AS

We first evaluate the waiting time. For results to be comparable between EVs and different traffic volumes, we normalize the waiting time over the driving time. That is, the time spent waiting at CSs as a fraction of the driving time.

Figure 6.3.1 shows the statistics in form of a boxplot of the normalized waiting time for different values of daily EV traffic volume. The results show that the waiting time is significantly reduced when using the AS approach. All descriptive statistics indicate a significant improvement in waiting time when applying our method.

The normalized waiting time provides a comparable measurement between EVs and traffic volumes, and a ratio between waiting time and driving time. A more intuitive measurement is presented in Figure 6.3.2. Here, we see the average equivalent driving

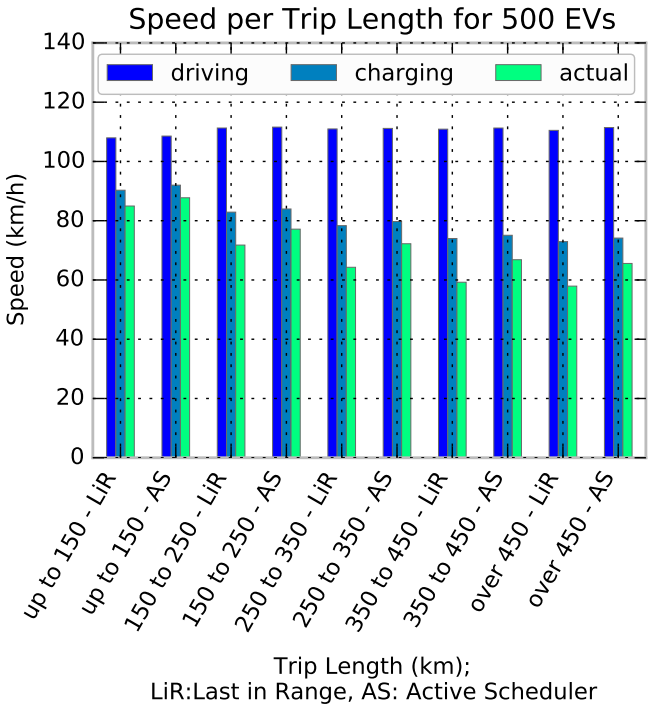

Figure 6.3.3: Mean equivalent driving speeds for 500 EVs by trip distance

speeds when the charging time and, cumulatively, the waiting time are taken into account. As depicted in this figure, for an average driving speed of 110 km/h, if we take into consideration the time needed only to charge, the equivalent speed would be 80 km/h. From this reference, the waiting time reduces the speed further. Using our approach increases the equivalent driving speed significantly, although the resulting speed is still low with respect to the driving speed due to the charging time.

The benefits of applying the proposed scheduling strategy become more evident as the traffic volume increases since the amount of available resources become proportionally scarcer. The benefits also become more evident as the length of trips increase. Figure 6.3.3 shows the influence of the trip length on the driving speed. In Figure 6.3.4 we see the proportion of the traveled time which is used for driving, charging, and waiting for trips of different lengths. Here we see that the scheduling algorithm succeeds in reducing the waiting time but also, due to the charging-time adjustment, we are able to reduce the time EVs spent charging.

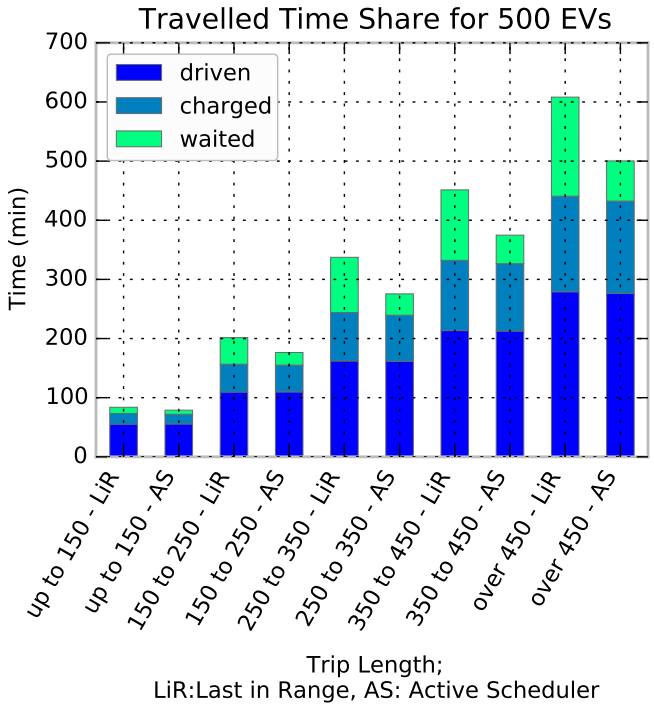

Figure 6.3.4: Proportion of traveled time (mean) for 500 EVs by trip distance

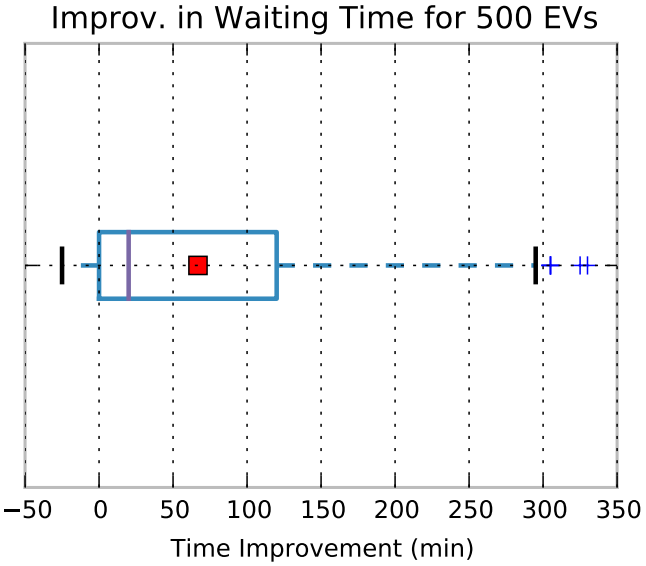

Figure 6.3.5: Vehicle-specific waiting time improvement for 500 EVs

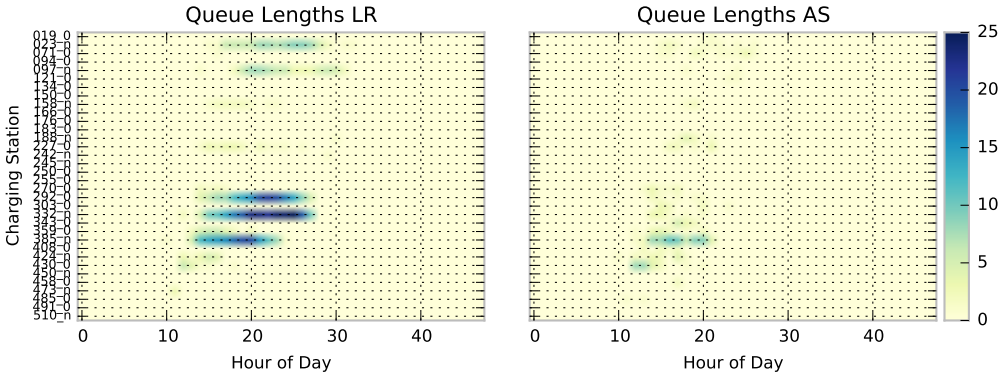

Figure 6.3.6: Queue lengths per CS and time for 500 EVs

We also compare the individual performance of every EV. In Figure 6.3.5 we see that most of the 500 EVs reduced their waiting time by several minutes. Few EVs ended up with a longer waiting time which was never longer than 30 minutes (the charging time for a single EV). This result suggests that although EVs optimize for their own benefit only, given the coupling effect of CSs, a collective benefit is also achieved.

Finally, we look into the queue lengths of the different CS vs. time of the day. Figure 6.3.6 shows the queue lengths for a daily traffic volume of 500 EVs. When the AS strategy is used, EVs tend to distribute themselves more uniformly among the available CSs. This is consistent with findings from previous work [23, 21] where a uniform use of CS is the objective for optimal utilization. Figure 6.3.7 shows the queue lengths for different daily numbers of EVs along the highway.

Energy consumption at the CS is also positively influenced by the active schedules. Although the daily peak energy consumption cannot be entirely avoided due to the charging demand, the energy consumption along the day is better distributed among the CSs. Figure 6.3.8 shows this effect for a daily traffic volume of 500 EVs.

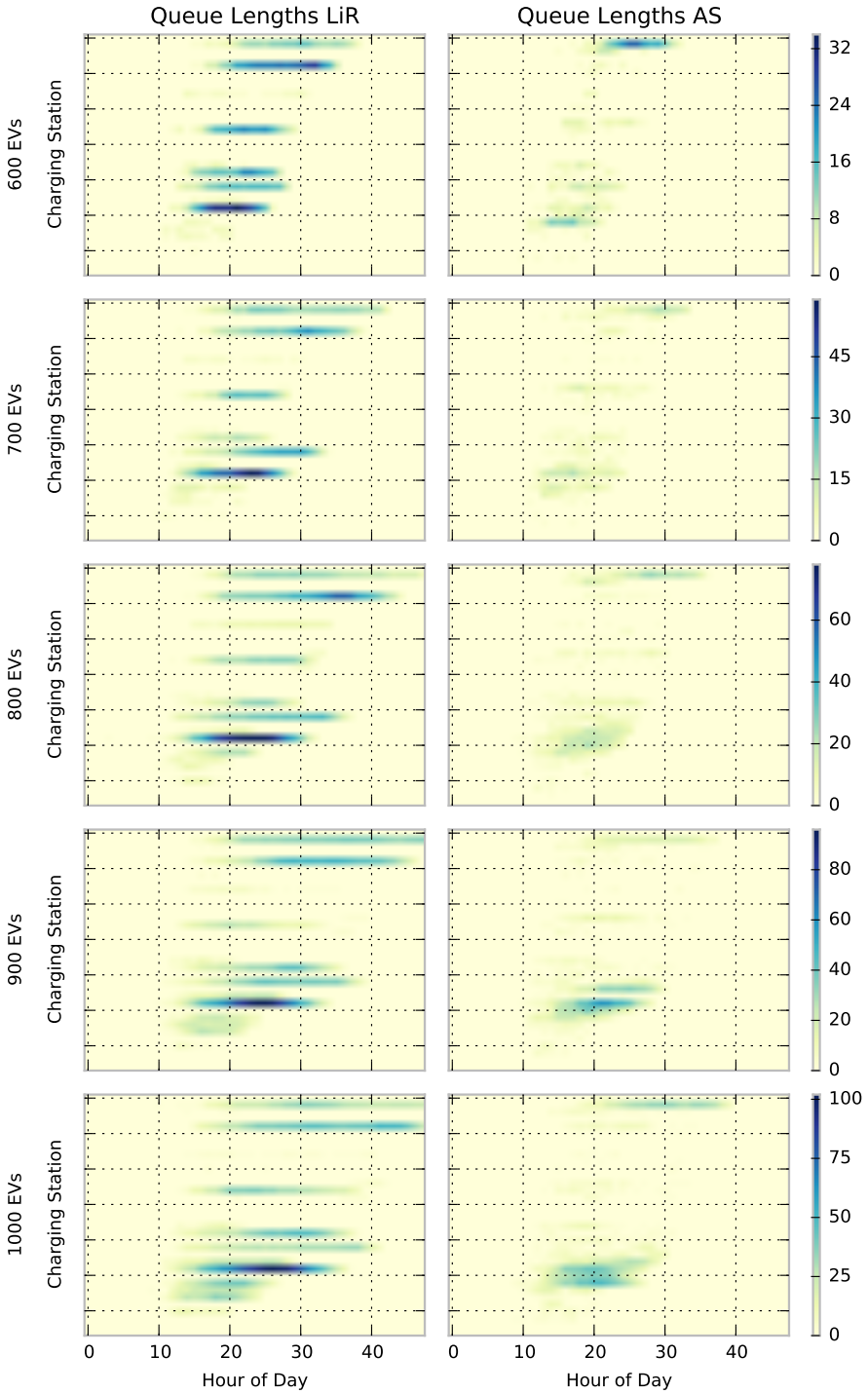

Figure 6.3.7: Queue lengths per CS and time for different traffic volumes

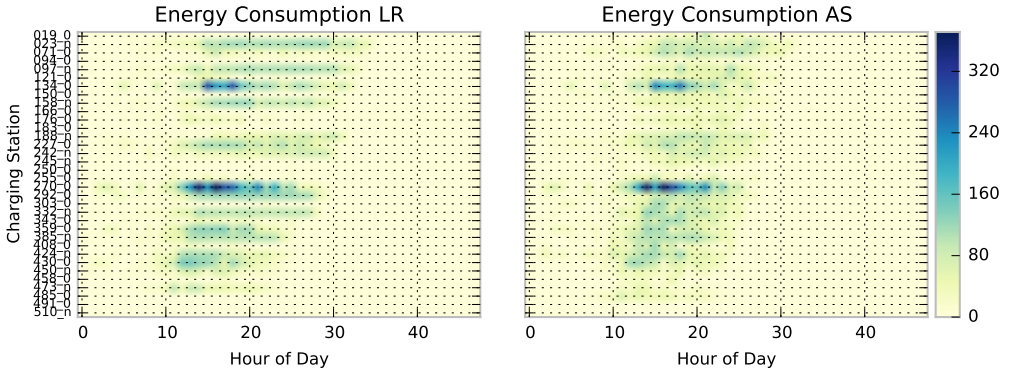

Figure 6.3.8: Energy consumption per CS and time for 500 EVs

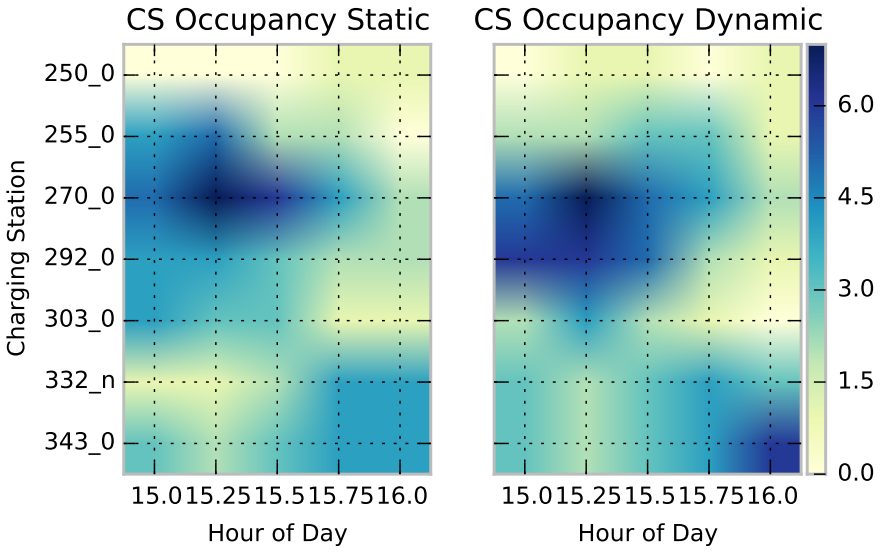

Figure 6.3.9: CS utilization on slow traffic

AS under varying traffic conditions

Since the scheduling algorithm considers the total travel time, one would expect it to readjust when a notice of a change in traffic conditions is added. In Figure 6.3.9, we see the utilization of CS (busy poles plus queues) and times of the inserted traffic notice for static and continuously updated schedules. One can see a more intense use of CS when updating the schedules which indicates that charging at the time of slow moving traffic was convenient for some of the vehicles.

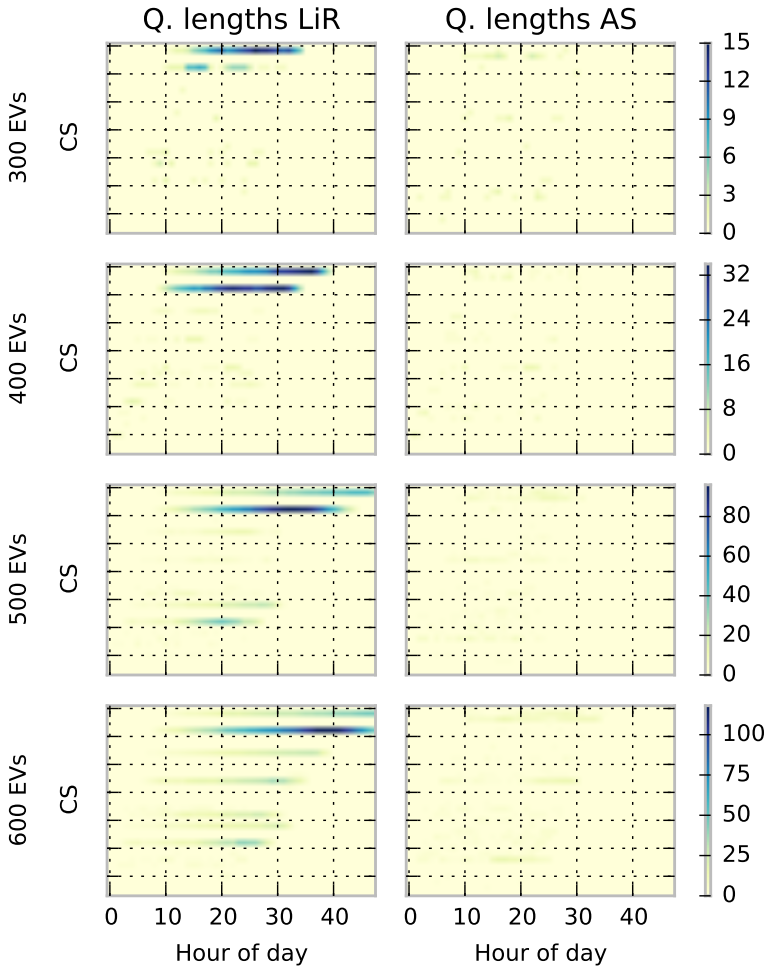

Figure 6.3.10: Queue lengths for uniform trip generation

Uniform trip generation

Figure 6.3.10 presents the results for the uniform-trip experiment. Since all EVs start from the same location, LiR is expected to perform poorly as many EVs will tend to stop at the same locations. However, a consistent trip length together with a uniform time distribution allows us to experimentally evaluate the performance of our approach in terms of the global optima. The authors in [23, 21] define a balanced distribution of EVs to CS as the objective for global optimization. In Figure 6.3.10, we see that, despite the high correlation between trips, the AS strategy results in balanced waiting queues.

Potential as planning methodology

The proposed framework can potentially be used for planning activities. Provided that the simulated trips are representative of the highway traffic, the simulation tool can be used to estimate the demand at the different CSs for a given charging strategy. In other words, this experiment provides insights on how to dimension the different target CS locations.

For this purpose, we run the simulation with an unlimited number of charging poles at each CS and evaluate their maximum and average demand. The results are shown in Figure 6.3.11. The demand at each CS varies depending on the chosen strategy, i.e., LiR or AS, however, one can already identify key CSs where demand is high for both strategies.

One can iteratively use such an approach to plan and dimension CS sites. For example, one could choose to remove CS sites with the lowest demand and repeat the experiments iteratively. Alternatively, one could assign a given amount of resources to each CS proportionally to the result of this experiment.

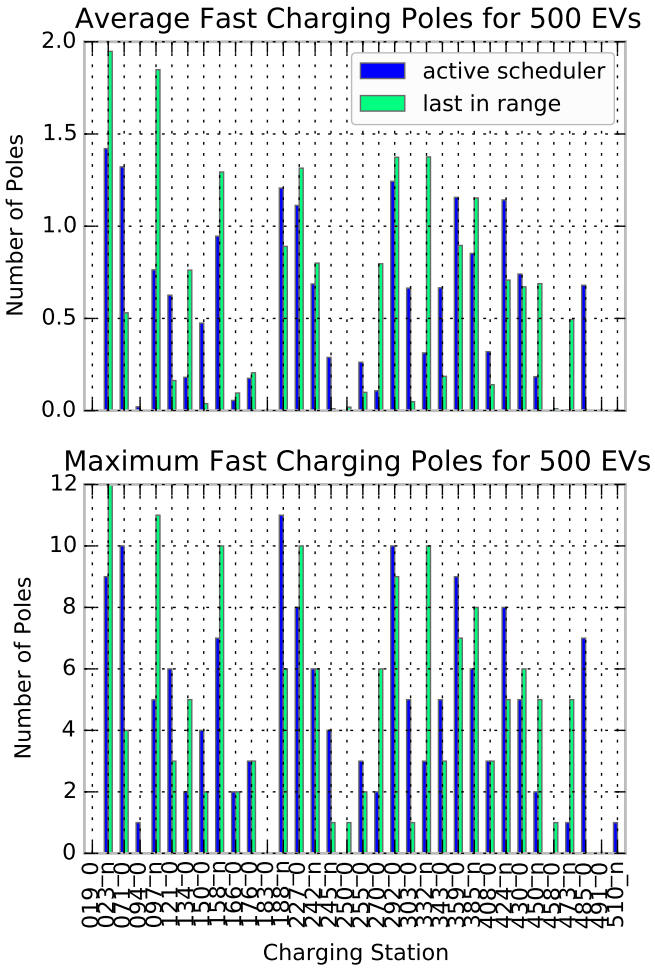

Figure 6.3.11: Average and maximum number of busy poles

Complexity

Figure 6.3.12 and 6.3.13 illustrate the mean, 75-percentile and maximum computation times of EV and CS operations, respectively, as the number of EVs increases.

The computation time of EV operations remains constant as the number of EVs increases. The worst case does increase slightly. This is not due to an increase of complexity itself. As the number of EVs increases and CSs become busy, certain EVs will in some cases need to search further for different CSs to find the shortest path.

The computation time of CS operations increases proportionally to the number of EVs but at a moderate rate. The worst case increases faster but this is mostly limited to peak demand times at the busiest CSs.

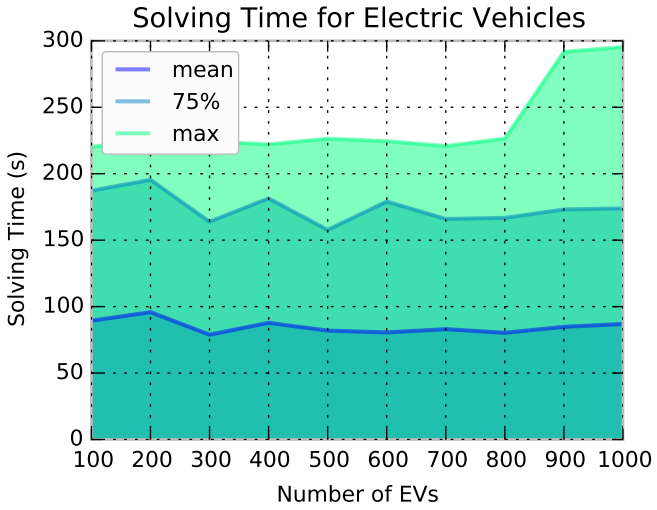

Figure 6.3.12: Computation times for EVs

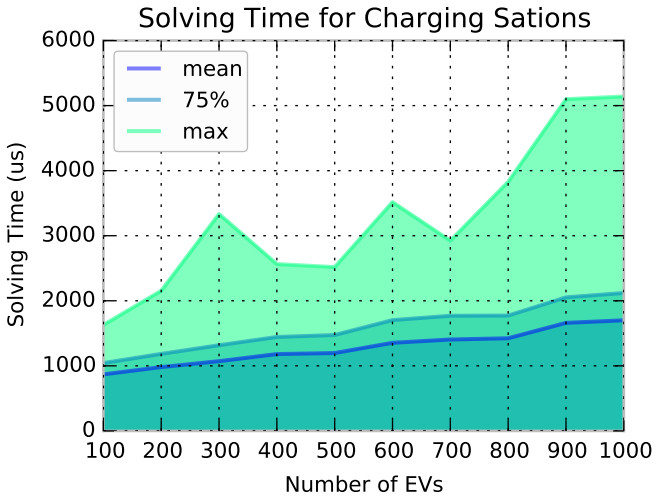

Figure 6.3.13: Computation times for CSs

6.4 Discussion of Active Scheduling on Highways

The proposed strategy for scheduling fast-charging stops in a highway environment considers a number of factors from the applicability perspective. First, the required information, such as CS location, estimated arrival times, and traffic situation, is already provided by commercial navigation products and is a target of further improvements with oncoming trends in inter-vehicular communication and GPS tracking. Second, the complexity of the algorithms that are to be executed in the EV is moderate and comparable to current capabilities of navigation products such as route planning. Third, the information exchange is limited since only the planned stop is communicated externally, meaning that data, such as EV-state, start, destination, speed, etc., remain private. Fourth, the communication requirements are also moderate and achievable with existing technology. Last, the solution is scalable due to its distributed nature.

As part of the EV's equipment or as a mobile device, communication technology is readily available for vehicles. Since CS infrastructure is relatively new, i.e., there is no significant legacy equipment in the field, one would expect CSs to be equipped with some kind of communication technology which, in addition to smart applications such as the one presented in this work, would be required at least for electronic payment purposes.

The proposed approach benefits from scalability since most of the computation is performed at the EV and some at the CS. Although the computational requirements of the CS are proportional to the number of EVs, this is only true for those EVs planning to stop at a particular CS and not the total number of EVs on the road.

Our approach is based on local decision making and execution for each EV without the direct influence of the actions of other EVs. However, the estimated queue lengths of each CS work as coupling variables. These estimates reflect the decision of other EVs and are constantly updated. Our results suggest that this coupling achieves a global benefit although we cannot qualify the result as a global optimum or social equilibrium.

A global approach could potentially improve the results. There are, however, a number of disadvantages, particularly from the applicability perspective. A centralized approach faces scalability challenges as the number of EVs and CSs increase. A distributed global approach would likely require more communication than the amount proposed here. Finally, a global approach would probably require more information from EVs to assign resources which could be undesirable from a privacy perspective.

We believe this work is relevant towards increasing EV penetration. Due to their limited range and long charging times, EVs are not the best choice for highway trips and their price does not justify them as a second "city-only" car. That said, even if we succeed in reducing the travel time, success can only be achieved if charging technology, battery prices, and energy density continue to evolve. Nevertheless, the proposed approach can be generalized to other candidate technologies such as hydrogen or battery swap since they all require new infrastructures and significant investments.

Since charging time is a major factor on highway trips, we do not consider ancillary or support services, such as frequency regulation, to the power grid. In our opinion, these services are provided by EVs which stay idle or parked generally longer than the time they need to charge; for example, at home or at work. By reducing the disadvantages of EVs for long trips, we hope that more EVs become available to provide these kind of services in urban and suburban environments. Alternatively, one could explore the use of CSs on highways (i.e., not EVs directly) for supporting the power grid, provided that they are equipped with local energy storage and generation capabilities; for example, batteries and photovoltaic panels.

A direct benefit of our approach for the power grid is the predictability of power requirements for the different CSs for a given day. Since CSs are booked and estimated arrival times are constantly updated, both medium and short term estimates of power consumption can be derived, facilitating the energy supply and balance tasks of the operator or utility.

From the simulation framework perspective, the data-driven trip generation is an important contribution but is also subject to further improvement. We concentrate

on publicly available data sources which in some cases are built from statistical studies. In particular, we are unable to separate commuting from long-distance traffic based only on counter data. Richer data sources, for example GPS traces or highway specific studies and surveys, could contribute to more realistic solutions.

In terms of accuracy of traffic models, our simulation network uses the highway speed value for simulating vehicle flows. Therefore, it can potentially be integrated with more evolved traffic simulation tools that provide the vehicle's speed as output. Furthermore, speed would also be the input in the real-life scenario where EVs drive to a given desired speed bounded either by speed limits or traffic conditions.

From the security perspective, our work assumes that EVs are honest and fair-players. However, security concerns should be studied further. A reliable authentication and monitoring mechanism is required to prevent EVs or intruders from intentionally overbooking CSs, for example. Although we partially protect privacy through distributed computation and limited information exchange, security best practices should be applied in both communication and data storage.

Another benefit of the proposed approach is that it can be extended to networked environments, that is, when more than one highway is used. EVs use their route as the planning starting point and the relevant information is the location and state of a CS along the route, independent of the highway on which they are located. Similarly, bookings depend on planned stops on a given CS and do not depend on the EV's origin, destination or specific route. This flexibility, however, does not apply to our simulation framework as, to date, only single highway simulation is supported. From the simulation framework perspective, one could look into an extension to networked environments and potential integration with specialized traffic simulation tools or open source projects such as OpenTraffic[88].

Potential future work includes the following. From the scheduling perspective, one could explore the benefits of considering driving speed as one of the decision variables. Also, a secondary load management between CS could be studied. Finally, a market-style scheduling with dynamic pricing based on CS state and EV preferences could be considered. In this case, energy prices could vary from CS to CS, where prices could be influenced by the charging demand from EVs and even power grid factors,

such as higher than predicted solar power generation.

From the battery perspective, one could explore the influence of driving styles (e.g., [72]) and battery aging. On the one hand, a more sportive driving style may influence the range significantly. On the other hand, since fast charging influences battery aging, one could explore how this could be considered in the decision variables.

Chapter 7

Conclusions

Renewable energies are a promising alternative to reduce CO2 emissions and mitigate climate change. While the share of energy generated from renewable sources has significantly increased, renewable generation incorporates new challenges into how electricity has been traditionally generated, transmitted, and consumed. As the share of energy from non-dispatchable renewable sources like wind and solar continues to increase, demand-side management and energy storage are becoming more relevant as methods to maintain this balance.

Transportation electrification, offers important advantages. First, it reduces local carbon emissions and fossil-fuel dependency. Second, it shifts energy needs towards a power system that is increasingly able to produce energy from renewable sources. EVs, in particular, allow for emission reduction in urban areas and, due to their use-patterns in urban environments, can potentially operate as flexible electric loads, or even as storage, to support the operation of power systems and the integration of renewable energies.

The environmental benefits of EVs can only be materialized if the number of EVs is large enough and the required technology and infrastructure are in place. On the one hand, control approaches for coordinated EV charging need to be efficient and realizable with moderate investments. On the other hand, known drawbacks of EVs

like range and charging time need to be addressed.

In this work, we analyze the use of EVs from two perspectives. First, we look into the EV as a tool for supporting power systems, and therefore the integration of renewable energies, by using them as controllable loads and even energy storage, particularly on residential environments. Second, we analyze strategies for the efficient use of fast charging infrastructure for long trips which contributes towards a higher EV adoption. In both perspectives, we put strong focus on the role of ICT technologies in the solution to these problems.

The Vehicle-Originating-Signals approach for real-time EV charging control aims at minimizing the variability of the aggregated power profile with respect to a given reference. First, we benchmark the VOS approach against a centralized optimization alternative and focus on mean squared error and solving time for the evaluation. Then, we perform a reliability analysis, where we determine the upper bound of the error with a given probability. Next, we introduce a method for reducing the communication overhead of the VOS approach, where we measure the improvements in terms of message reduction and the impact on performance in terms of error percentiles. Last, we show how alternative signals can be produced and their effect on global and individual performance. For the evaluation, we use a load leveling scenario for Munich based on real power consumption data and a driving survey.

The VOS approach benefits from distributed computation that enables scalability, some degree of privacy-preserving, and use-case-specific adaptation such as message reduction. Results show an attractive trade-off between computational resources and performance and a reliable behavior, measured not only on average but also in percentile, at least in the presented use cases. Furthermore, we show that it is possible to reduce the message requirements with limited effects on performance.

In terms of the efficient use of fast charging infrastructure for long trips, we propose a dynamic scheduling approach, based on a modified A* algorithm with constraint verification, for EVs to plan charging stops in a highway environment and minimize the total travel time. These schedules are continuously updated to account for changes in traffic and charging station utilization along the trip. The computation and communication requirements of the proposed solution remain moderate, which

contributes to applicability. We also introduce a simulation framework that includes the generation of EV trips using a data-driven approach and support for time-dependent highway parameters. We apply our approach to a use-case for the German highway A9 from Munich to Berlin.

Using the proposed approach, waiting times and overall travel times can be significantly reduced, leading to the more efficient use of resources. By considering the estimated state of the CSs as input for the algorithm, we achieve indirect coordination between EVs. Additionally, by dynamically adjusting the schedules, the proposed approach accounts for changes on the highway, such as slow traffic on a given segment.

Future work related to the VOS approach includes (i) more elaborate and alternative designs for NfC and WtS signals with different objectives, both for EVs and the aggregator, e.g., for improved battery life or better aggregated performance; (ii) including a DN topology, its corresponding power flow, and a set of aggregators allocated to certain neighborhoods; (iii) exploring different reference profiles and other renewable sources. Moreover, one could look into the extension of the approach to other flexible loads like heating, ventilation and air conditioning. From the game theoretic perspective, an interesting direction for future work could be the analysis of EVs following different strategies within the same fleet.

In terms future work on EV charging on highways, one could explore the benefits of considering driving speed as one of the decision variables. Also, a secondary load management between CS could be studied. Additionally, a market-style scheduling with dynamic pricing based on CS state and EV preferences could be considered. In this case, energy prices could vary from CS to CS, where prices could be influenced by the charging demand from EVs and even power grid factors, such as higher than predicted solar power generation. Finally, one could explore the influence of driving styles (e.g., [72]) and battery aging.

The VOS approach provides promising starting points for designing resource-efficient flexible load and storage control systems. It can be generalized to different loads and objectives and could enable new business models for aggregators. With market price

differences of 15%-30% between base and peak loads, 5%-15%[1] in futures contracts and probably more in bilaterally agreed long-term contracts, we believe that there are sufficient economic incentives to realize the type of systems evaluated in this paper.

To fully take advantage of such an approach, a large number of EVs is necessary. Our work on fast charging scheduling on highways has the potential to improve the driving experience and EV adoption rates with a limited cost, both economical and computational. With ongoing projects for fast-charging infrastructures [82, 90], the use of this type of approach can have a positive impact in terms of investment and success of these projects and the overall EV adoption.

[1] From random price samples [89]

List of Figures

List of Tables

List of Algorithms

Bibliography

[1] IEA, International Energy Agency. "Tracking Clean Energy Progress 2015: Energy Technology Perspectives 2015 Excerpt IEA Input to the Clean Energy Ministerial." In: *OECD/IEA* (2015). URL: http://www.iea.org/publications/freepublications/publication/clean-energy-progress-report.html (visited on 11/26/2015).

[2] United Nations. *United Nations Framework Convention on Climate Change*. 1992. URL: https://unfccc.int/resource/docs/convkp/conveng.pdf.

[3] Intergovernmental Panel on Climate Change. *Climate Change 2014: Mitigation of Climate Change: Working Group III Contribution to the Fifth Assessment Report of the Intergovernmental Panel on Climate Change*. Assessment report. Cambridge University Press, 2015. ISBN: 9781107058217.

[4] IEA, International Energy Agency. *CO2 EMISSIONS FROM FUEL COMBUSTION: HIGHLIGHTS*. 2015 Edition. OECD/IEA, 2015.

[5] Organisation for Economic Co-operation and Development/International Energy Agency and International Renewable Energy Agency. *IEA/IRENA Global Renewable Energy Policies and Measures Database*. URL: http://www.iea.org/policiesandmeasures/renewableenergy/ (visited on 04/2015).

[6] P. Kundur, N. J. Balu, and M. G. Lauby. *Power system stability and control*. New York and London: McGraw-Hill, 1994. ISBN: 9780070359581.

[7] B. Metz, O. Davidson, P. Bosch, et al. *Climate change 2007: Mitigation of climate change : contribution of Working Group III to the Fourth Assessment Report of the Intergovernmental Panel on Climate Change*. Cambridge and New York: Cambridge University Press, 2007. ISBN: 9780511366512.

[8] B. Bilgin, P. Magne, P. Malysz, et al. "Making the Case for Electrified Transportation." In: *IEEE Transactions on Transportation Electrification* 1.1 (2015), pp. 4–17.

[9] A. Emadi. "Transportation 2.0." In: *IEEE Power and Energy Magazine* 9.4 (2011), pp. 18–29.

[10] B. K. Sovacool and R. F. Hirsh. "Beyond batteries: An examination of the benefits and barriers to plug-in hybrid electric vehicles (PHEVs) and a vehicle-to-grid (V2G) transition." In: *Energy Policy* 37.3 (2009), pp. 1095–1103.

[11] S. Han, S. Han, and K. Sezaki. "Development of an Optimal Vehicle-to-Grid Aggregator for Frequency Regulation." In: *IEEE Transactions on Smart Grid* 1.1 (2010), pp. 65–72.

[12] A. Y. Saber and G. K. Venayagamoorthy. "Intelligent unit commitment with vehicle-to-grid – A cost-emission optimization." In: *Journal of Power Sources* 195.3 (2010), pp. 898–911.

[13] J. Rivera, C. Goebel, and H.-A. Jacobsen. "Distributed Convex Optimization for Electric Vehicle Aggregators." In: *IEEE Transactions on Smart Grid* (2016), pp. 1–12. DOI: 10.1109/TSG.2015.2509030.

[14] G. Binetti, A. Davoudi, D. Naso, et al. "Scalable Real-Time Electric Vehicles Charging With Discrete Charging Rates." In: *IEEE Transactions on Smart Grid* (2015).

[15] M. D. Galus, S. Koch, and G. Andersson. "Provision of Load Frequency Control by PHEVs, Controllable Loads, and a Cogeneration Unit." In: *IEEE Transactions on Industrial Electronics* 58.10 (2011), pp. 4568–4582.

[16] W. Yao, J. Zhao, F. Wen, et al. "A Hierarchical Decomposition Approach for Coordinated Dispatch of Plug-in Electric Vehicles." In: *IEEE Transactions on Power Systems* 28.3 (2013), pp. 2768–2778.

[17] C. Goebel and D. S. Callaway. "Using ICT-Controlled Plug-in Electric Vehicles to Supply Grid Regulation in California at Different Renewable Integration Levels." In: *IEEE Transactions on Smart Grid* 4.2 (2013), pp. 729–740.

[18] A. Schroeder and T. Traber. "The economics of fast charging infrastructure for electric vehicles." In: *Energy Policy* 43 (2012), pp. 136–144.

[19] S. S. Zhang. "The effect of the charging protocol on the cycle life of a Li-ion battery." In: *Journal of Power Sources* 161.2 (2006), pp. 1385–1391.

[20] S.-N. Yang, W.-S. Cheng, Y.-C. Hsu, et al. "Charge scheduling of electric vehicles in highways." In: *Mathematical and Computer Modelling* 57.11-12 (2013), pp. 2873–2882.

[21] H. Qin and W. Zhang. "Charging scheduling with minimal waiting in a network of electric vehicles and charging stations." In: *Proceedings of the Eighth ACM International Workshop on Vehicular Inter-networking*. VANET '11. New York, NY, and USA: ACM, 2011, pp. 51–60.

[22] C. Bodet, A. Schulke, K. Erickson, and R. Jablonowski. "Optimization of charging infrastructure usage under varying traffic and capacity conditions." In: *Smart Grid Communications (SmartGridComm), 2012 IEEE Third International Conference on*. 2012, pp. 424–429.

[23] A. Gusrialdi, Z. Qu, and M. A. Simaan. "Scheduling and cooperative control of electric vehicles' charging at highway service stations." In: *2014 IEEE 53rd Annual Conference on Decision and Control (CDC)*. 2014, pp. 6465–6471.

[24] V. del Razo and H.-A. Jacobsen. "Smart Charging Schedules for Highway Travel with Electric Vehicles." In: *IEEE Transactions on Transportation Electrification* 2.2 (2016).

[25] V. del Razo, C. Goebel, and H.-A. Jacobsen. "Vehicle-Originating-Signals for Real-Time Charging Control of Electric Vehicle Fleets." In: *IEEE Transactions on Transportation Electrification* 1.2 (2015), pp. 150–167.

[26] V. del Razo, C. Goebel, and H.-A. Jacobsen. "Reducing Communication Requirements for Electric Vehicle Charging using Vehicle-Originating-Signals." In: *IEEE SmartGridComm*. 2014, pp. 7–12.

[27] V. del Razo, C. Goebel, and H.-A. Jacobsen. "On the effects of signal design in electric vehicle charging using vehicle-originating-signals." In: *Computer Science-Research and Development* 31.1 (2016), pp. 49–56.

[28] V. del Razo, C. Goebel, and H.-A. Jacobsen. "Benchmarking a Car-Originated-Signal Approach for Real-Time Electric Vehicle Charging Control." In: *IEEE PES ISGT*. 2014.

[29] B. M. Weedy, B. J. Cory, N. Jenkins, et al. *Electric Power Systems*. Wiley, 2012. ISBN: 9781283645065.

[30] M. H. J. Bollen and F. Hassan. *Integration of distributed generation in the power system*. IEEE press series on power engineering. Hoboken: Wiley-Blackwell, 2011. ISBN: 9781118029015.

[31] J. Zhu. *Optimization of power system operation*. Second edition. Vol. 47. IEEE press series on power engineering. Wiley, 2014. ISBN: 9781118854150.

[32] W. Su, H. Eichi, W. Zeng, and M.-Y. Chow. "A Survey on the Electrification of Transportation in a Smart Grid Environment." In: *IEEE Transactions on Industrial Informatics* 8.1 (2012), pp. 1–10.

[33] V. C. Gungor, D. Sahin, T. Kocak, et al. "A Survey on Smart Grid Potential Applications and Communication Requirements." In: *IEEE Transactions on Industrial Informatics* 9.1 (2013), pp. 28–42.

[34] A. Woyte, V. Thong, R. Belmans, and J. Nijs. "Voltage Fluctuations on Distribution Level Introduced by Photovoltaic Systems." In: *IEEE Transactions on Energy Conversion* 21.1 (2006), pp. 202–209.

[35] L. Pieltain Fernandez, T. Gomez San Roman, R. Cossent, et al. "Assessment of the Impact of Plug-in Electric Vehicles on Distribution Networks." In: *IEEE Transactions on Power Systems* 26.1 (2011), pp. 206–213.

[36] J. Lassila, V. Tikka, J. Haakana, and J. Partanen. "Electric cars as part of electricity distribution – who pays, who benefits?" In: *IET Electrical Systems in Transportation* 2.4 (2012), pp. 186–194.

[37] P. Papadopoulos, S. Skarvelis-Kazakos, I. Grau, et al. "Electric vehicles' impact on British distribution networks." In: *IET Electrical Systems in Transportation* 2.3 (2012), pp. 91–102.

[38] L. Gan, U. Topcu, and S. H. Low. "Optimal Decentralized Protocol for Electric Vehicle Charging." In: *IEEE Transactions on Power Systems* 28.2 (2013), pp. 940–951.

[39] Y. He, B. Venkatesh, and L. Guan. "Optimal Scheduling for Charging and Discharging of Electric Vehicles." In: *IEEE Transactions on Smart Grid* 3.3 (2012), pp. 1095–1105.

[40] P. Richardson, D. Flynn, and A. Keane. "Local Versus Centralized Charging Strategies for Electric Vehicles in Low Voltage Distribution Systems." In: *IEEE Transactions on Smart Grid* 3.2 (2012), pp. 1020–1028.

[41] N. Rotering and M. Ilic. "Optimal Charge Control of Plug-In Hybrid Electric Vehicles in Deregulated Electricity Markets." In: *IEEE Transactions on Power Systems* 26.3 (2011), pp. 1021–1029.

[42] S. Martinenas, A. B. Pedersen, M. Marinelli, et al. "Electric vehicle smart charging using dynamic price signal." In: *IEEE International Electric Vehicle Conference (IEVC)*. 2014.

[43] K. Clement-Nyns, E. Haesen, and J. Driesen. "The Impact of Charging Plug-In Hybrid Electric Vehicles on a Residential Distribution Grid." In: *IEEE Transactions on Power Systems* 25.1 (2010), pp. 371–380.

[44] T. van der Klauw, M. E. T. Gerards, G. J. M. Smit, and J. L. Hurink. "Optimal scheduling of electrical vehicle charging under two types of steering signals." In: *IEEE PES Innovative Smart Grid Technologies Conference Europe (ISGT-Europe)*. 2014.

[45] M. Huber, A. Trippe, P. Kuhn, and T. Hamacher. "Effects of large scale EV and PV integration on power supply systems in the context of Singapore." In: *2012 ISGT Europe*. 2012.

[46] Z. Ma, D. S. Callaway, and I. A. Hiskens. "Decentralized Charging Control of Large Populations of Plug-in Electric Vehicles." In: *IEEE Transactions on Control Systems Technology* 21.1 (2013), pp. 67–78.

[47] W. Tushar, W. Saad, H. V. Poor, and D. B. Smith. "Economics of Electric Vehicle Charging: A Game Theoretic Approach." In: *IEEE Transactions on Smart Grid* 3.4 (2012), pp. 1767–1778.

[48] C. Harris, I. Dusparic, A. Marinescu, et al. "Set Point Control for Charging of Electric Vehicles on the Distribution Network." In: *IEEE PES ISGT*. 2014.

[49] W. Kempton and J. Tomić. "Vehicle-to-grid power fundamentals: Calculating capacity and net revenue." In: *Journal of Power Sources* 144.1 (2005), pp. 268–279.

[50] Y.-W. Wang and C.-C. Lin. "Locating road-vehicle refueling stations." In: *Transportation Research Part E: Logistics and Transportation Review* 45.5 (2009), pp. 821–829.

[51] Y.-W. Wang and C.-R. Wang. "Locating passenger vehicle refueling stations." In: *Transportation Research Part E: Logistics and Transportation Review* 46.5 (2010), pp. 791–801.

[52] N. Sathaye and S. Kelley. "An approach for the optimal planning of electric vehicle infrastructure for highway corridors." In: *Transportation Research Part E: Logistics and Transportation Review* 59.C (2013), pp. 15–33.

[53] S.-Y. Kim, H.-W. Jung, J.-D. Hwang, et al. "A study on the construction of EV charging infrastructures in highway rest area." In: *Power Engineering, Energy and Electrical Drives (POWERENG), 2013 Fourth International Conference on*. 2013, pp. 396–400.

[54] Y. Nie and M. Ghamami. "A corridor-centric approach to planning electric vehicle charging infrastructure." In: *Transportation Research Part B: Methodological* 57 (2013), pp. 172–190.

[55] S. Bae and A. Kwasinski. "Spatial and Temporal Model of Electric Vehicle Charging Demand." In: *IEEE Transactions on Smart Grid* 3.1 (2012), pp. 394–403.

[56] Q. Gong, Y. Li, and Z.-R. Peng. "Trip based optimal power management of plug-in hybrid electric vehicles using gas-kinetic traffic flow model." In: *American Control Conference, 2008*. 2008, pp. 3225–3230.

[57] M. Rahman, Qi Duan, and E. Al-Shaer. "Energy efficient navigation management for hybrid electric vehicles on highways." In: *Cyber-Physical Systems (ICCPS), 2013 ACM/IEEE International Conference on*. 2013, pp. 21–30.

[58] S. Pourazarm, C. G. Cassandras, and A. Malikopoulos. "Optimal routing of electric vehicles in networks with charging nodes: A dynamic programming approach." In: *2014 IEEE International Electric Vehicle Conference (IEVC)*. 2014, pp. 1–7.

[59] S. Storandt. "Quick and energy-efficient routes." In: *the 5th ACM SIGSPATIAL International Workshop on Computational Transportation Science*. Ed. by S. Winter and M. Müller-Hannemann. 2012, pp. 20–25.

[60] D. Helbing, A. Hennecke, V. Shvetsov, and M. Treiber. "Micro- and macro-simulation of freeway traffic." In: *Mathematical and Computer Modelling* 35.5-6 (2002), pp. 517–547.

[61] M. Treiber, A. Kesting, and D. Helbing. "Three-phase traffic theory and two-phase models with a fundamental diagram in the light of empirical stylized facts." In: *Transportation Research Part B: Methodological* 44.8-9 (2010), pp. 983–1000.

[62] S. P. Boyd and L. Vandenberghe. *Convex optimization*. Cambridge University Press, 2004.

[63] F. C. Schweppe and S. K. Mitter. "Hierarchical system theory and electric power systems." In: *Proceedings Symposium on Real Time Control of Electric Power Systems*. 1972, pp. 259–277.

[64] U. S. DOE. "Communications requirements of Smart Grid technologies." In: *US Department of Energy, Tech. Rep* (2010), pp. 1–69.

[65] SWM Infrastruktur GmbH. *Netzdaten*. 2013. URL: `http://www.swm-infrastruktur.de/strom/netzstrukturdaten/netzdaten.html`.

[66] infas / DLR. *MiD 2008: Mobilität in Deutschland 2008: Nutzerhandbuch*. 2010. (Visited on 06/08/2013).

[67] The MathWorks Inc. *MATLAB R2013a*. 2013.

[68] J. Löfberg. "YALMIP: A Toolbox for Modeling and Optimization in MATLAB." In: *Proceedings of the CACSD Conference*. 2004.

[69] G. O. Inc. *Gurobi Optimizer Reference Manual*. 2013. URL: http://www.gurobi.com.

[70] J. A. Storer. *An introduction to data structures and algorithms*. Birkhäuser and Springer, 2002.

[71] J. W. Pratt. "Risk Aversion in the Small and in the Large." In: *Econometrica* 32.1/2 (1964), p 122–136.

[72] M. Jafari, A. Gauchia, K. Zhang, and L. Gauchia. "Simulation and Analysis of the Effect of Real-World Driving Styles in an EV Battery Performance and Aging." In: *IEEE Transactions on Transportation Electrification* 1.4 (2015), pp. 391–401.

[73] W. Zeng and R. L. Church. "Finding shortest paths on real road networks: the case for A*." In: *International Journal of Geographical Information Science* 23.4 (2009), pp. 531–543.

[74] M. J. De Smith, M. F. Goodchild, and P. Longley. *Geospatial analysis: A comprehensive guide to principles, techniques and software tools*. Leicester: Matador, 2007. ISBN: 9781905886609.

[75] A. A. Hagberg, D. A. Schult, and P. J. Swart. "Exploring network structure, dynamics, and function using NetworkX." In: *Proceedings of the 7th Python in Science Conference (SciPy2008)*. Pasadena and CA USA, 2008, pp. 11–15.

[76] geotools.org. *GeoTools: The Open Source Java GIS Toolkit*.

[77] PTV Group. *PTV Visum*. URL: http://www.ptvgroup.com/.

[78] matsim.org. *MATSim: Agent-Based Transport Simulations*. URL: http://www.matsim.org.

[79] A. Fitschen and H. Nordmann. *Verkehrsentwicklung auf Bundesfernstraßen 2012*. Vol. 236. Berichte der Bundesanstalt für Strassenwesen - Verkehrstechnik (V). Bremen: Wirtschaftsverlag NW, 2014. ISBN: 9783956060731. URL: http://www.bast.de/.

[80] Kraftfahrt-Bundesamt. *Bestandsbarometer Personenkraftwagen am 1. Januar 2013 nach ausgewählten Merkmalen (Teil 1)*. 2013. (Visited on 07/29/2014).

[81] P. Scholl. *Autobahn Atlas Online*. URL: http://www.autobahnatlas-online.de/ (visited on 10/2015).

[82] T. M. Inc. *Tesla Super Chargers*. 2014. URL: http://www.teslamotors.com/supercharger (visited on 05/22/2015).

[83] T. Williams. *Nissan LEAF range chart for 24 kWh battery. 100% Capacity*. 2011. URL: http://www.mynissanleaf.com/viewtopic.php?f=31%5C&t=4295 (visited on 04/09/2014).

[84] BMW AG. *BMW i3. Technische Daten*. 2014. URL: http://www.bmw.de/de/neufahrzeuge/bmw-i/i3/2013/techdata.html (visited on 04/07/2014).

[85] BMWi3Owner. *Range for speed*. 2014. URL: http://bmwi3owner.com/2014/03/range-for-speed/l (visited on 04/16/2014).

[86] E. Musk and J. B. Straubel. *Model S Efficiency and Range*. 2012. URL: http://www.teslamotors.com/de%5C_DE/blog/model-s-efficiency-and-range (visited on 04/08/2014).

[87] J. Haendel. "An Approach for Scheduling Fast Electric Vehicle Charging on the A9 Highway by Employing an Event-Based Traffic Model." MA thesis. Technische Universität München, 2014.

[88] opentraffic.io. *Open Traffic: A free, global traffic speed data set linked to OpenStreetMap*. URL: `http://opentraffic.io/`.

[89] European Energy Exchange AG. URL: `www.eex.com`.

[90] H. Bünder. "Stromtankstellen: Spannung an der Autobahn." In: *Frankfurter Allgemeine* (16.Nov.2015). URL: `http://www.faz.net/-i2l-896c7`.